Shcherban' V. Yu.
Halavska L.E.
Kolysko O.Z.
Shcherban' Yu.Yu.
Ielina T.V.
Kolysko M.I.

Ministry of education and science of Ukraine

Kyiv national university of technologies and design

Department of computer sciences and technologies

Department of textile technology and design

MATHEMATICAL SOFTWARE MODELS FOR DETERMINING TECHNOLOGICAL EFFORTS IN THE PRODUCTION OF TECHNICAL FABRICS AND KNITWEAR FOR MILITARY NEEDS

SHCHERBAN' V. Yu., HALAVSKA L.E., KOLYSKO O.Z.,
SHCHERBAN' Yu.Yu., IELINA T.V., KOLYSKO M.I.

MATHEMATICAL SOFTWARE MODELS FOR DETERMINING TECHNOLOGICAL EFFORTS IN THE PRODUCTION OF TECHNICAL FABRICS AND KNITWEAR FOR MILITARY NEEDS

Monograph

Kyiv – 2021

Recommended by the Academic Council of the Kyiv National University of Technology and Design for a wide range of teachers, scientists, graduate students, masters and students of specialized universities, engineering and technical staff of the computer industry
(Minutes №9 of 28 April 2021)
Team of authors:

SHCHERBAN' V. Yu. – laureate of the State Prize of Ukraine in the field of science and technology, academician of the International Academy of Computer Science and Systems, Doctor of Technical Sciences, Professor, Head of the Department of Computer Science and Technology, Kiev National University of Technology and Design;

HALAVSKA L.E. - Doctor of Technical Sciences, Professor, Head of the Department of Technology and Design of Textile Materials, Kiev National University of Technology and Design;

KOLYSKO O.Z. - Candidate of Technical Sciences, Associate Professor of the Department of Computer Science and Technology, Kiev National University of Technology and Design;

SHCHERBAN' Yu.Yu. – Laureate of the State Prize of Ukraine in the field of science and technology, Doctor of Technical Sciences, Professor, Deputy Director of the Kiev Professional College of Applied Sciences;

IELINA T.V. - Candidate of Technical Sciences, Associate Professor of the Department of Technology and Design of Textile Materials, Kiev National University of Technology and Design;

KOLYSKO M.I. - Candidate of Technical Sciences, Associate Professor of the Department of Computer Science and Technology, Kiev National University of Technology and Design.

Reviewers:

SHCHUTSKA G.V. – Doctor of Technical Sciences, Associate Professor, Director of the Kiev Professional College of Applied Sciences;

RIABCHYKOV M.L. – Doctor of Technical Sciences, Associate Professor, Professor of the Department of Technology and Design of the Ukrainian Engineering and Pedagogical Academy.

The results of research on the development of technical fabrics, knitted fabrics and high-strength products with high anti-bullet, anti-fragment, anti-cutting and puncture resistance on textile and knitting equipment that can be used as components of individual human armor (military servicemen) Ukraine, law enforcement agencies, other military formations of Ukraine, persons - participants in hostilities, military, volunteers, journalists and security guards) and equipment; with antibacterial properties and deodorizing effect; resistant to open flames or intense heat flux.

CONTENT

INTRODUCTION

In the current political and military situation, there is a question of reliable individual protection of the military, police and representatives of the executive branch. Body armor of various degrees of protection and accessories to them are used as means of individual protection. With the advent of new modern weapons, personal armor needs to be improved to improve their strength, reliability, preservation of their properties in different climatic conditions and extreme situations, and ease and comfort in carrying. Despite significant achievements in this field in recent years, science still faces the task of developing new materials and design solutions that will make durable textiles lighter and more comfortable.

At the same time, the qualitative characteristics of the equipment and the level of comfort of the serviceman's property are quite important factors that affect his endurance during marches and combat operations, the effectiveness of the tasks. In particular, servicemen who have been in a limited space of military equipment for a long time are at risk of moisture accumulation in the clothing space, development of pathogenic microflora (bacteria, fungi) and the appearance of an unpleasant odor of sweat. Therefore, the elements of property that are in direct contact with the body of the serviceman must provide thermal and physiological comfort, so that the crew of military equipment during its operation was satisfied with the thermal environment, without feeling heat or cold, and vapor moisture (sweat) evaporates freely. On the other hand, there is a risk of damage to combat vehicles due to explosion and fire and ignition of clothing. Therefore, clothing should serve as a means of personal protection against open flames or intense heat flux. Given this, there is a need to improve tangible assets and tactical equipment by developing multifunctional knitted fabrics using new innovative types of raw materials.

The scientific novelty of the received results lies in development of scientifically justified methods of improvement of the thread feeding system of

large diameter circular knitting machines based on strain stabilization. In this case: based on a system of differential equations, which describes the conditions of interaction of a variable cross-section hard-bent thread, which is crumpled in the contact zone, with larger and lesser curvature guiding surfaces, the dependences of the outgoing strain with account of the change in the incoming strain were obtained; based on numeric resolution of a transcendental equation using the dichotomy method, the dependence for definition of the reduced friction ratio was obtained, taking account of the radial embrace of thread with the guide rail; dependences were obtained for determining the incoming strain for the existing and improved thread straining devices and compensators with account of the uneven cross-section diameter, uneven incoming strain, bending and crushing stiffness in the contact zone; based on the research using active planning of experiment, regressive dependences of strain of complex thread and yarn as functions of the thread feeding system constituent elements' parameters, incoming strain, radial and normal embrace angles in the contact zone with high and low curvature guide rails, were obtained; based on the dependences of the thread and yarn incoming strain during their interaction with the structural elements of the thread feeding system on large diameter feeding machines, using the recursive method, systems of equations were obtained, which describe the dependence of strain in the knitting zone from the structural parameters of the constituent elements of the thread feeding system, with account of the change in the cross-section, radial embrace in the contact zone, angles of embrace at entry and exit points, and of the law of change of the incoming strain and the physical and mechanical properties of thread.

The practical value of the work results obtained lies in the following: a computer software was developed for numeric resolution of a system of transcendental equations when determining the incoming strain of a hard-bent thread of a variable cross-section, crumpled in the contact zone, with the large and small curvature guide surfaces with account of the incoming strain change;

a computer software was developed for determining the reduced friction ratio in case of interaction of complex thread and yarn with high and low curvature guide rails, with account of the radial embrace of thread with the guide rail; improved structures were suggested for thread tensioner and compensators, thus allowing, with account of the uneven cross-section of thread and yarn, to reduce the unevenness of strain for the pin-type thread tensioner from 7.5% to 2.2%, of a pin-type compensator – from 68-83% to 10-14%, of a disk compensator – from 71-88% to 8-12%; a structure of a tubular compensator was suggested, the use of which allows reducing the unevenness of strain more than twice, compared with a disc compensator.

The main results of the research were implemented at "Danish Textile" SC in the course of improvement of the technological processes of knitting jersey fabrics from cotton yarn with addition of polyester and lycra on "Mayer&Cie", "Terrot", "Pailung", "Keum Yong" high-performance large-diameter circular knitting machines, based on stabilization of yarn strain in the working zone during formation of jersey fabric. The results of the research work enabled to determine the value of technological forces appearing in thread and yarn in the course of their processing in the working zone of circular knitting machines, thus allowing to reduce the strain to the minimum necessary value. This enabled obtaining the technological effect: reduction of thread and yarn breakages by 4-12% and increase of jersey fabrics quality indicators by 10-15% due to decrease in cutting defective areas and stabilization of the loop shape.

1. MATHEMATICAL SUPPORT OF A COMPUTER PROGRAM FOR DETERMINING THE TENSION OF THE THREAD WHEN INTERACTING WITH THE GUIDING SURFACE

To simplify the process of assembling systems of differential equations that describe the equilibrium of the thread element on the guide surface, it is advisable to use models of threads that are closest in structure and appearance to the real ones [1-28]. In fig. 1.1 presents the most common schemes for cases where a real thread or yarn is replaced by a single cylindrical body, or a real thread is represented as an object consisting of a system of individual cylindrical bodies whose diameter is close to the diameter of individual filaments of a real complex thread or yarn [1- 5, 8, 28]. In this case we are dealing with a system of material bodies. Using the basic principles of the method of kinetostatics, it is necessary to add the appropriate reactions of connections and forces of inertia that act on the body or system of bodies to achieve conditional equilibrium to actively given forces and moments.

To compile systems of differential equations that describe the equilibrium of a thread element on the guide surface, it is necessary to present all external forces and reactions of bonds, threads acting on an element of infinitesimal length dS, as the main vector R_0 and the main moment M_0. The vector data is reduced to the point A * - the center of mass of the selected element of the thread. The resulting force of inertia Φ* and the vector of moment of inertia Mϕ are brought to this point. The main triangle $\tau * n * b *$, with vertex at point A *, serves as a coordinate system in relation to which the conditional equilibrium of all forces and moments is considered [7].

Isolation of the element [5, 7] infinitesimal thickness of the Sun by crossing the thread with two planes perpendicular to the axis of the thread at points B and C, allows all internal force factors in each of them to lead to the main vector and the main moment: to point B (M, R) - for the left section; to the point C (R + ∂R, M + ∂M) - for the right section.
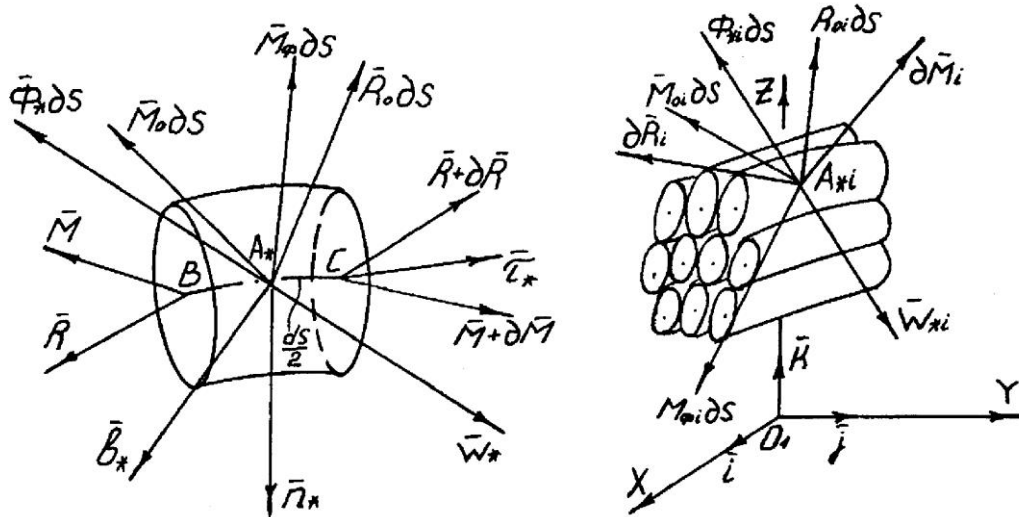
Fig.1.1. Physical models of monofilament and complex thread and yarn

When constructing this scheme, it was believed that the movement occurs from left to right [116, 117, 122]. Vector equations

$$\frac{\partial \vec{R}}{\partial S} + \vec{R}_0 - \vec{\Phi}_* = 0; \quad \frac{\partial \vec{M}}{\partial S} + \vec{M}_0 + \vec{\tau}_* \times \vec{Q} - \vec{M}_\Phi = 0, \tag{1.1}$$

describe the motion of an infinitesimal element of the thread.

In the case when a real thread is represented as an object consisting of a system of individual cylindrical bodies whose diameter is close to the diameter of individual filaments of a real complex thread or yarn, to compile a system of differential equations with two planes perpendicular to the axis of the complex thread or yarn, cut off the element of infinitesimal length ds, consisting of n elementary filaments [2, 8, 11]. According to the above method of kinetostatics [8, 9-28] it is necessary to apply the above forces to each i-th elementary filament.

The reduction center of each i-th elementary fiber will be the point A^*_i - the center of mass. All actively given forces and the corresponding reactions of the bonds are reduced to the main vector R_0i and the main moment M_0i. By analogy with the first option, the internal forces in the two sections are also reduced to the center of mass [8]. Their effect on the elementary filament is replaced by the principal vector dR_i and the principal moment dM_i.

We reduce the forces of inertia to the main vector $\Phi^* i$ and the main moment of inertia $M_{\phi i}$ [2, 8].

For the i-th filament, the vector equilibrium equations will have the form [8]

$$\frac{\partial \vec{R}_i}{\partial S} + \vec{R}_{0i} - \vec{\Phi}_{*i} = 0; \quad \frac{\partial \vec{M}_i}{\partial S} + \vec{M}_{0i} - \vec{M}_{\Phi i} = 0. \tag{1.2}$$

Summarize these dependences for n elementary fibers, which make up a complex thread or yarn, the reactions of the bonds (except for internal forces) will be destroyed as mutually balanced forces for each pair of fibers [1, 8].

We design a system of differential equations (1.2) on the coordinate axes X, Y, Z, and we obtain a system of six differential equations

$$\sum_{i=1}^{n}\left(\frac{\partial R_{ix}}{\partial S} + R_{0ix}^- - \Phi_{*ix}\right) = 0; \quad \sum_{i=1}^{n}\left(\frac{\partial M_{ix}}{\partial S} + M_{0ix}^- - M_{\phi ix}\right) = 0;$$

$$\sum_{i=1}^{n}\left(\frac{\partial R_{iy}}{\partial S} + R_{0iy}^- - \Phi_{*iy}\right) = 0; \quad \sum_{i=1}^{n}\left(\frac{\partial M_{iy}}{\partial S} + M_{0iy}^- - M_{\phi iy}\right) = 0;$$

$$\sum_{i=1}^{n}\left(\frac{\partial R_{iz}}{\partial S} + R_{0iz}^- - \Phi_{*iz}\right) = 0; \quad \sum_{i=1}^{n}\left(\frac{\partial M_{iz}}{\partial S} + M_{0iz}^- - M_{\phi iz}\right) = 0,$$

where the corresponding index x, y or z indicates the projection on the corresponding coordinate axis.

However, when a real thread is represented as an object consisting of a system of individual cylindrical bodies whose diameter is close to the diameter of individual filaments of a real complex thread or yarn, there are problems with the adequacy of the process of interaction of the thread with the guide surface. Models of this type are quite cumbersome [2, 4, 8]. For example, in its construction, the filaments are considered to be arranged in a straight line. In fact, the elementary fibers are intertwined with each other, and this significantly changes the nature of the interaction between them. In addition, in solving the above system of equations face very serious difficulties. This concerns the difficulty in determining the projections of force vectors and moments on the corresponding coordinate axes.

Thus, given all the above, the most acceptable, in terms of simplicity of the results, is a model of the thread, in which the entire volume is evenly filled with material.

The main vector R is equal

$$\vec{R} = P\vec{\tau}_* + Q_2\vec{n}_* + Q_3\vec{b}_*, \tag{1.3}$$

and the main moment M is equal

$$\vec{M} = M_k\vec{\tau}_* + M_{u2}\vec{n}_* + M_{u3}\vec{b}_*. \tag{1.4}$$

To obtain a system of differential equations, it is necessary to design the vector equations (1.3) - (1.4) on the axis of the main trihedron $\tau * n * b *$ (Fig. 1.2).

Differentiate expressions (1.3) and (1.4) by the arc coordinate

$$\frac{\partial \vec{R}}{\partial S} = \left(\frac{\partial P}{\partial S} - Q_2 q_1 + Q_3 p_1\right)\vec{\tau}_* + \left(\frac{\partial Q_2}{\partial S} + P q_1 + Q_3 r_1\right)\vec{n}_* + \left(\frac{\partial Q_3}{\partial S} - P p_1 + Q_2 r_1\right)\vec{b}_*,$$

$$\frac{\partial \vec{M}}{\partial S} = \left(\frac{\partial M_k}{\partial S} - M_{u2} q_1 + M_{u3} p_1\right)\vec{\tau}_* + \left(\frac{\partial M_{u2}}{\partial S} + M_k q_1 + M_{u3} r_1\right)\vec{n}_* + \tag{1.5}$$

$$+ \left(\frac{\partial M_{u3}}{\partial S} - M_k p_1 + M_{u2} r_1\right)\vec{b}_*,$$

where P - is the thread tension; Q2, Q3 - projections of the cutting force on the normal and binormal; Mk - torque; Mu2, Mu3 - bending moments in the corresponding sections of the thread.

The force of inertia will be determined by the formula [1, 3-8, 28]

$$\vec{\Phi}_* = T\vec{W}_* = T \times$$

$$\times\left\{\left[\frac{\partial(V_\tau + U'_\tau)}{\partial t} + (\omega_{0n} + \omega_{un})(V_b + U'_b) - (\omega_{0b} + \omega_{ub})(V_n + U'_n)\right]\vec{\tau}_* + \right.$$

$$+ \left[\frac{\partial(V_n + U'_n)}{\partial t} - (\omega_{0\tau} + \omega_{u\tau})(V_b + U'_b) + (\omega_{0b} + \omega_{ub})(V_\tau + U'_\tau)\right]\vec{n}_* + \tag{1.6}$$

$$+ \left.\left[\frac{\partial(V_b + U'_b)}{\partial t} + (\omega_{0\tau} + \omega_{u\tau})(V_n + U'_n) - (\omega_{0n} + \omega_{un})(V_\tau + U'_\tau)\right]\vec{b}_*\right\},$$

where T - is the linear density of the thread.

To determine the value of M_ϕ use the ratio known from theoretical mechanics [1-5, 8, 27], then for the thread element

$$\vec{M}_\phi = \frac{J}{\partial S}\frac{\partial \vec{\omega}}{\partial t}, \qquad (1.7)$$

where J - is the inertia tensor (given that the axes of the main trihedron located in the center of mass of the element BC (Fig. 1.2) are the axes of symmetry and the main axes of inertia, we assume that the centrifugal moments of inertia are zero and significant will be located only on the main diagonal of the matrix inertia tensor).

The components of the inertia tensor located on the main diagonal of the matrix are determined by the formulas [5]

$$J_{\tau*} = \gamma_{\text{н}}\left[J_{\tau_0} \pm \Delta_\tau(\vec{U})\right]\partial S,$$
$$J_{n*} = \gamma_{\text{н}}\left[J_{n_0} \pm \Delta_n(\vec{U})\right]\partial S, \qquad (1.8)$$
$$J_{b*} = \gamma_{\text{н}}\left[J_{b_0} \pm \Delta_b(\vec{U})\right]\partial S,$$

where $J_{\tau*}$, J_{n*}, J_{b*} - respectively, the moments of inertia of the selected element relative to the axes of the main trihedron;

$J_{\tau0}$, J_{n0}, J_{b0} - geometric moments of inertia about the axes of the main trihedron to the crumpled thread;

$\Delta_\tau(U)$, $\Delta_n(U)$, $\Delta_b(U)$ – functional coefficients that determine the change of geometric moments of inertia due to wrinkling in the contact zone;

γ_H - bulk density.

Taking into account the dependence (1.8), expression (1.7) will take the form

$$\vec{M}_\phi = \gamma_{\text{н}}\left\{\left[J_{\tau_0} \pm \Delta_\tau(\vec{U})\right]\varepsilon_1\vec{\tau}_* + \left[J_{n_0} \pm \Delta_n(\vec{U})\right]\varepsilon_2\vec{n}_* + \left[J_{b_0} \pm \Delta_b(\vec{U})\right]\varepsilon_3\vec{b}_*\right\}, \qquad (1.9)$$

where ε_1, ε_2, ε_3 - projections of the vector of angular acceleration of the thread element $\varepsilon*$ on the axis of the main trihedron.

The projections of the main vector of all external forces, for the case of interaction of the thread with the guide, can be expressed as follows

$$\vec{R}_0 = F_\tau \vec{\tau}_* + F_n \vec{n}_* + F_b \vec{b}_*,$$

where F_τ, F_n, F_b - projections of the vector R0 on the axis of the main trihedron.

Figure 1.2 shows a diagram of the interaction of the thread with the guides at the break points of the refueling line
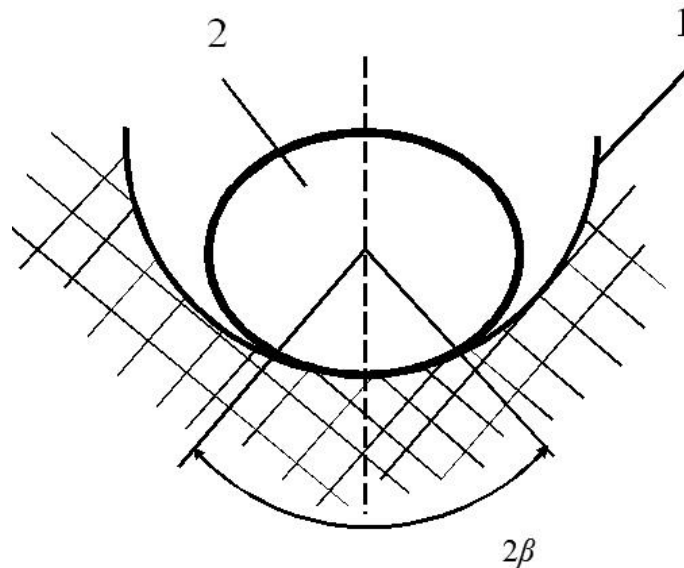
Fig.1.2. The scheme of interaction of a thread with guides in break points of a line of refueling

Then the equation for the main vector of all external forces will take the form [8, 25-28]

$$\vec{R}_0 = F_\tau \vec{\tau}_* + F_n \vec{n}_* + F_b \vec{b}_*,$$
$$F_\tau = \mu N, \quad F_n = N,$$
$$\mu = \frac{\beta}{\sin\beta} \frac{aR^b}{P_0^b}, \tag{1.10}$$

where μ – coefficient of friction; N – specific normal surface reaction; β – half the angle of the arc of contact of the thread with the guides at the break points of the filling line; a, b – constant coefficients for a specific type of complex yarn or yarn (for nylon yarn 28 Tex (a= 0,1765, b= 0,1186), viscose complex thread 16,7 Tex (a= 0,1580, b= 0,1160), woolen yarn 29,9 Tex (a= 0,1330, b =

12

0,0910), cotton yarn 27,6 Tex (a= 0,1656, b = 0,0590), viscose staple yarn 28,8 Tex (a= 0,1470, b= 0,0690)); P_0 – tension of the driven branch of a thread; R – radius of curvature of the guide.

Dependence for the main moment of external forces Mo will look like

$$\vec{M}_0 = M_\tau \vec{\tau}_* + M_n \vec{n}_* + M_b \vec{b}_*,\tag{1.11}$$

where M_τ , M_n , M_b - corresponding projections on the axis of the main trihedron.

$$\frac{\partial P}{\partial S} - Q_2 q_1 + Q_3 p_1 - \frac{\beta}{\sin\beta}\frac{aR^b}{P_0^b}N\cos\varphi_t = T \times$$

$$\times\left[\frac{\partial(V_\tau + U_\tau')}{\partial t} + (\omega_{0n} + \omega_{un})(V_b + U_b') - (\omega_{0b} + \omega_{ub})(V_n + U_n')\right];$$

$$\frac{\partial Q_2}{\partial S} + P\,q_1 + Q_3 r_1 - N = T \times$$

$$\times\left[\frac{\partial(V_n + U_n')}{\partial t} - (\omega_{0\tau} + \omega_{u\tau})(V_b + U_b') + (\omega_{0b} + \omega_{ub})(V_\tau + U_\tau')\right];$$

$$\frac{\partial Q_3}{\partial S} - P\,p_1 + Q_2 r_1 + \frac{\beta}{\sin\beta}\frac{aR^b}{P_0^b}N\sin\varphi_t = T \times$$

$$\times\left[\frac{\partial(V_b + U_b')}{\partial t} + (\omega_{0\tau} + \omega_{u\tau})(V_n + U_n') - (\omega_{0n} + \omega_{un})(V_\tau + U_\tau')\right];$$

$$\frac{\partial M_\kappa}{\partial S} - M_{u2}q_1 + (c_0 + c_1 K_r + c_2 K_r^2)q_1 p_1 + M_\tau = \gamma_{_H}\left[J_{\tau_0} \pm \Delta_\tau(\vec{U})\right]\varepsilon_1;$$

$$\frac{\partial M_{u2}}{\partial S} + M_k q_1 + (c_0 + c_1 K_r + c_2 K_r^2)q_1 r_1 - Q_3 + M_n = \gamma_{_H}\left[J_{n_0} \pm \Delta_n(\vec{U})\right]\varepsilon_2;$$

$$\frac{\partial[(c_0 + c_1 K_r + c_2 K_r^2)q_1]}{\partial S} - M_k p_1 + M_{u2}r_1 + Q_2 +$$

$$+ r_x\frac{\beta}{\sin\beta}\frac{aR^b}{P_0^b}N = \gamma_{_H}\left[J_{b_0} \pm \Delta_b(\vec{U})\right]\varepsilon_3,$$

$$N = b_2 E_1\delta(1 - b_3\delta^{b_4}) + \eta\dot{\delta}^{b_5}(1 - b_5\dot{\delta}^{b_6}),\ \delta = \frac{r - r_x}{r},\ \dot{\delta} = \frac{\partial U_\nu}{r\partial t},$$

$$q_1 = \frac{\cos\Psi_0}{\rho_0} + \frac{\partial\beta}{\partial S} + \frac{\alpha}{\rho_{01}} + \alpha\frac{\partial\Psi_0}{\partial S},\ p_1 = \frac{\sin\Psi_0}{\rho_0} + \frac{\partial\alpha}{\partial S} - \frac{\beta}{\rho_{01}} - \beta\frac{\partial\Psi_0}{\partial S};$$

$$r_1 = \frac{1}{\rho_0} + \frac{\partial\Psi_0}{\partial S} - \alpha\frac{\cos\Psi_0}{\rho_0} + \frac{\sin\Psi_0}{\rho_0}\beta,\ \gamma = \frac{\partial U_\tau}{\partial S} - \frac{\cos\Psi_0}{\rho_0}U_\nu + \frac{\sin\Psi_0}{\rho_0}U_\beta;$$

$$\beta = \frac{\partial U_\nu}{\partial S} + \frac{\cos\Psi_0}{\rho_0}U_\tau - \frac{U_\beta}{\rho_{01}} - U_\beta\frac{\partial\Psi_0}{\partial S},\ \alpha = \frac{\sin\Psi_0}{\rho_0}U_\tau - \frac{\partial U_\beta}{\partial S} - \frac{U_\nu}{\rho_{01}}_\nu - U_\nu\frac{\partial\Psi_0}{\partial S}.$$

$$(1.12)$$

where r_x - the distance from the point A * of the axis of the thread element to the guide (r_x = r - Uv, where r is the calculated radius of intersection of the thread);

ρ_0, ρ_{01} - radii of curvature and geometric rotation of the thread axis;

ψ_0 - corner of Saint-Venan;

$U\tau$, Uv, $U\beta$ – of projection of the cross-sectional deformation vector on the axis of a natural trihedron [8, 25-28];

b_2 - contact trace width;

$\delta^{'}$ - the rate of relative deformation of the cross section of the thread;

η - coefficient characterizing the viscous properties of the thread during its transverse deformation;

E_1 - the current modulus of stiffness of the thread on the deformation of its cross section;

b_3, b_4, b_5, b_6 - experimental coefficients determined from the load-strain diagram [8-12];

c_0, c_1, c_3 - experimental coefficients, which are determined from the diagram "load - deformation" when bending the thread at the appropriate angle;

K_r – the number of complete rotations of the thread relative to its axis per unit length [8].

The resulting system of differential equations in the projection on the axis of the main trihedron, which describes the motion of the threads taking into account their real physical and mechanical properties on the guide surface, taking into account (1.1) - (1.11) has the form [8, 25-28].

A few words need to be said about the dependence of the value of specific pressure on the rate of deformation and the value of the relative deformation of the cross section of the thread. The thread tension decreases with increasing speed. As the size of the cross section of the thread decreases, the effect of its speed of movement on the tension decreases. The obtained results are valid only for monofilaments. The opposite pattern is observed for complex

threads and yarns. As will be shown below, as the speed of the thread increases, its tension increases. The same trend is observed with increasing relative deformation of the cross section of the thread. In our opinion, the explanation of this phenomenon should be sought when determining the rate of propagation of deformations.

The resulting system is a closed nonlinear system of 12 differential and 4 algebraic equations. This system contains 16 unknown functions for the arguments S and t.

The integration of this system of differential equations is associated with great difficulties and is possible only with the use of computers. The difficulty of integration lies in the choice of boundary and initial conditions for the derivatives of the respective degrees (above the second).

2. WARP YARN TENSION DURING FABRIC FORMATION

Tension of warp yarn, before it enters fabric weaving area, is a value determining intensity of the weaving process and cloth structure [21]. Tension of warp yarns, before they enter fabric weaving area, comprises both input tension and additional tension, which arises by virtue of frictional forces between warp yarns and surfaces of guiding and working components having cylinder form or one close to it [2, 7, 21]. Figure 2.1a, b represents guiding and working components of the loom the warp yarn interacts with when entering the weaving area. Curvature radius of the provided surfaces, which have cylinder form or one close to it, both significantly longer as compared to radius of the cross-section a warp yarn and commensurate with it [2, 21]. Such type of interation also occurs in implementation of similar technological processes [1, 4].

a   b

Figure 2.1 Guides and working components of the loom: a – tension rail; b –
heddle eyes

Simulation of the warp yarn processing using a loom involves study of
interaction between warp yarns and cylindrical surfaces. These surfaces are
dummies for surface of separating rods, which are components of the yarn break
detector, as well as heddle eyes for automatic shuttleless pneumatic rapier looms
[1, 2, 3, 21]. When drafting the plan of the experiment, the direction connected
to slip of rubbing surfaces [9], speed of yarn or guiding surface [10, 21] and
radius of the curvature of cylindrical surface [4, 7] should be taken into account.
Keeping in mind that spun yarn and multi-filaments are used as warp yarns,
flexural rigidity can be ignored [3-4, 7-8, 21].

Figure 2.2 shows warp yarn threading system for a loom. It is divided
into three areas for our purpose: I area – between warp beam and separating warp
stop motion; II area – between tension rail and heddle frames; III area – between
separating warp stop motion and fell of the cloth. Increase in intensity of warp
yarn tension divided into areas represented by green, blue and red color. These
colors have been used during modelling of response surfaces and plotting of

warp yarn tension. Indexes for designation warp yarn tension, contact angles, curvature radius of the cylindrical surfaces shall correspond to areas' numbers.
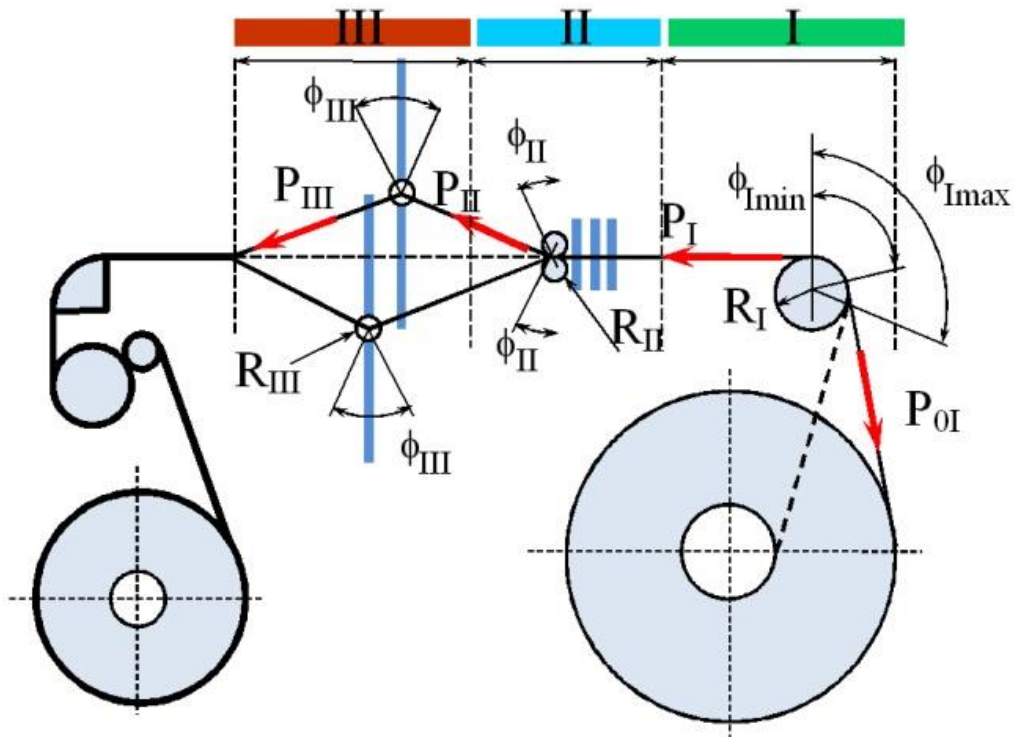
Figure 2.2 Warp yarn threading system for a loom

Three types of yarn have been chosen for experiment. Series A: carded cotton yarn 18.5x2 Tex. It is used as warp yarns for spring-autumn fabric of tartan twill weave Series B: bleached flax of wet spun 41 Tex, obtained from dressed flax. It is used as warp yarns to manufacture sindon. Series C: wool 31.2x2 Tex. It is used as warp yarns to manufacture pure-wool suit cloth of boston twill.

For each series A, B, and C to define joint impact of input tension of warp yarn P0, radius of cylinder guide R and computed value of contact angle φ_P on output tension of the warp yarn P, the secondary orthogonal design was prepared and implemented for three factors [3, 7, 21]. Standard form of regression equation shall be as follows

$$P = b_0 + b_1 x_1 + b_2 x_2 + b_3 x_3 + b_{12} x_1 x_2 + b_{13} x_1 x_3 + b_{23} x_2 x_3 +$$
$$+ b_{11} x_1^2 + b_{22} x_2^2 + b_{33} x_3^2 \tag{2.1}$$

The range of factors variability in equation (2.1) is determined by real conditions of yarns processing on looms. Threading line for warp yarn is divided into three areas: I is the area from warp yarn run-off point from beam to stop motion; II is the area from warp yarn entrance into stop motion to heddle frame; III is the area from warp yarn exit from stop motion to the fell of the cloth (Figure 2). Within the I area warp yarn interacts with tension rail. Within the II area warp yarn contacts separating stop motion rod. Within the III area warp yarn contacts heddle eye.

Factor x_1 is the value of the threading tension within I area before tension rail for shuttle looms, shuttleless looms, and pneumatic rapier looms: A - for carded cotton yarn - $P_{0I} = 20$ cN; B - for bleached flax of wet spun made - $P_{0I} = 25$ cN; C - for wool - $P_{0I} = 35$ cN.

Factor x_2 – cylinder (tension rail) radius within I area for: shuttle looms – $R_I = 56$ mm; shuttleless looms – $R_I = 63$ mm; pneumatic rapier looms – $R_I = 32$ mm.

Factor x_2 – cylinder (left separating rod in stop motion) radius within II area for: pneumatic rapier looms shuttle looms - $R_{II} = 9$ mm; shuttleless looms – $R_{II} = 4$ mm; pneumatic rapier looms – $R_{II} = 3$ mm.

Factor x_2 – cylinder (heddle eye) radius within III area for: shuttle looms – $R_{III} = 1.1$ mm; shuttleless looms – $R_{III} = 0.6$ mm; pneumatic rapier looms – $R_{III} = 0.5$ mm.

Factor x_3 – calculated value of the contact angle with cylinder (tension rail) within I area for: shuttle looms – $\varphi_{IP} = 60^0$ with maximum beam diameter 600 mm and $\varphi_{IP} = 110^0$ with minimum beam diameter 146 mm; shuttleless looms – $\varphi_{IP} = 70^0$ with maximum beam diameter 600 mm and $\varphi_{IP} = 100^0$ with minimum

beam diameter 220 mm; pneumatic rapier looms – $\varphi_{IP} = 90^0$ with maximum beam diameter 600 mm and $\varphi_{IP} = 115^0$ with minimum beam diameter 100 mm.

Factor x_3 – calculated value of the contact angle with cylinder (left separating rod in the stop motion) within II area for: shuttle looms – $\varphi_{IIP} = 75^0$ with maximum shed opening and 0^0 with closed shed; shuttleless looms – $\varphi_{IIP} = 75^0$ with maximum shed opening and 0^0 with closed shed; pneumatic rapier looms – $\varphi_{IIP} = 76^0$ with maximum shed opening and 0^0 with closed shed.

Factor x_3 – calculated value of the contact angle with cylinder (heddle eye) within III area for: shuttle looms – $\varphi_{IIIP} = 29^0$ with open shed and $\varphi_{IIIP} = 0^0$ with closed shed; shuttleless looms – $\varphi_{IIIP} = 22^0$ with open shed and $\varphi_{IIIP} = 0^0$ with closed shed; pneumatic rapier looms – $\varphi_{IIIP} = 41^0$ with open shed and $\varphi_{IIIP} = 0^0$ with closed shed.

At the first stage the tension within the I area after the tension rail is determined. Table 2.1 shows orthogonal matrix of the second order for three series A, B and C.

Table 2.1

No.	Factors							
	Input tension				Curvature radius		Contact angle	
	x_1	P_{0I}, cN			x_2	R_I,	x_3	φ_{IP},
		A	B	C		mm		degrees
1	+1	25	35	45	+1	65	+1	120
2	-1	15	15	25	+1	65	+1	120
3	+1	25	35	45	-1	35	+1	120
4	-1	15	15	25	-1	35	+1	120
5	+1	25	35	45	+1	65	-1	100
6	-1	15	15	25	+1	65	-1	100
7	+1	25	35	45	-1	35	-1	100

8	-1	15	15	25	-1	35	-1	100
9	-1.215	14	14	23	0	50	0	110
10	+1.215	26	26	47	0	50	0	110
11	0	20	25	35	-1.215	32	0	110
12	0	20	25	35	+1.215	68	0	110
13	0	20	25	35	0	50	-1.215	98
14	0	20	25	35	0	50	+1.215	122
15	0	20	25	35	0	50	0	110

Connection between natural and encoded values for I area shall be as follows:

series A

$$x1 = \frac{P_{0I} - 20}{5}, \quad x2 = \frac{R_I - 50}{15}, \quad x3 = \frac{\varphi_{IP} - 110}{10}, \tag{2.2}$$

series B

$$x1 = \frac{P_{0I} - 25}{10}, \quad x2 = \frac{R_I - 50}{15}, \quad x3 = \frac{\varphi_{IP} - 110}{10}, \tag{2.3}$$

series C

$$x1 = \frac{P_{0I} - 35}{10}, \quad x2 = \frac{R_I - 50}{15}, \quad x3 = \frac{\varphi_{IP} - 110}{10}. \tag{2.4}$$

At the second stage the tension within the I area after the left separating rod in stop motion is determined. As an input tension P_{0II} we shall take the output tension of the warp yarns after I area P_I. Table 2.2 shows orthogonal matrix of the second order for three series A, B and C.

Table 2.2

No.	Factors		
	Input tension	Curvature radius	Contact angle

	x_1	P_{0II}, cN			x_2	R_{II},	x_3	$\varphi_{II P}$,
		A	B	C		mm		degrees
1	+1	36	48	60	+1	8	+1	80
2	-1	20	18	30	+1	8	+1	80
3	+1	36	48	60	-1	2	+1	80
4	-1	20	18	30	-1	2	+1	80
5	+1	36	48	60	+1	8	-1	10
6	-1	20	18	30	+1	8	-1	10
7	+1	36	48	60	-1	2	-1	10
8	-1	20	18	30	-1	2	-1	10
9	-1.215	18	15	27	0	5	0	45
10	+1.215	38	51	63	0	5	0	45
11	0	28	33	45	-1.215	1	0	45
12	0	28	33	45	+1.215	9	0	45
13	0	28	33	45	0	5	-1.215	3
14	0	28	33	45	0	5	+1.215	88
15	0	28	33	45	0	5	0	45

Connection between natural and encoded values for II area shall be as follows:

series A

$$x1 = \frac{P_{0II} - 28}{8}, \quad x2 = \frac{R_{II} - 5}{3}, \quad x3 = \frac{\varphi_{II P} - 45}{35}, \tag{2.5}$$

series B

$$x1 = \frac{P_{0II} - 33}{15}, \quad x2 = \frac{R_{II} - 5}{3}, \quad x3 = \frac{\varphi_{II P} - 45}{35}, \tag{2.6}$$

series C

$$x1 = \frac{P_{0II} - 45}{15}, \quad x2 = \frac{R_{II} - 5}{3}, \quad x3 = \frac{\varphi_{II P} - 45}{35}. \tag{2.7}$$

At the third stage the tension within the III area after the heddle eye. As an input tension P_{0III} we shall take the output tension of the warp yarns after II area P_{II}. Table 2.3 shows orthogonal matrix of the second order for three series A, B and C.

Table 2. 3

No.	Factors							
	Input tension				Curvature radius		Contact angle	
	x_1	P_{0III}, cN			x_2	R_{III},	x_3	$\varphi_{III\,P}$,
		A	B	C		mm		degrees
1	+1	50	58	70	+1	1.4	+1	40
2	-1	20	18	30	+1	1.4	+1	40
3	+1	50	58	70	-1	0.6	+1	40
4	-1	20	18	30	-1	0.6	+1	40
5	+1	50	58	70	+1	1.4	-1	4
6	-1	20	18	30	+1	1.4	-1	4
7	+1	50	58	70	-1	0.6	-1	4
8	-1	20	18	30	-1	0.6	-1	4
9	-1.215	17	14	26	0	1	0	22
10	+1.215	53	62	74	0	1	0	22
11	0	35	38	50	-1.215	0.5	0	22
12	0	35	38	50	+1.215	1.5	0	22
13	0	35	38	50	0	1	-1.215	0
14	0	35	38	50	0	1	+1.215	44
15	0	35	38	50	0	1	0	22

Connection between natural and encoded values for II area shall be as follows:
series A

$$x1 = \frac{P_{0III} - 35}{15}, \quad x2 = \frac{R_{III} - 1}{0.4}, \quad x3 = \frac{\varphi_{III\,P} - 22}{18},$$

(2.8)

series B

$$x1 = \frac{P_{0III} - 38}{20}, \quad x2 = \frac{R_{III} - 1}{0.4}, \quad x3 = \frac{\varphi_{III\,P} - 22}{18},$$

(2.9)

series C

$$x1 = \frac{P_{0III} - 50}{20}, \quad x2 = \frac{R_{III} - 1}{0.4}, \quad x3 = \frac{\varphi_{III\,P} - 22}{18}.$$

(2.10)

Figure 2.3 shows experimental setup, which includes 9 units. The first unit 1 is a device for threading and tension of warp yarn. In order to avoid ballooning, warp yarns 9 were wound on a cylindrical take-up which fed it into the measurement zone. Slack-side tension was created using cymbal tension device.

The second 2 and third 3 units (figure 2.3) are intended to measure input and output tension of the warp yarn 9. Based on the value of the input tension of the warp yarn 9 two types of measuring assembly were used in the work. For tension range 50 cN to 500 cN the fixed tension meter for moving monofilament MT 320M by METROTEKS company with movable outer rollers was used (Figure 2.4): range of the motion speed for warp yarn 9: 1- 6000 m/min, metering accuracy – 2 %, velocity – 0.1 sec, analog output – 0-1 B. For tension range 20 cN to 50 cN the second type of the measuring assembly was used. The one that includes two rollers mounted in bearing parts on the fixed axles. The third roller mounted on the cantilever fitted beam in such a way that inner bearing ring was fixed on the beam itself, and outer bearing ring stiffened to roller that interacts with yarn. Friction forces in bearings can be ignored. A warp yarn was supplied to the pulleys in such a manner that slack-side and tight-side appeared to be on the sides of an isosceles triangle. The middle bar flexed under the warp yarn tension, and that led to changing resistance of the tension meter. This has been registered at the corresponding channel of the amplifier 8АНЧ-7М [7, 21].
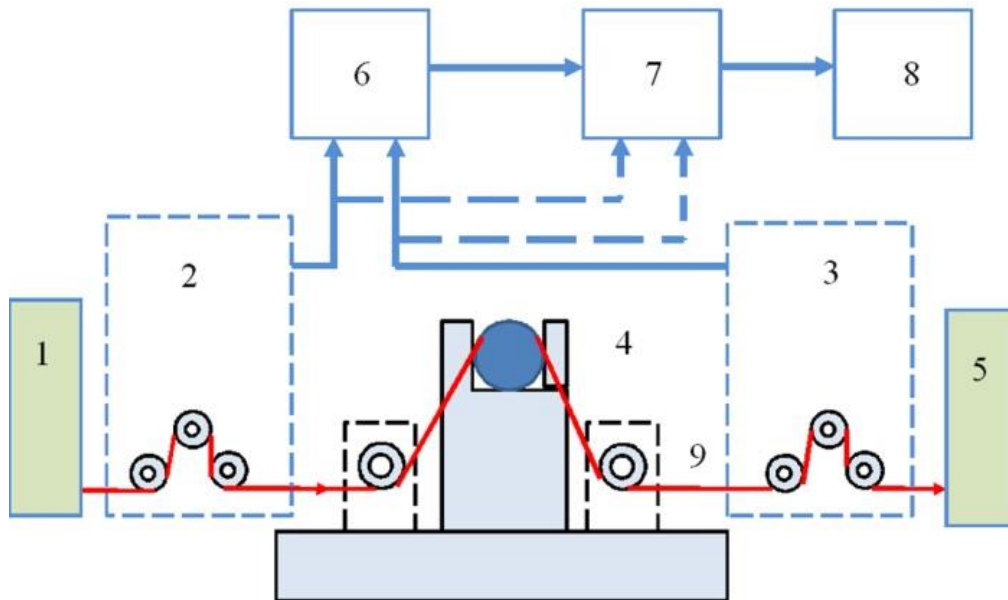
Figure 2.3 Scheme of the experimental setup: 1 – warp yarn threading unit; 2 – metering unit for warp yarn input tension; 3 – metering unit for warp yarn output tension; 4 – environment modelling unit; 5 – warp yarn take up unit; 6 – amplifier; 7 – analog to digital converter ADC; 8 – personal computer; 9 – warp yarn

Crosswise and lengthwise dimensions of the beam have been chosen to make its natural oscillation frequency equal to 1400 Hz. This frequency is many times higher than he frequency of the highest component of tension.

Figure 2.4 Input and output warp yarn tension metering unit MT 320M

Figure 2.5 shows the fourth main unit 4 of the experimental setup. It is intended for simulation of interaction conditions between warp yarn 9 and cylinder guides [1,2]. Two slider pairs, on which aluminum rollers are fixed in rotation bearings, are installed on the foundation in the horizontal grooves. The position of the slider pairs with respect to the central fixed bracket is changed by turning the two levers on the left and on the right. The central, fixed vertical bracket serves to secure the cylinder guides of different diameters, needles of knitting machine, heddles. The fastening is carried out by two screw pairs and clamping bars.

The warp yarn 9 speed was varied due to a fixed-ratio round belt transmission (the fifth unit in Figure 2.3). Driving pulley of the transmission is rotated by AC motor, that was firmly fixed to the foundation of the main measurement system.

Figure 2.5 Unit for simulation of interaction conditions

Analog signals from the 3rd and 4th units measuring warp yarn tension (for the first type of the measurement assembly) or from the amplifier 6 (for the second type of the measurement assembly) is being received by analogue-to-digital converter ADC 7 (figure 2.6), enabled as a multifunction board L-780M

with signaling processor ADC 14 bit/400 kHz having 16 differential input analog and output digital channels, which is connected to the PCI-connector 8. Generation of interrupts according to padding of the part of the FIFO-buffers of ADC and DAC.

Figure 2.6 Analogue-to-digital converter ADC

As a result of implementation of experimental designs (tables 2.1-3) for each series A, B, and C, as well as for each area I, II, and III, 10 concurrent metering were conducted. Table 2.4 shows their average values.

Table 2.4

Experiment No.	Output tension of warp yarn Pi, cN								
	Cotton yarn 18.5x2 Tex			Flax 41 Tex			Wool 31x2 Tex		
	i=I	i=II	i=III	i=I	i=II	i=III	i=I	i=II	i=III
1	36.12	44.77	56.71	48.06	57.72	64.45	60.08	70.48	77.03
2	21.92	25.06	22.84	20.99	21.92	20.18	33.91	35.61	33.27
3	35.67	44.79	58.75	47.47	57.60	66.32	59.18	70.32	79.55
4	21.64	25.08	23.71	20.71	21.88	20.81	33.38	35.53	34.44

5	33.97	37.20	52.12	45.59	49.35	60.05	57.26	61.56	72.65
6	20.58	20.69	20.89	19.85	18.54	18.69	32.24	30.83	31.23
7	33.63	37.76	54.23	45.13	49.96	62.05	56.56	62.42	75.35
8	20.36	21.02	21.79	19.63	18.79	19.36	31.82	31.29	32.49
9	19.75	20.52	18.81	18.98	16.82	15.28	30.29	29.84	28.27
10	36.22	43.03	58.25	34.81	56.67	67.08	60.84	69.12	79.85
11	27.78	32.62	40.17	33.22	37.51	42.63	45.17	50.61	56.20
12	28.17	31.81	38.05	33.69	36.80	40.78	45.95	49.54	53.45
13	27.00	28.51	36.62	32.45	33.51	39.47	44.34	45.71	52.20
14	29.05	35.59	40.59	34.58	40.47	43.05	46.95	53.73	56.08
15	28.00	31.81	38.56	33.49	36.78	41.22	45.62	49.51	54.11

Applying well-known methodics to determine coefficient in the regression equation (2.1) for orthogonal design of the second order [21], taking into account dependences (2.2)-(2.10), the following regressional dependences are obtained:

for area I:

series A

$$P_I = 0.02 + 0.91P_{0I} + 0.01R_I + 0.01P_{0I}\varphi_{IP}, \quad (2.11)$$

series B

$$P_I = 211.44 + 1.91P_{0I} - 0.72R_I - 3.71\varphi_{IP} + $$
$$+ 0.003P_{0I}\varphi_{IP} - 0.02P_{0I}^2 + 0.01R_I^2, \quad (2.12)$$

series C

$$P_I = 0.37 + 0.92P_{0I} + 0.02R_I + 0.01\varphi_{IP} + 0.001P_{0I}R_I + $$
$$+ 0.003P_{0I}\varphi_{IP} - 0.0002R_I^2, \quad (2.13)$$

for area II:

series A

$$P_{II} = 1.28 + 0.99 P_{0II} - 0.32 R_{II} - 0.001 \varphi_{IIP} + 0.003 P_{0II} \varphi_{IIP} +$$
$$+ 0.001 R_{II} \varphi_{IIP} + 0.02 R_{II}^2 , \qquad (2.14)$$

series B

$$P_{II} = 1.68 + 0.98 P_{0II} - 0.29 R_{II} - 0.002 \varphi_{IIP} + 0.002 P_{0II} \varphi_{IIP} +$$
$$+ 0.0012 R_{II} \varphi_{IIP} + 0.018 R_{II}^2 , \qquad (2.15)$$

series C

$$P_{II} = 2.45 + 0.99 P_{0II} - 0.44 R_{II} - 0.002 \varphi_{IIP} + 0.002 P_{0II} \varphi_{IIP} +$$
$$+ 0.002 R_{II} \varphi_{IIP} + 0.03 R_{II}^2 , \qquad (2.16)$$

for area III:

series A

$$P_{III} = 2.86 + 1.08 P_{0III} - 4.21 R_{III} + 0.004 \varphi_{IIIP} + 0.002 P_{0III} \varphi_{IIIP} -$$
$$- 0.05 P_{0III} R_{III} + 2.02 R_{III}^2 , \qquad (2.17)$$

series B

$$P_{III} = 2.66 + 1.06 P_{0III} - 3.67 R_{III} + 0.004 \varphi_{IIIP} + 0.002 P_{0III} \varphi_{IIIP} -$$
$$- 0.04 P_{0III} R_{III} + 1.77 R_{III}^2 , \qquad (2.18)$$

series C

$$P_{III} = 3.96 + 1.07 P_{0III} - 5.54 R_{III} + 0.007 \varphi_{IIIP} + 0.002 P_{0III} \varphi_{IIIP} -$$
$$- 0.04 P_{0III} R_{III} + 2.62 R_{III}^2 . \qquad (2.19)$$

Figure 2.7 shows response surfaces Warp yarn tension dependence on tension and radius of the cylinder were obtained subject to fixed value of the calculated contact angle of the cylinder. This value corresponded to the centre of the experiment (tables 2.1-3)

Adequacy of the obtained regressional dependences was verified using SPSS software application for statistical processing of experimental findings [21]. Analysis of significance of the coefficient of the regression equations (2.11)-(2.19) allowed to discard insignificant ones [3, 7, 21].
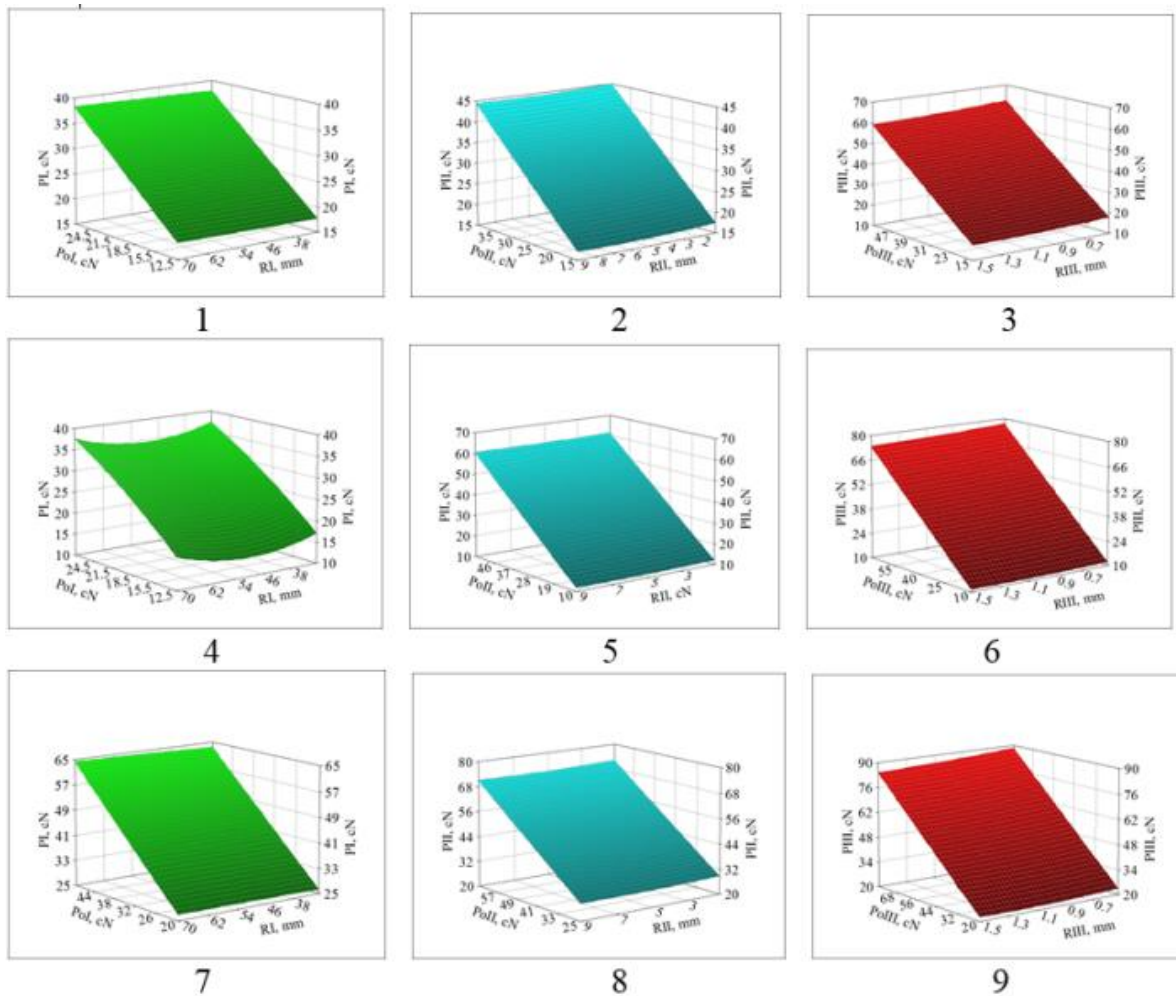
Figure 2.7 Curve based on warp yarn tension according to loom zones (■ - zone I, ■ - zone II, ■ - zone III) : 1, 2, 3 - for series A; 4, 5, 6 - for series B, 8, 9 - for series C

Obtained graphical dependences between warp yarn tension and cylinder radius are of interest, taking into account fixed value of the input tension and calculated contact angle of the cylinder. These values corresponded to the center of the experiment (tables 2.1-3) Having been analyzed, graphical dependences provided existing bending points. These points have the minimum warp yarns tension within I, II, and III areas. This allows to raise a question of geometric sizing of guiding and working components of a loom.
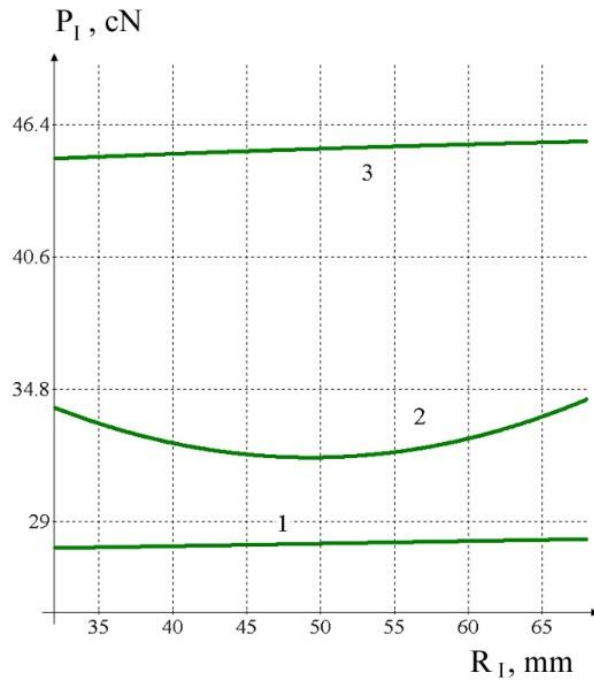
Figure 2.8 Dependence of the warp yarns tension after I area: 1 - for series A; 2 - for series B; 3 - for series C
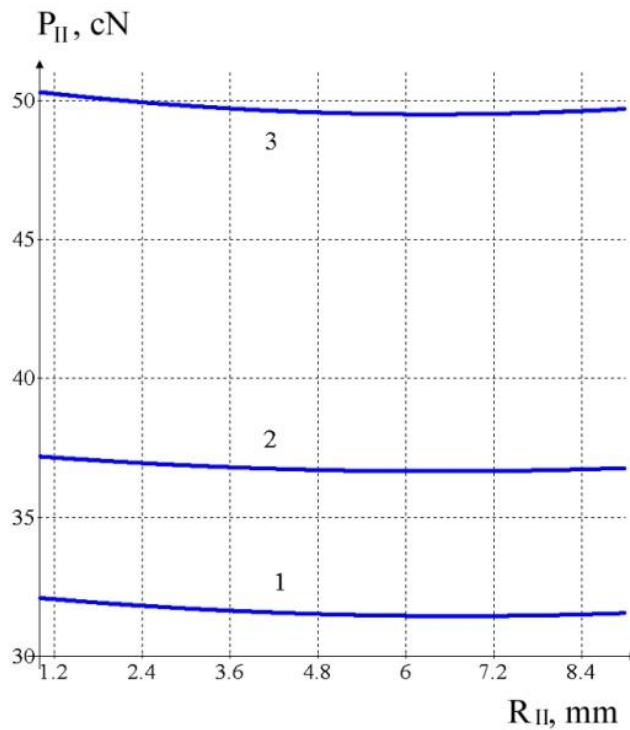
Figure 2.9 Dependence of the warp yarns tension after II area: 1 - for series A; 2 - for series B; 3 - for series C
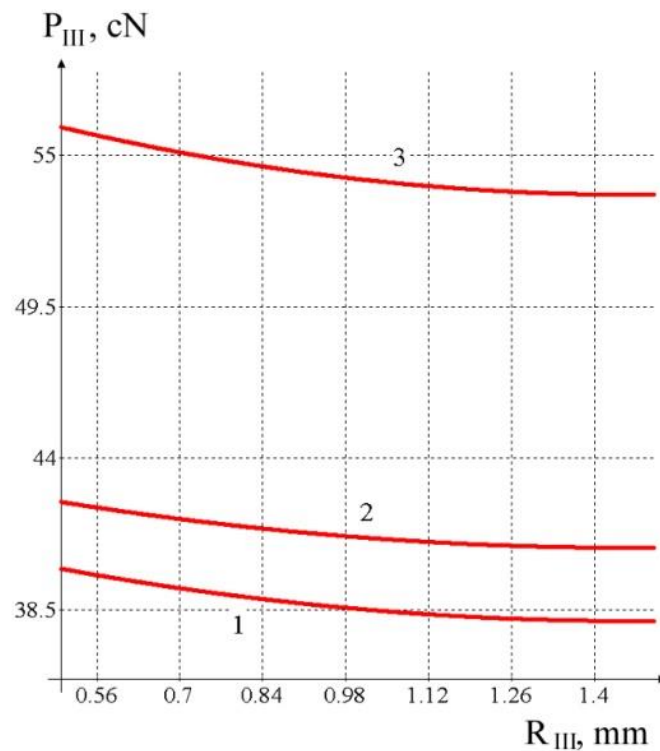
Figure 2.10 Dependence of the warp yarns tension after III area: 1 - for series A;
2 - for series B; 3 - for series C

Using regression dependences (2.11) - (2.19) we have found values of the warp yarn tension in the III area before fell of the cloth for different moments of the cloth components formation at the shuttleless looms. Values of the deflection of warp yarns, during shedding, battening and removal of cloth, was taken into account as a value of the input tension in I area.

Having been analyzed, graphical dependences (Figure 2.11) allowed to determine that the toughest formation conditions will be for series B during manufacture of sindon; abovementioned is based on bleached flax of wet spun 41 Tex. This can be explained by the high value of the rigidity coefficient of the strain and flexure of the warp yarns.

Obtained results can be applied for weaving development to determine the tension at a primary stage when forming fabric.
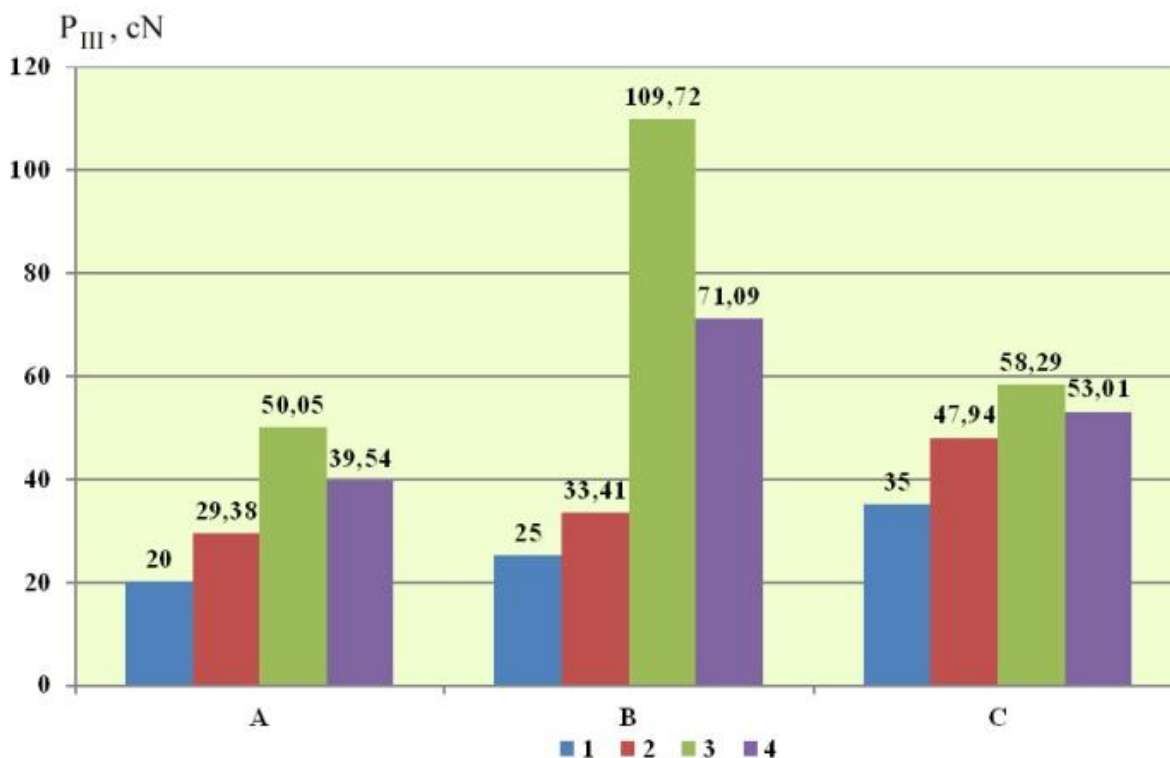
Figure 2.11 Warp yarns tension P_{III} histogram before fell when forming fabric:
A – tartan (warp - carded cotton yarn 18.5x2 Tex);   B – sindon (warp - bleached flax of wet spun 41 Tex); C – boston twill (warp - wool 31.2x2 Tex); ■ – threading tension of warp yarns; ■ – warp yarns tension working with closed shed; ■ – tension of warp yarns with fully opened shed; ■ – tension of warp yarns during battening

Resulting from conducted integral experimental research of the interaction process between warp yarns and cylinder guiding surfaces — the latter simulate guiding surfaces and working components of looms — we obtained regression dependences, that allow to determine changes in tension of the warp yarns in the areas from warp beam to the area of fabric formation. Dependences were obtained taking into account types of feedstock processed and construction of the specific looms. Obtained results may be used to optimize weaving process flow in terms of optimizing construction peculiarities, reducing number of yarn breaks, and improving quality of the manufactured fabrics.

3. YARN TENSION WHILE KNITTING TEXTILE FABRIC

Simulation of the yarn processing using a (loom) knitting machines involves study of interaction between yarns and surfaces in the form of torus. These surfaces are dummies for surface of yarn guides, the yarn break detectors, needles and push downs of the looms with two types of tackings: an umbrella tacking, which is placed above knitting area; a tacking which is placed on the floor [1- 8, 22]. When drafting the plan of the experiment, the direction connected to slip of rubbing surfaces [2, 10, 22], yarn tension prior to guide [1, 2, 4, 8], yarn thickness and type of feedstock [5, 8, 22] should be considered. Flexural rigidity of the multifilaments and spun yarn with slight twist can be ignored while processing on the looms [1, 3, 22]. The above restrictions required development of all-new scheme of the experimental setup, which is different from previously developed [22].

Figure 3.1 shows looms with tacking in different places. Figure 1a shows the loom DL–4M with umbrella tacking placed above the knitting area. The loom DL–4M is intended for knitting rib fabric to produce underwear and sportswear. Figure 1b shows the loom PaiLung with tacking placed on the floor. It is intended for knitting fabric with stockinette structure [8].
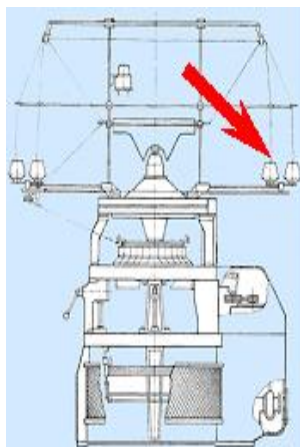
a   b

Figure 3.1 Looms: a - DL–4M; b - PaiLung

Figure 3.2 shows structural schemes of threading on the looms DL–4M and PaiLung. For the loom DL–4M (I – figure 2) threading line may be divided into 11 sections (Figure 3.2 shows in red): 1r – from bobbin to guiding yarn; 2r – from guiding yarn to break detector; 3r – from break detector to guiding yarn; 4r – from guiding yarn to guiding yarn; 5r – from guiding yarn to cylindrical tensioner; 6r – from cylindrical tensioner to break detector; 7r – from break detector to vertical thread storage in the form of cylinder; 8r – from vertical thread storage in the form of cylinder to break detector; 9r – from break detector to inlet of yarn thread guide; 10 (Figure 3.2 shows in brown) – from inlet of yarn thread guide to knitting area; 11 (Figure 3.2 shows in yellow) – from knitting area to formed textile fabric.
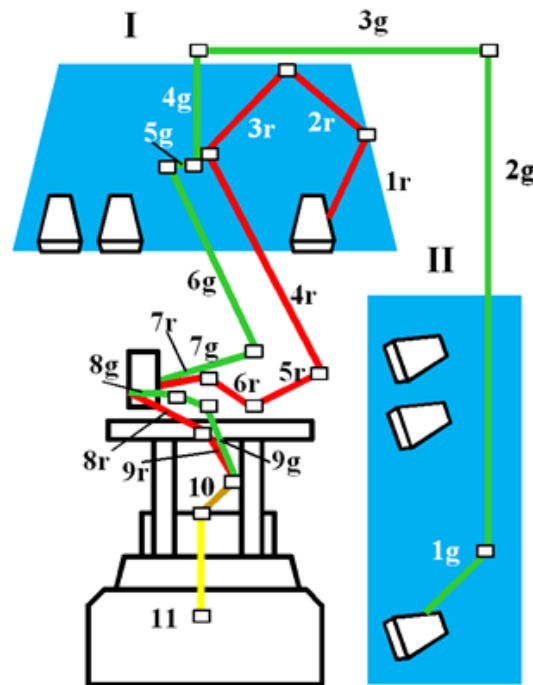
Figure 3.2 Structural scheme of threading on the looms DL–4M and PaiLung
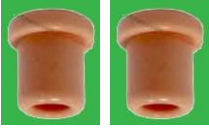
For the loom PaiLung (II – figure 3.2) threading line may be divided into 11 sections (Figure 3.2 shows in green): 1g – from bobbin to inlet of vertical cylindrical guide tube; 2g – from vertical cylindrical guide tube to rectangular connecting element; 3g – horizontal cylindrical guide tube between rectangular

connecting elements; 4g – from rectangular connecting element to yarn tensioner in the form of two washers; 5g – from tensioner in the form of two washers to guiding yarn; 6g – from guiding yarn to vertical yarn storage in the form of cylinder; 7g – from vertical yarn storage in the form of cylinder to guiding yarn; 8g – from guiding yarn to break detector; 9g – from break detector to inlet of yarn thread guide; 10 (figure 3.2 shows in brown) – from inlet of yarn thread guide to knitting area; 11 (figure 3.2 shows in yellow) – from knitting area to formed textile fabric.

Sections 10 and 11 for looms DL–4M and PaiLung are identical, that is why in figure 3.2 they are shown in one colour. Yarn tension in the sections 1r and 1g will be equal to tension of the yarn when going off the bobbin. Threading line has the form of spatial zigzag line. Table 3.1 shows elements of yarn supply system on the knitting machines DL–4M and PaiLung, which divide threading line into corresponding sections (figure 3.2).

Table 3.1 Elements of yarn supply system

No.	Umbrella tacking (loom DL-4M)		A tacking on the floor (loom PaiLung)	
	Area	Guide	Area	Guide
1	1r-2r		1g-2g	
2	2r-3r		2g-3g	
3	3r-4r		3g-4g	
4	4r-5r		4g-5g	

5	5r-6r		5g-6g	
6	6r-7r		6g-7g	
7	7r-8r		7g-8g	
8	8r-9r		8g-9g	
9	9r-10		9g-10	
10	10-11		10-11	

Analysis of the structural scheme of the threading line shows its very complicated geometrical configuration both in plane and in space. In threading line inflection point the yarn or spun yarn are contacting with guide eyes in form of torus, tension devices, and control devices.

Figure 3.3 shows yarn thread guides and working components of the looms with which the yarn or the spun yarn interacts during its entry into the area of knitting the textile fabric.

Curvature radius of these surfaces having the form of torus both significantly exceeds yarn cross-section radius and commensurable with it. Such type of interaction also occurs in implementation of similar technological processes [4, 6, 8, 22]. Figure 4 shows scheme of interaction between the yarn or spun yarn and cylindrical surface (figure 3.4a) and surface in the form of torus (figure 3.4b). Analysis shows that in the second case the forces of normal pressure in the section of the yarn, act not along a straight line, but along a

curved surface in the form of a torus. In this case, frictional forces do not obey the friction laws known [8, 22].
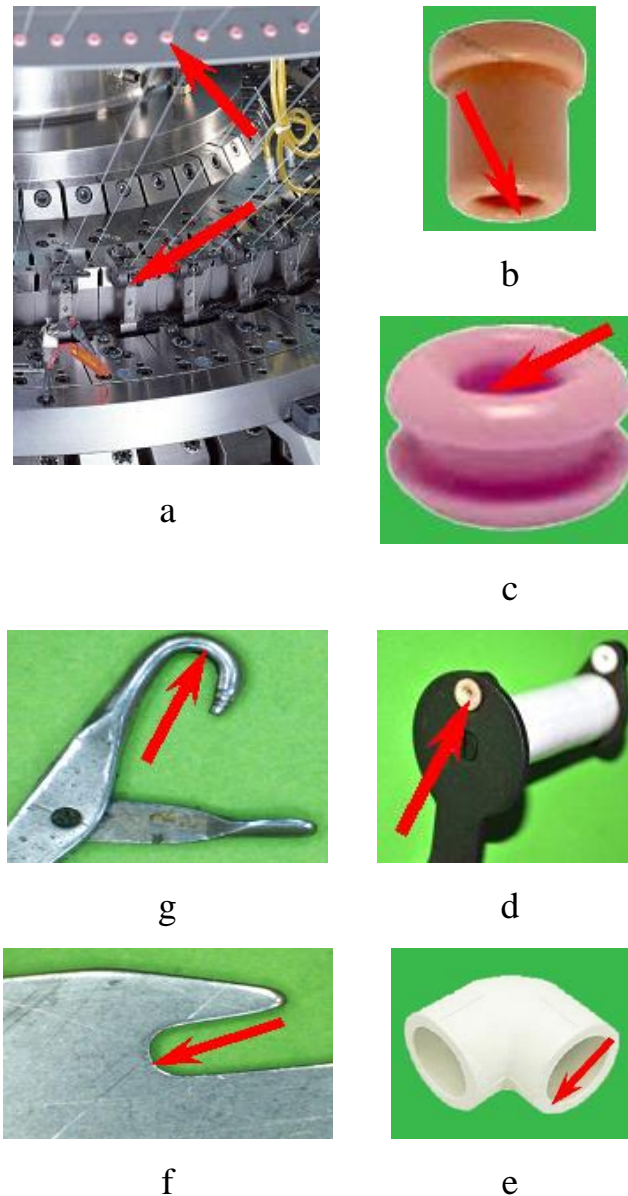
Figure 3.3 Structural elements in the form of torus of the threading system on the looms: a, c - yarn thread guides; b - components of break detectors; d - cylindrical yarn tensioner; e – rectangular connecting component; g – needles; f - push downs

For the experiment, five types of yarns and spun yarns were chosen. Series A: Cotton yarn 29 Tex Series B: wool 28 Tex. Series C: Flax 30 Tex. Series D: viscose yarn 29 Tex. Series E: Caprone multifilament 15.2x2 Tex.

The following yarn guides were chosen: I – ceramic yarn guide (figure 3.3c); II – ceramic yarn guide at input and output in break detector (figure 3.3b) and cylindrical yarn tensioner (figure 3.3d); III – rectangular connecting element (figure 3.3 e); IV – needles and push downs of the loom (figure 3.3g, 3f).
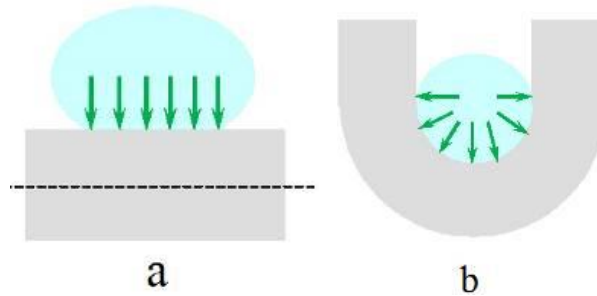
Figure 3.4 Scheme of interaction between the yarn and guiding surfaces: a – cylindrical; b - form of torus

For each structural element I-IV (figure 3.3) of the treading system on the loom, to determine joint influence of input tension of the yarn, radius of guide in the form of torus and calculated value of contact angle on output tension of yarn P, in our work we planned and implemented orthogonal design of the second order for three factors. Standard form of regression equation shall be as follows [8]

$$P = b_0 + b_1 x_1 + b_2 x_2 + b_3 x_3 + b_{12} x_1 x_2 + b_{13} x_1 x_3 + b_{23} x_2 x_3 + \\ + b_{11} x_1^2 + b_{22} x_2^2 + b_{33} x_3^2 \tag{3.1}$$

The range of factors variability in equation (3.1) is determined by real conditions of yarns and spun yarn processing on looms.

Factor x1 - value of yarn or spun yarn tension up to structural element I-IV of the threading system of the loom: for guide of the yarn I changed within the range from P0I = 3 cN to P0I =33 cN; for ceramic guide of the yarn II at the entry and output in the break detector and cylindrical tensioner of the yarn changed from P0II =4 cN to P0II =16 cN; for rectangular connecting element III changed from P0III =4 cN to P0III =10 cN; for needles and push downs IV of the loom changed from P0IV =5 cN to P0IV =11 cN. The range of tension change is

determined by position of the structural element I-IV in threading line on the loom (figure 3.2).

Factor x2 – curvature radius of the guide: for ceramic guide of the yarn I in the form of torus within the range from RI = 2 mm to RI = 4mm; for ceramic guide of the yarn II in the form of torus at the entry and output in the break detector and cylindrical tensioner of the yarn within the range from RII = 1 mm to RII = 3 mm; for rectangular connecting element III of the yarn within the range from RIII = 1 mm to RIII = 3 mm; for needles and push downs IV of the loom within the range from RIV = 2 mm to RIV = 4mm.

The value of radii was determined using digital microscope (USB Digital microscope Sigeta).

Factor x3 – calculated value of the contact angle: for ceramic guide I of the yarn in the form of torus within the range from φI = 190 to φI = 920; for ceramic guide of the yarn II in the form of torus at the input and output in the break detector and cylindrical yarn tensioner within the range from φII = 170 to φII = 900; for rectangular connecting element III of the yarn calculated value of contact angle remained unchanged φIII = 900 ; for needles and push downs IV of the loom within the range from φIV = 600 to φIV = 1800.

The value of the calculated contact angle is determined by the form of threading line and position of the structural element I-IV in the threading system. At the first stage tension after the structural element I is determined. Table 3.2 shows matrix of orthogonal design of the second order for ceramic yarn guide I.

Table 3.2

Matrix of orthogonal design of the second order for ceramic yarn guide I

No.	Factors					
	Input tension		Curvature radius		Contact angle	
	x_1	P_{0I} [cN]	x_2	R_I [mm]	x_3	φ_{IP} [°]
1	+1	30	+1	4	+1	85

2	-1	6	+1	4	+1	85
3	+1	30	-1	2	+1	85
4	-1	6	-1	2	+1	85
5	+1	30	+1	4	-1	25
6	-1	6	+1	4	-1	25
7	+1	30	-1	2	-1	25
8	-1	6	-1	2	-1	25
9	-1.215	3	0	3	0	55
10	+1.215	33	0	3	0	55
11	0	18	-1.215	1.8	0	55
12	0	18	+1.215	4.2	0	55
13	0	18	0	3	-1.215	19
14	0	18	0	3	+1.215	92
15	0	18	0	3	0	55

Connection between natural and encoded values for ceramic yarn guide I shall be as follows:

$$x1 = \frac{P_{0I} - 18}{12}, \quad x2 = \frac{R_I - 3}{1}, \quad x3 = \frac{\varphi_I - 55}{30}. \qquad (3.2)$$

At the second stage tension after the structural element II is determined. Table 3.3 shows matrix of orthogonal design of the second order for ceramic yarn guide II at the input and output: in the break detector and cylindrical tensioner.

Table 3.3

Matrix of orthogonal design of the second order for ceramic yarn guide II

No.	Factors					
	Input tension		Curvature radius		Contact angle	
	x_1	P_{0II} [cN]	x_2	R_{II} [mm]	x_3	$\varphi_{II\,P}$ [°]
1	+1	15	+1	3	+1	83

2	-1	5	+1	3	+1	83
3	+1	15	-1	1	+1	83
4	-1	5	-1	1	+1	83
5	+1	15	+1	3	-1	23
6	-1	5	+1	3	-1	23
7	+1	15	-1	1	-1	23
8	-1	5	-1	1	-1	23
9	-1.215	4	0	2	0	53
10	+1.215	16	0	2	0	53
11	0	10	-1.215	0.8	0	53
12	0	10	+1.215	3.2	0	53
13	0	10	0	2	-1.215	17
14	0	10	0	2	+1.215	90
15	0	10	0	2	0	53

Connection between natural and encoded values for ceramic yarn guide II shall be as follows:

$$x1 = \frac{P_{0II} - 10}{5}, \quad x2 = \frac{R_{II} - 2}{1}, \quad x3 = \frac{\varphi_{II} - 53}{30}. \tag{3.3}$$

At the third stage the tension after the structural element III is determined. Table 3.4 shows matrix of orthogonal design of the second order for rectangular connecting element III.

Table 3.4

Matrix of orthogonal design of the second order for rectangular connecting element III

No.	Input tension		Curvature radius	
	x_1	P_{0III} [cN]	x_2	R_{III} [mm]

1	+1	10	+1	20
2	-1	4	+1	20
3	+1	10	-1	10
4	-1	4	-1	10
5	-1	4	0	15
6	+1	10	0	15
7	0	7	-1	10
8	0	7	+1	20
9	0	7	0	15

Connection between natural and encoded values for rectangular connecting element III shall be as follows:

$$x1 = \frac{P_{0III} - 7}{3}, \quad x2 = \frac{R_{III} - 15}{5}. \tag{3.4}$$

At the fourth stage tension after the structural elements IV is determined. Table 3.5 shows matrix of orthogonal design of the second order for needles and push downs of the loom IV.

Table 3.5

Matrix of orthogonal design of the second order for needles and push downs of the loom IV

No.	Factors					
	Input tension		**Curvature radius**		**Contact angle**	
	x_1	P_{0I} [cN]	x_2	R_I [mm]	x_3	φ_{IP} [°]
1	+1	10	+1	0.9	+1	170
2	-1	6	+1	0.9	+1	170
3	+1	10	-1	0.5	+1	170
4	-1	6	-1	0.5	+1	170
5	+1	10	+1	0.9	-1	70

6	-1	6	+1	0.9	-1	70
7	+1	10	-1	0.5	-1	70
8	-1	6	-1	0.5	-1	70
9	-1.215	5.6	0	0.7	0	120
10	+1.215	10.4	0	0.7	0	120
11	0	8	-1.215	0.45	0	120
12	0	8	+1.215	0.94	0	120
13	0	8	0	0.7	-1.215	60
14	0	8	0	0.7	+1.215	180
15	0	8	0	0.7	0	120

Connection between natural and encoded values for needles and push downs of the loom IV shall be as follows:

$$x1 = \frac{P_{0IV} - 8}{2}, \quad x2 = \frac{R_{IV} - 0.7}{0.2}, \quad x3 = \frac{\varphi_{IV} - 120}{50}. \tag{3.5}$$

Figure 3.5 shows the scheme of experimental setup. Its assembly detailed in the work [22]. Distinctive feature is that unit 4 of the simulated conditions of interaction with surface in the form of torus included such structural elements as I – IV of the threading system of the loom (figure 3.3)
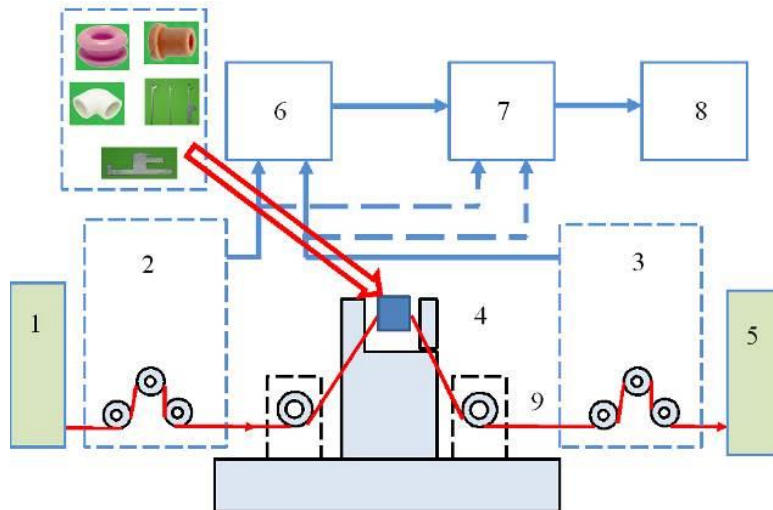
Figure 3.5 Scheme of the experimental setup: 1 – yarn threading unit; 2 – metering unit for yarn input tension; 3 – metering unit for yarn output tension; 4

– environment modelling unit for surface in the form of torus; 5 – yarn take up unit; 6 – amplifier; 7 – analogue to digital converter ADC; 8 – personal computer; 9 – yarn

The value of radii was determined using digital microscope (USB Digital microscope Sigeta) (figure 3.6).

Figure 3.6 Setup for determining geometric dimensions of the structural elements I – IV of the threading system of the loom

As a result of implementation of orthogonal design of the second order for three factors (tables 3.2-5) for each of the series A, B, C, D, E (for five types of natural, synthetic and artificial spun yarn and yarns) for four types I, II, III and IV of yarns and spun yarn guides, 10 concurrent metering were conducted. Their average values represented in the tables 3.6-10.

Table 3.6

Tension values – series A: cotton spun yarn 29 Tex

Expe rime nt No.	Tension of natural spun yarn, cN			
	Series A (Cotton spun yarn 29 Tex)			
	I	II	III	IV

1	44.82	22.31	14.78	33.05
2	8.79	7.31	5.93	18.28
3	48.79	27.36	14.79	51.98
4	9.07	8.13	5.93	25.67
5	34.62	17.22	5.93	18.77
6	6.79	5.15	14.78	10.53
7	37.18	20.51	10.36	27.48
8	6.99	6.21	10.36	14.01
9	3.87	5.22	10.36	14.18
10	44.47	21.75		30.05
11	25.22	16.23		30.83
12	23.38	12.93		18.92
13	20.38	11.41		15.32
14	27.96	15.69		30.74
15	23.82	13.35		21.72

Table 3.7

Tension values – series B: wool 28 Tex

Expe riment nt No.	Tension of natural spun yarn, cN			
	Series B (Wool 28 Tex)			
	I	II	III	IV
1	41.51	20.70	13.85	26.96
2	8.21	6.83	5.57	15.19
3	44.29	24.26	13.83	38.88
4	8.41	7.41	5.55	19.95
5	33.68	16.77	5.56	16.87
6	6.64	5.52	13.83	9.59

7	35.62	19.26	9.69	23.09
8	6.79	5.96	9.71	12.12
9	3.7	4.97	9.70	12.13
10	41.95	20.49		25.02
11	23.61	14.74		24.39
12	22.26	12.33		16.38
13	19.91	11.13		13.71
14	25.71	14.41		24.39
15	22.59	12.64		18.31

Table 3.8

Tension values – series C: flax spun yarn 30 Tex

Experiment No.	Tension of natural spun yarn, cN			
	Series C (Flax spun yarn 30 Tex)			
	I	II	III	IV
1	43.23	21.53	14.32	29.77
2	8.51	7.08	5.75	16.65
3	46.48	25.64	14.33	44.25
4	8.74	7.75	5.74	22.38
5	34.13	16.98	5.74	17.68
6	6.71	5.58	14.32	10.01
7	36.29	19.73	10.04	24.71
8	6.89	6.06	10.04	12.85
9	3.79	5.09	10.03	13.04
10	43.20	21.09		27.17
11	24.37	15.36		26.93
12	22.84	12.63		17.55

13	20.12	11.25		14.35
14	26.87	15.05		27.24
15	23.21	12.99		19.79

Table 3.9

Tension values – series D: viscose yarn 29 Tex

Expe rime nt No.	Tension of natural spun yarn, cN			
	Series D (Viscose yarn 29 Tex)			
	I	II	III	IV
1	41.82	20.83	14.04	25.79
2	8.31	6.89	5.64	14.83
3	43.75	23.27	14.02	33.38
4	8.44	7.31	5.63	17.97
5	33.57	16.70	5.63	16.03
6	6.65	5.52	14.03	9.27
7	34.95	18.44	9.83	19.97
8	6.76	5.83	9.84	10.97
9	3.72	4.98	9.84	11.23
10	41.79	20.34		22.99
11	23.32	14.04		20.92
12	22.37	12.37		15.81
13	19.79	11.02		12.79
14	25.89	14.44		22.85
15	22.59	12.59		17.09

Table 3.10

Tension values – series B: caprone multifilament 15.2x2 Tex

Expe riment No.	Tension of natural spun yarn, cN			
	Series E (Caprone multifilament 15.2x2 Tex)			
	I	II	III	IV
1	47.18	23.45	15.37	38.67
2	9.17	7.63	6.15	20.95
3	52.45	30.17	15.42	66.83
4	9.54	8.71	6.16	31.67
5	35.31	17.55	6.15	20.53
6	6.89	5.73	15.38	11.35
7	38.53	21.71	10.79	32.36
8	7.14	6.43	10.76	15.97
9	3.98	5.39	10.77	16.05
10	46.38	22.73		35.05
11	26.51	17.63		38.03
12	24.14	13.34		21.15
13	20.75	11.63		16.88
14	29.57	16.63		36.93
15	24.71	13.88		24.99

Applying well-known methods to determine coefficient in the regression equation (3.1) for orthogonal design of the second order [22], considering dependences (3.2-3.10), the following regression dependences are obtained:

Series A (Cotton yarn 29 Tex):

for yarn guide I

$$P_{IA} = 1.22P_{0I} - 0.86R_I - 0.01\varphi_I + 0.33R_I^2 - 0.06P_{0I}R_I + 0.006P_{0I}\varphi_I - 0.98, \qquad (3.6)$$

for yarn guide II

$$P_{IIA} = 1.42P_{0II} + 0.51R_{II} - 0.01\varphi_{II} - 0.17P_{0II}R_{II} + 0.01P_{0II}\varphi_{II} - 1.65,$$ (3.7)

for yarn guide III

$$P_{IIIA} = 0.31 + 1.44P_{0III},$$ (3.8)

for yarn guide IV

$$P_{IVA} = 4.44P_{0IV} - 32.07R_{IV} + 0.07\varphi_{IV} + 50.99R_{IV}^2 - 5.24P_{0IV}R_{IV} + $$
$$+ 0.02P_{0IV}\varphi_{IV} - 0.18R_{IV}\varphi_{IV} - 3.68.$$ (3.9)

Series B (wool 28 Tex):

for yarn guide I

$$P_{IB} = 0.59P_{0I} + 0.04R_I + 0.01\varphi_I - 0.05P_{0I}R_I + 0.002P_{0I}\varphi_I + 2.39$$ (3.10)

for yarn guide II

$$P_{IIB} = 1.31P_{0II} + 0.36R_{II} - 0.004\varphi_{II} - 0.13P_{0II}R_{II} + 0.01P_{0II}\varphi_{II} - 0.81$$ (3.11)

for yarn guide III

$$P_{IIIB} = 0.29 + 1.34P_{0III}$$ (3.12)

for yarn guide IV

$$P_{IVB} = 3.4P_{0IV} - 22.92R_{IV} + 0.04\varphi_{IV} + 33R_{IV}^2 - 3.4P_{0IV}R_{IV} + $$
$$+ 0.02P_{0IV}\varphi_{IV} - 0.09R_{IV}\varphi_{IV} - 1.33$$ (3.13)

Series C (Flax 30 Tex):

for yarn guide I

$$P_{IC} = 1.03P_{0I} - 0.69R_I - 0.01\varphi_I + 0.005P_{0I}\varphi_I + 1.66$$ (3.14)

for yarn guide II

$$P_{IIC} = 1.34P_{0II} + 0.4R_{II} - 0.006\varphi_{II} - 0.14P_{0II}R_{II} + 0.01P_{0II}\varphi_{II} - 1.29$$ (3.15)

for yarn guide III

$$P_{IIIC} = 0.28 + 1.39P_{0III}$$ (3.16)

for yarn guide IV

$$P_{IVC} = 3.73P_{0IV} - 25.72R_{IV} + 0.05\varphi_{IV} + 39.25R_{IV}^2 - 4.05P_{0IV}R_{IV} + $$
$$+ 0.02P_{0IV}\varphi_{IV} - 0.13R_{IV}\varphi_{IV} - 2.38$$ (3.17)

Series D (Viscose yarn 29 Tex):

for yarn guide I

$$P_{ID} = 1.01P_{0I} - 0.003\varphi_I + 0.005P_{0I}\varphi_I - 0.22 \tag{3.18}$$

for yarn guide II

$$P_{IID} = 1.03P_{0II} - 0.62R_{II} - 0.003\varphi_{II} + 0.005P_{0II}\varphi_{II} + 1.01 \tag{3.19}$$

for yarn guide III

$$P_{IIID} = 0.29 + 1.36P_{0III} \tag{3.20}$$

for yarn guide IV

$$P_{IVD} = 2.4P_{0IV} + 6.65R_{IV} - 0.02\varphi_{IV} - 2.1P_{0IV}R_{IV} + 0.01P_{0IV}\varphi_{IV} - 5.45 \tag{3.21}$$

Series E (Caprone multifilament 15.2x2 Tex):

for yarn guide I

$$P_{IE} = 1.28P_{0I} + 0.39R_I - 0.009\varphi_I - 0.08P_{0I}R_I + 0.01P_{0I}\varphi_I - 1.92 \tag{3.22}$$

for yarn guide II

$$P_{IIE} = 1.54P_{0II} + 0.67R_{II} - 0.01\varphi_{II} - 0.23P_{0II}R_{II} + 0.01P_{0II}\varphi_{II} - 2.23 \tag{3.23}$$

for yarn guide III

$$P_{IIIE} = 0.29 + 1.49P_{0III} \tag{3.24}$$

for yarn guide IV

$$P_{IVE} = 5.84P_{0IV} - 43.85R_{IV} + 0.11\varphi_{IV} + 75R_{IV}^2 - 7.7P_{0IV}R_{IV} + \\ + 0.03P_{0IV}\varphi_{IV} - 0.28R_{IV}\varphi_{IV} - 6.92 \tag{3.25}$$

Figures 3.7-3.11 show response surfaces of the regression dependences (3.6) - (3.25). Tension dependencies after the yarn guide from input tension and curvature radius of the surface guide in the form of torus were constructed at a fixed value of the calculated contact angle of the cylinder. This value corresponded to the centre of the experiment (tables 3.1-3.4).

Adequacy of the obtained regression dependences was verified using SPSS software application for statistical processing of experimental findings [22]. Analysis of significance of the coefficient of the regression equations (3.6) - (3.25) allowed to discard insignificant ones [8, 21, 22].
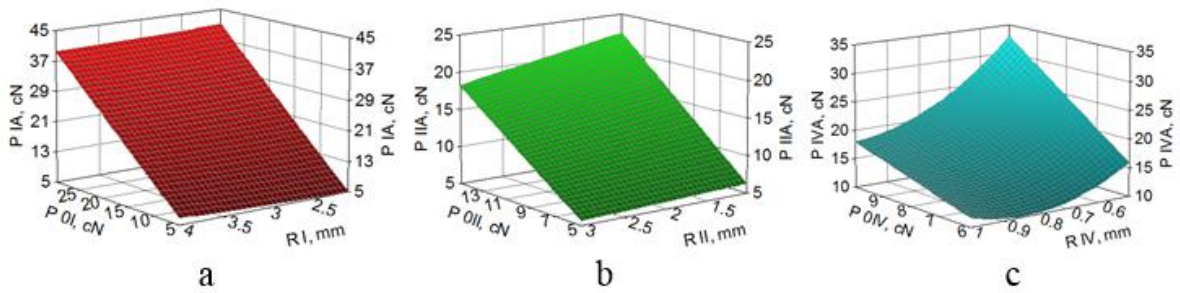
Figure 3.7 Response surfaces of the series A: a - for yarn guide I; b - for yarn guide II; c - for yarn guide IV
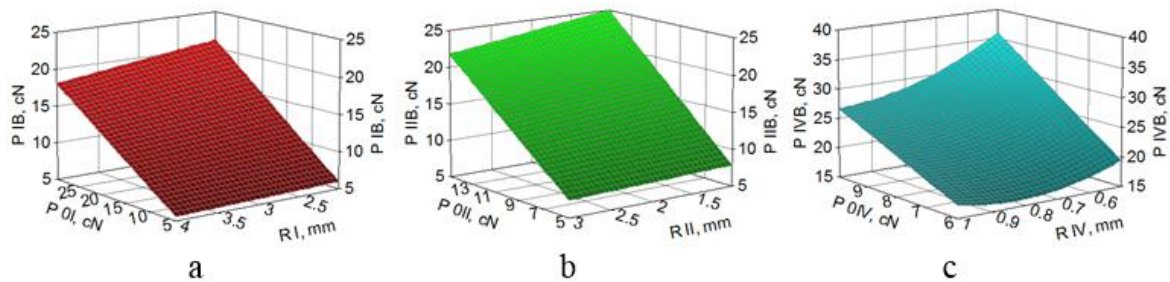
Figure 3.8 Response surfaces of the series B: a - for yarn guide I; b - for yarn guide II; c - for yarn guide IV
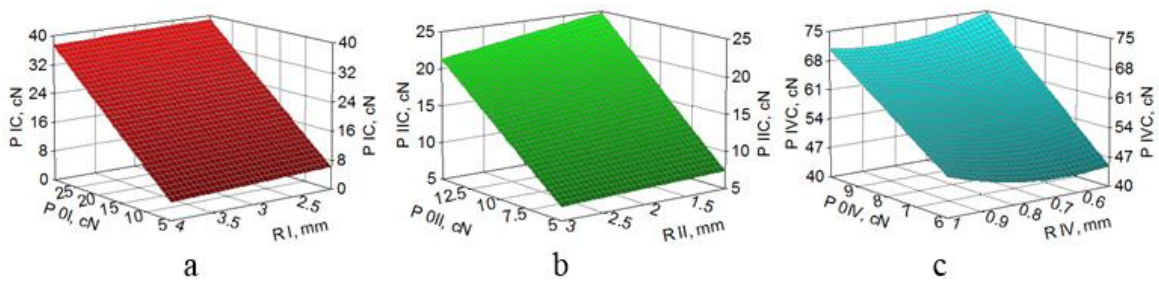
Figure 3.9 Response surfaces of the series C: a - for yarn guide I; b - for yarn guide II; c - for yarn guide IV
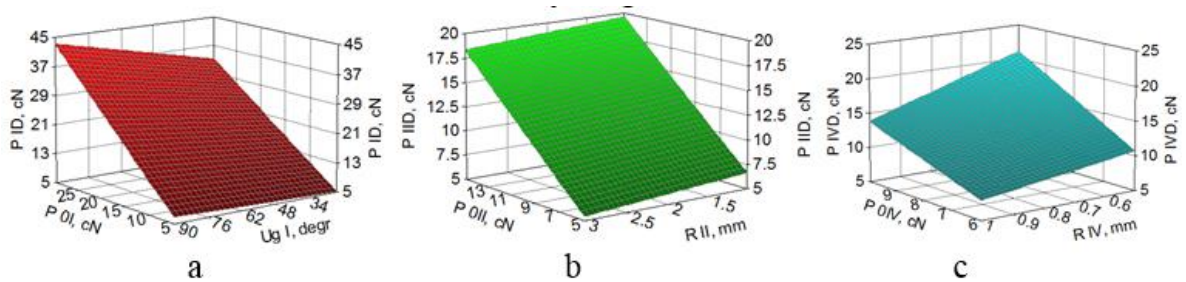
Figure 3.10 Response surfaces of the series D: a - for yarn guide I; b - for yarn guide II; c - for yarn guide IV

51
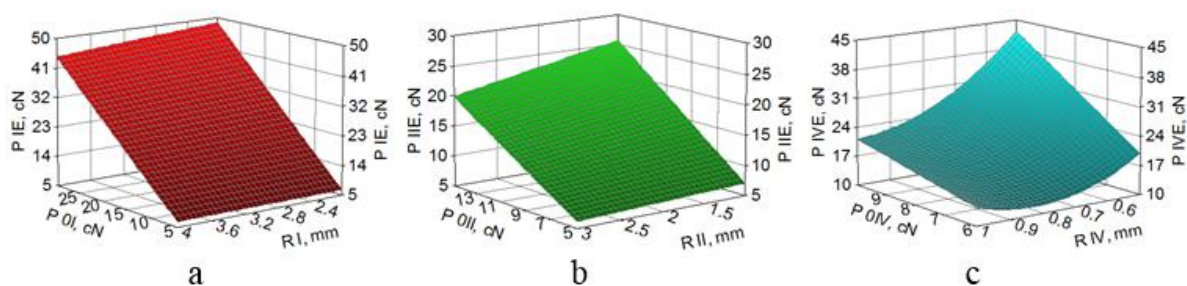
Figure 3.11 Response surfaces of the series E: a - for yarn guide I; b - for yarn guide II; c - for yarn guide IV

Using regression dependencies (3.6) - (3.25) the values of yarn and spun yarn tension were determined in the knitting area on the looms DL–4M и PaiLung. The value of the yarn and spun yarn tension when going off the bobbin was considered constant and such as not depending on its diameter.

Having been analysed, graphical dependences (Figure 3.12) allowed to determine that yarn tension is increasing from area to area an reaches its maximum before the mechanism of active yarn supply: area 6r-7r for loom DL–4M; area 5g-6g for loom PaiLung. After the mechanism of active supply the yarn will have the minimum tension. Its tension will gradually increase before knitting area at the expense of its interaction with structural elements I-IV. It should be noted that, loom PaiLung will have for different yarns nad spun yarns (series A-E), the tension varied within 14-24 cN.

Received results may be used to optimize technological process of knitting of the textile fabric, when yet at the initial stage the intensity of the yarn and spun yarn processing on the looms may be determined.
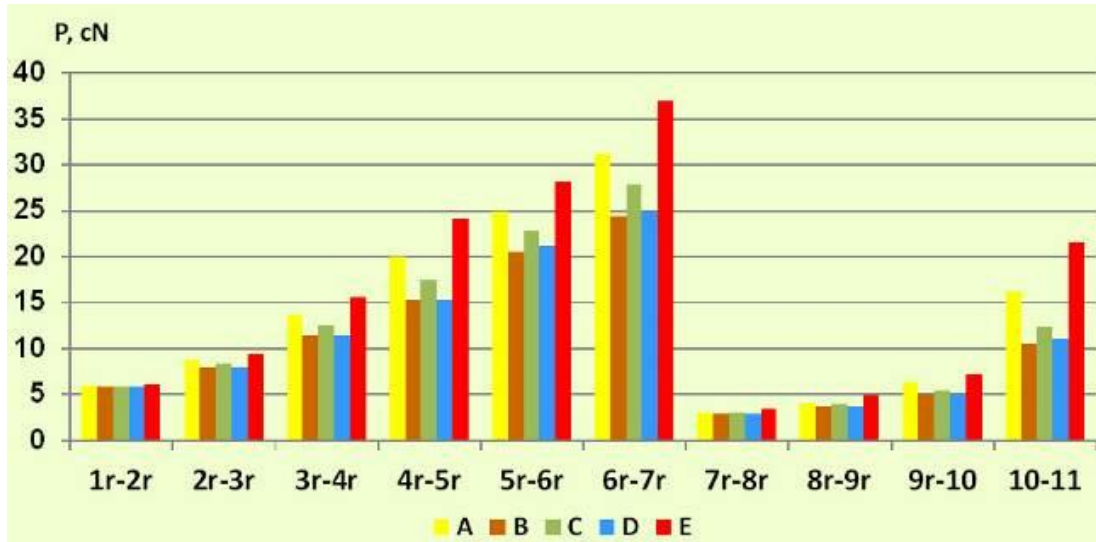
a
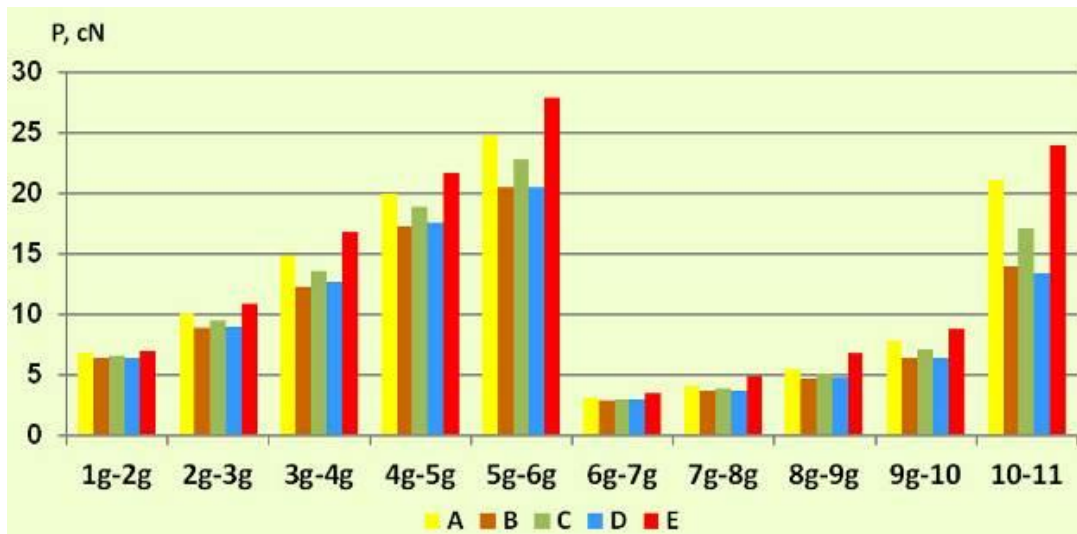
b

Figure 3.12 Yarns tension change histogram according to areas of yarn threading: a – loom DL–4M; b – loom PaiLung; ▪ – Series A(cotton spun yarn 29 Tex); ▪ – Series B(wool 28 Tex); ▪ – Series C(flax 30 Tex); ▪ – Series D(viscose spun yarn29 Tex); ▪ – Series E(caprone multifilament 15.2x2 Tex)

Resulting from conducted comprehensive experimental research of the process of interaction between yarns and surfaces in the form of torus, simulating surfaces of the yarn guides, elements of break detector devices, needles and push downs of looms, the regression dependencies were obtained. These dependencies

53

allow to determine changes in yarn tension from the bobbin to the area of textile fabric knitting. Dependencies were obtained considering types of feedstock processed and constructions of the specific looms. Obtained results may be used to optimize technological process of knitting in terms of optimizing of geometrical form of yarn threading line on the loom, decreasing breaks, and increasing quality of the produced textile fabrics.

4. IMPROVEMENT OF STRUCTURE AND TECHNOLOGY OF MANUFACTURE OF MULTILAYER TECHNICAL FABRIC

At present during construction and operational commissioning of main oil and gas lines pipes with external factory polyethylene coating are used (figure 1a). Factory insulation of pipes is the reliable protection against corrosion. Polymer coating prevents from rust formation and early wear of steel utilities. Corrosion protection is applied to steel pipelines, which are laid under ground or in high humidity. Constant contact with wet ground, air and water may led to rapid damage of metalware. Polymeric factory insulation protects metal against contact with aggressive external environments, and by several times extends the service life of pipelines. Comparing to field coating of pipelines with insulation material introduction of factory insulation of pipes technology allowed for both getting a boost of pipes construction and significantly improve efficiency of its anticorrosive protection. In both, the first and the second, cases for backing up and laying pipes with external factory insulation coating the chains and cords cannot be used [23]. Extreme pressure in the contact area leads to damage of insulation coating, inducing metal corrosion where sections when damaged insulation contacts with water and soil.

Woven power grips (figure 1b) are used for laying pipes with factory insulation coating. These grips are manufactured of multilayer technical fabrics [8,16, 23]. Structure of multilayer technical fabrics and conditions of its

formation on a weaving machine determine effectiveness of the woven power
grips manufacturing process [1, 4, 23, 24].

a

b

Figure 4.1 Components and way of laying oil and gas pipelines: a – pipes with
external factory insulation coating b – woven power grips

Design of woven power grips represented on the figure 4.2.
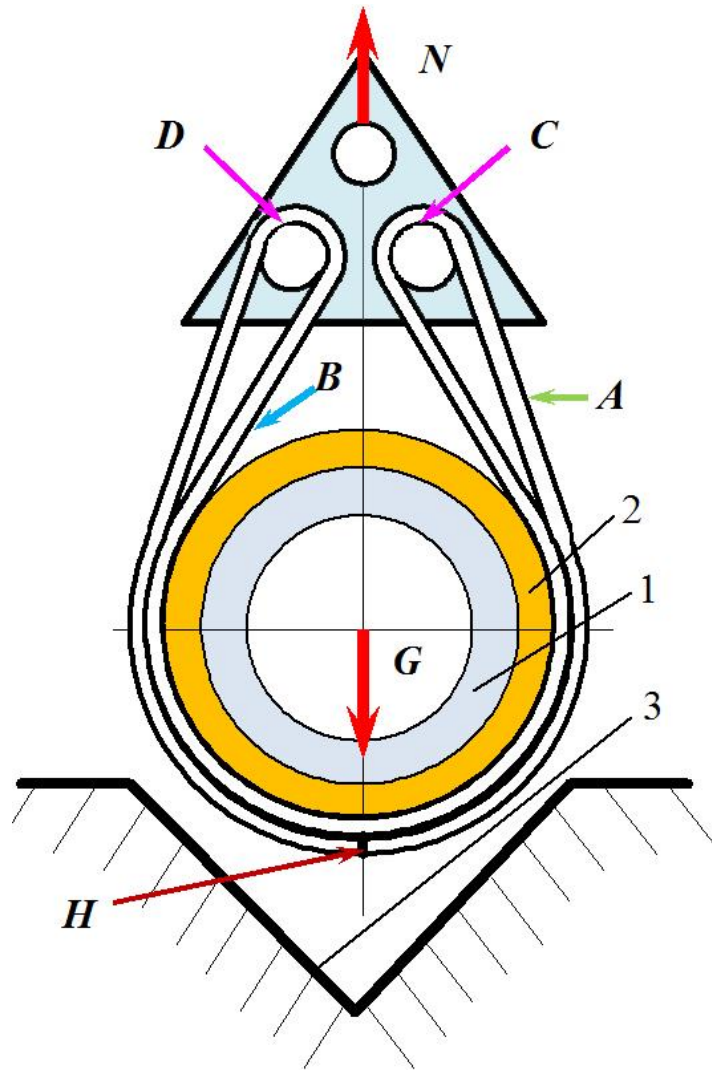
Figure 4.2 Design of woven power grip: 1 – pipe; 2 – insulation coating; 3 –
ground surface; A – surface of the woven power grip, which is in contact with
ground; B - surface of the woven power grip, which is in contact with insulation
coating; C, D - surface of the woven power grip, which is in contact with rollers
of the lifting machine; H – area of edge-joint of multilayer technical fabric; G –
gravitation force of the pipe; N – lifting force

Woven power grip represents locked loop from 20cm multilayer
technical fabric, ends of which are joined in the H area. Surface of grip A
contacts with ground surface. Surface of grip B contacts with insulation coating
of the pipe. In the areas C and D the grip contacts with rollers of the lifting
machine. These four areas provide for maximum wear of the surface of

multilayer technical fabric. Process of friction between the surface of the woven power grip and indicated areas is of great importance [8, 22, 23]. Should gravitation force of the pipe G increase, width of the grip may be extended by means of adding another strip of 20cm multilayer technical fabric (figure 4.1b).

Multilayer technical fabric MTF – 1 (figure 4.3a) was used for woven power grip. This fabric consists of 5 layers. Figure 4.3b shows cross-section of fabric along wrap yarns. Wrap yarns of external protective layers (PL) are shown in red colour, wrap yarns of force layers (FL) are shown in blue colour. Wrap yarns for binding external protective layers and force layers (BIN) are shown in green colour. Main element of woven power grip is wrap yarns of the force layers (FL). External protective layers are meant for protection of the force layers (figure 4.3c). For fabric MTF – 1(width 20cm) 816 hard-twisted caprone multifilaments 29 Tex S110x2 S300 Z 180 were used as wrap yarns of external protective layers (PL) [4]. 544 caprone multifilaments 93.5 Tex S 30 Z 60 were used as wrap yarns of force layers (FL). 136 caprone multifilaments 29 Tex S110x2 S300 Z 180 were used as wrap yarns for binding of external protective layers and force layers (BIN).

a

b

c

d
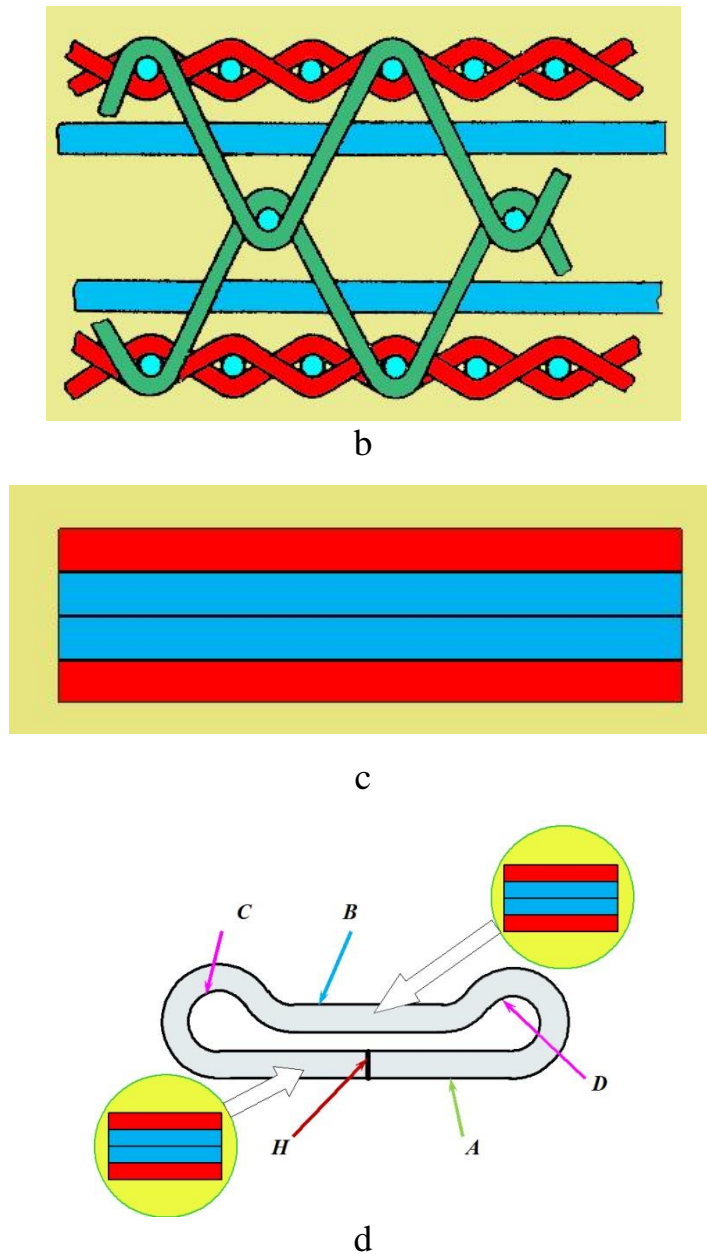
Figure 4.3 Multilayer technical fabric MTF – 1: a – general view; b – cross-section of fabric along wrap yarns; c – conventional design of cross-section of fabric along wrap yarns represented as layers; d - woven power grip represented as locked loop from multilayer technical fabric MTF – 1

Figure 4.4a shows elastic system of wrap yarns threading while manufacturing of multilayer technical fabric MTF – 1. Automatic weaving machine with center-shed dobby for 8 heddle frames was used to manufacture the fabric. Wrap yarns are arranged on three beams. It significantly aggravates servicing of the weaving machine [8, 24]. Different contraction of wrap yarns

(figure 4.3b) involves creation of different input tension for each type of wrap yarns [1,4-6, 23].
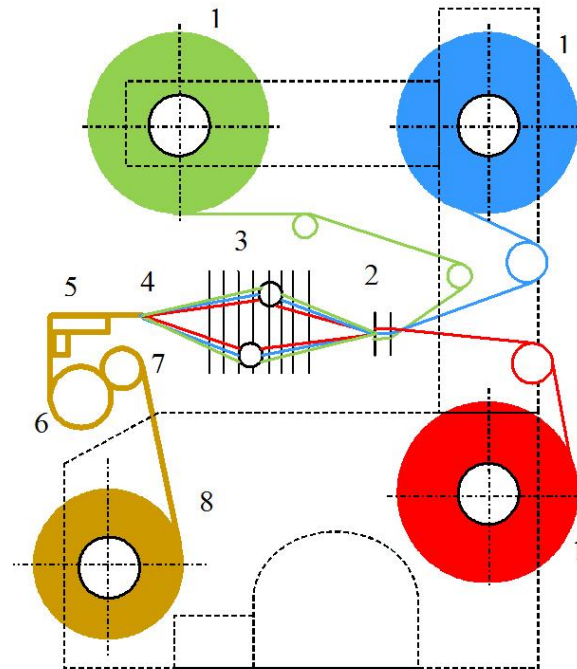
a
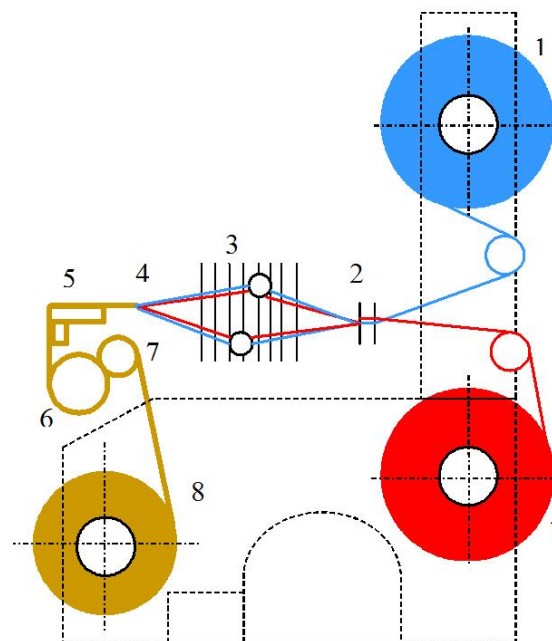
b

Figure 4.4 Elastic system of threading for wrap yarns on weaving machines:

a – during manufacture of multilayer technical fabric MTF – 1 ; b – during manufacture of multilayer technical fabric MTF – 9 ; 1 – weaver beam; 2 – wrap

yarn break detector; 3 – heddle frames of shed development mechanism; 4 – area of multilayer technical fabric formation; 5 – breast beam; 6 – roller; 7 – roller for fabric pressing; 8 – shaft for winding of fabric; ■ – wrap yarns for binding external protective layers and force layers (BIN); ■ – wrap yarns of force layers (FL); ■ – wrap yarns of protective layers (PL); ■ – multilayer technical fabric

Analysis of woven power grip as locked loop from multilayer technical fabric MTF – 1 (figure 4.3d) shows that top protective layer is inside the loop and does not protect force layers. It is formed of hard-twisted caprone multifilaments, which are significantly more expensive in manufacturing comparing to manufacture of wrap yarns of the force layers. This layer is virtually extra one in the structure of the multilayer technical fabric. This condition should be considered while improving the structure of the multilayer technical fabric.

Four plans of experimental researches were implemented to determine the influence of the structure of the multilayer technical fabric for power grips on conditions of its formation on the weaving machine [2,5, 6, 8-23]. Two multilayer technical fabrics MTF – 1 and MTF – 9 were chosen for experiment.

Tables 4.1 and 4.3 represent matrixes of the experimental researches that were carried out to determine influence of the input tension of wrap yarns of the protective layers on beat-up force value for multilayer technical fabric MTF – 1 and MTF – 9. Position of the backrest over the middle level and value of spade corresponded to the center of the experiment that was carried out to determine joint influence of the spade and different tension of shed on the beat-up force value. For multilayer technical fabric MTF – 1 the input tension of wrap yarns of the protective layers changed within the limits from 164.7 cN to 223.4 cN. For multilayer technical fabric MTF – 9 the input tension of wrap yarns of the protective layers changed within the limits from 125.8 cN to 175.4 cN.

Tables 4.2 and 4.4 show matrixes of orthogonal design of the second order for two factors that determine joint influence of spade and different tension of shed on the beat-up force value for multilayer technical fabric MTF – 1 and MTF – 9. Increase or decrease of the said parameters lead to change of contact angles between wrap yarns and guides and conditions of relative movement of the filling yarn towards wrap yarns in the multilayer fabric formation area. [2, 8, 14, 23].

Table 4.1

Matrix of the plan that determines influence of the input tension of the wrap yarns of the protective layers on the beat-up force value for multilayer technical fabric MTF – 1

№	Position of the backrest over the middle level		Value of spade		Input tension of the wrap yarns of the protective layers
	x_1	h [mm]	x_2	φ_Z [degrees]	P_S [cN]
I-1	0	0	0	45	192.2
I-2	0	0	0	45	164.7
I-3	0	0	0	45	178.3
I-4	0	0	0	45	208.3
I-5	0	0	0	45	223.4

For multilayer technical fabric MTF – 1 Value of spade changed within limits from 35 to 55 degrees. This value of spade is explained by the formation of external protective layers of this fabric with plain weave (figure 4.3b). Different tension of shed was created by means of vertical displacement of the top point of backrest in reference to middle position. This value was changing within limits from 10 to -10 mm. Minus indicates that backrest descended below middle position. For multilayer technical fabric MTF – 9 Value of spade changed within limits from 6 to 22 degrees. This value of spade allows to realize normal

formation of external protective layer. Different tension of shed was changing within limits from 10 to -10 mm.

Table 4.2

Matrix of orthogonal design of the second order for two factors that determine joint influence of spade and different tension of shed on beat-up force value for multilayer technical fabric MTF – 1

№.	Position of the backrest over the middle level		Value of spade	
	x_1	h [mm]	x_2	φ_Z [degrees]
I-6	-1	-10	-1	35
I-7	-1	-10	+1	55
I-8	+1	10	-1	35
I-9	+1	10	+1	55
I-10	0	0	-1	35
I-11	0	0	+1	55
I-12	-1	-10	0	45
I-13	+1	10	0	45
I-14	0	0	0	45

Connection between denominated and coded values for multilayer technical fabric MTF – 1 shall be as follows:

$$x1 = \frac{h}{10}, \quad x2 = \frac{\varphi_Z - 45}{10}, \tag{4.1}$$

for multilayer technical fabric MTF – 9 shall be as follows:

$$x1 = \frac{h}{10}, \quad x2 = \frac{\varphi_Z - 14}{8}. \tag{4.2}$$

Table 4.3

Matrix of the plan that determines the influence of the input tension of wrap yarns of protective layers on the beat-up force value for multilayer technical fabric MTF – 9

№.	Position of the backrest over the middle level		Value of spade		Input tension of the wrap yarns of the protective layers
	x_1	h [mm]	x_2	φ_Z [degrees]	P_S [cN]
II-1	0	0	0	14	150.6
II-2	0	0	0	14	125.8
II-3	0	0	0	14	143.2
II-4	0	0	0	14	162.0
II-5	0	0	0	14	175.4

Experimental setup for determining technological efforts during formation of multilayer technical fabrics is described in the work in reasonable details [1, 2, 8, 24]. It included eight-channel amplifier 8АНЧ-7М, oscillograph H-700, power modules for them. Separate measuring tensometric units were intended to determine tension of wrap yarns, beat-up force, and tension of fabric. Time records after 0.2 seconds were recorded by the oscillograph H-700 itself. Figure 4.5 shows an example of oscillogram. 3 repetitive oscillograms were done for each series. Calibration charts were obtained for each measuring tensometric unit for determining tension of wrap yarns, beat-up force, and tension of fabric. These charts were used for interpretation of oscillograms.
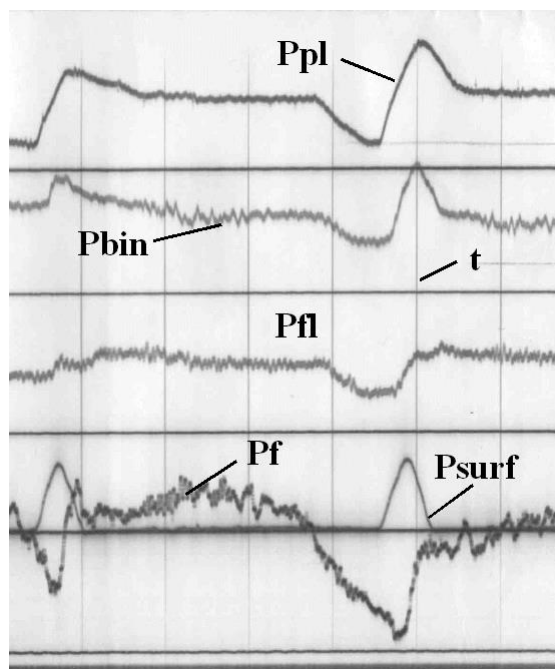
Figure 4.5 example of oscillography record of technological efforts during formation of multilayer technical fabrics: PSURF – beat-up force; PPL – tension of the wrap yarns of the external protective layers (PL); PBIN – tension of wrap yarns for binding of external protective and force layers (BIN); PFL – tension of wrap yarns of the force layers (FL); PF – tension of fabric; t – time

Table 4.4

Matrix of orthogonal design of the second order for two factors that determine joint influence of spade and different tension of shed on beat-up force value for multilayer technical fabric MTF – 1

№.	Position of the backrest over the middle level		Value of spade	
	x_1	h [mm]	x_2	φ_Z [degrees]
II-6	-1	-10	-1	6
II-7	-1	-10	+1	22
II-8	+1	10	-1	6
II-9	+1	10	+1	22

II-10	0	0	-1	6
II-11	0	0	+1	22
II-12	-1	-10	0	14
II-13	+1	10	0	14
II-14	0	0	0	14

The work contains a series of experimental researches that determines influence of the structure of the multilayer technical fabric and conditions of its manufacturing on the weaving machine on the breaking load value of 20cm strip. Taking into account that breaking load of 20cm strip of fabric is 100-160 kN, conventional tensile-testing machines used in materials science and engineering cannot be used for experiment [1, 8, 23]. This series of experiments was carried out in the Institute of strength problems of the Academy of Sciences of Ukraine. Experiments were carried out using INSTRON 8802 tensile-testing machine (breaking force up to 250 kN). 10 replicated experiments were carried out for each series.

To fasten 20cm strip of the multilayer technical fabric shaped clamps with movable axles (70mm in diameter) were inserted into the upper and lower grips of INSTRON 8802 tensile-testing machines [23]. Loose ends of fabric wrapping around these axles and were joined. To fix the joint the area of joining was clamped on both sides with metal plates, fixed by 5 screws with nuts on each end of the sample. Such a fastening scheme made it possible to exclude slippage of the loaded branch of the fabric against the unloaded end of the fabric during tensile tests.

In result of researches carried out for woven power grip the multilayer technical fabric MTF – 9 (figure 4.6a) was offered. This fabric includes 6 layers. Figure 4.6b shows cross-section of fabric along wrap yarns. Wrap yarns of external protective layers (PL) are shown in red colour, wrap yarns of force layers (FL) are shown in blue colour. Main element of the woven power grip is

wrap yarns of the force layers (FL). External protective layers are intended for protection of the force layers (figure 4.6c). For fabric MTF – 9 (width 20 cm) 488 caprone multifilaments 29 Tex S110x2 S300 Z 180 were used as wrap yarns of the external protective layers (PL). 952 caprone multifilaments 93.5 Tex S 30 Z 60 were used as wrap yarns of force layers (FL). In this structure connection between the layers is due to wrap yarns of the external protective layers (PL).

a

b

c

d
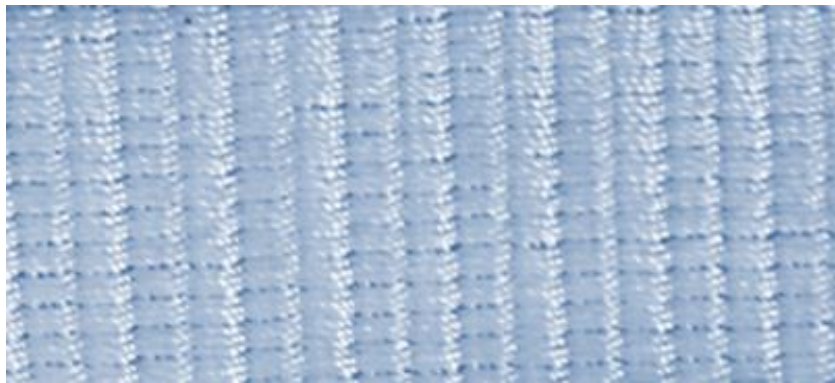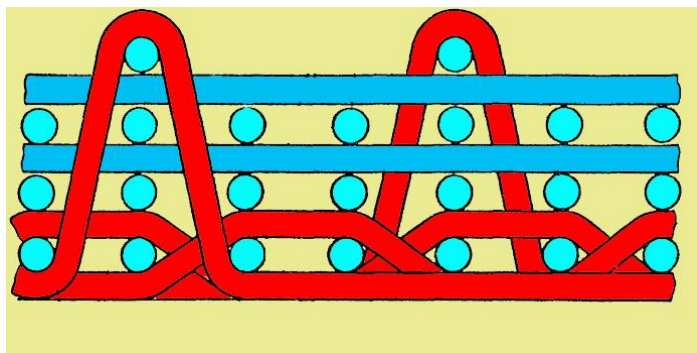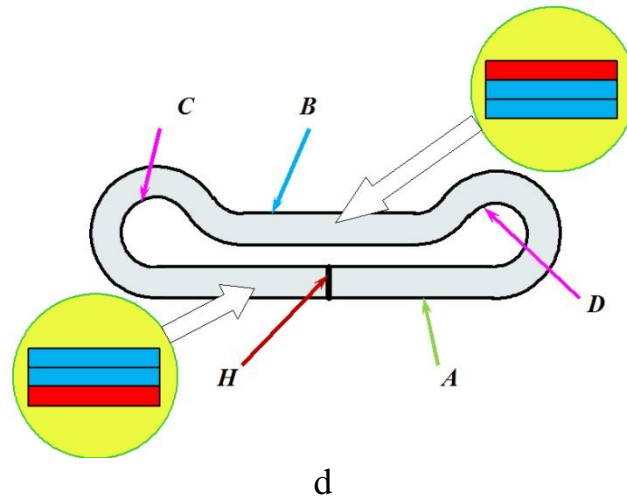
Figure 4.6 Multilayer technical fabric MTF – 9: a – general appearance; b – cross-section of fabric along wrap yarns; c – conventional representation of cross-section of fabric along wrap yarns in the form of layers; d – woven power grip in the form of locked loop made of multilayer technical fabric MTF – 9

Figure 4.4b shows elastic system of wrap yarns threading while manufacturing of multilayer technical fabric MTF – 9. Wrap yarns are located on two beams. It makes servicing of the weaving machine much easier while manufacturing of fabric comparing to multilayer technical fabric MTF – 1.

Analysis of the woven power grip in the form of locked loop made of multilayer technical fiber MTF – 9 (figure 4.6d) shows that wrap yarns of the two force layers (FL) will be placed inside the woven power grip. While using the woven power grip, force layers will not contact with ground surface, pipe surface, and rollers of the lifting device (figure 4.2). It will allow to avoid damage to the force layers. Exclusion of upper protective layer allowed to increase number of wrap yarns in the two force layers (FL).

Figure 4.7 shows results of tensile test for 20cm strips of multilayer technical fabrics MTF – 1 and MTF – 9. Where the same density of fabric along the filling yarns breaking strength of the multilayer technical fabric MTF – 9 is higher by 53% comparing to its prototype. The influence of density along the filling yarns of the multilayer technical fabric MTF – 9 on the breaking force value was determined separately. It was established that the higher the density

along the filling yarns the lower breaking force value. It is explained by more strained conditions of fabric formation on the machine.

According to experiment plans the data was obtained that determined the influence of threading tension of the wrap yarns on the conditions of multilayer technical fabric formation MTF – 1(table 4.5) and MTF – 9 (table 4.6). For multilayer technical fabrics MTF – 1 if threading tension of the ground/back wrap yarns increases from 164.7 cN (variant I-2) to 223.4 cN (variant I-5) the beat-up force increases from 139.3 cN to 152.5 cN by one yarn. At the same time the value of the beat strip decreases from 22.3 mm to 12.6 mm.

Where threading tension increases, wrap tension at the fell of the fabric in the moment of beat increases as follows: ground/back wrap yarns from 239.0 cN (variant I-2) to 289.6 cN (variant I-5) and filling wrap yarns from 168.7 cN (variant I-2) to 244.2 cN (variant I-5).
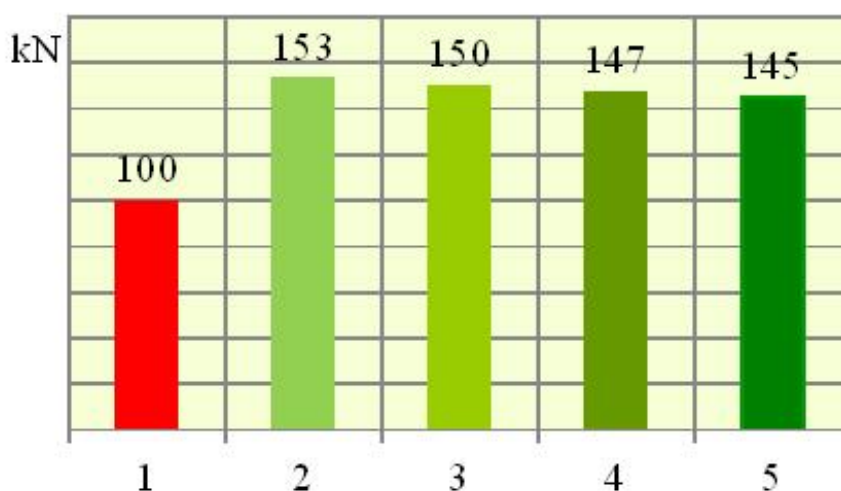
Figure 4.7 breaking force value of the multilayer technical fabric: 1 - MTF – 1 (density of filling yarns 100 yarns/decimetre); 2 - MTF – 9 (density of filling yarns 100 yarns/decimetre); 3 - MTF – 9 (density of filling yarns 120 yarns/decimetre); 4 - MTF – 9 (density of filling yarns 130 yarns/decimetre); 5 - MTF – 9 (density of filling yarns 140 yarns/decimetre)

Table 4.5

Results that determines influence of the input tension of wrap yarns of the protective layers on the beat-up force value for multilayer technical fabric MTF – 1

№.	Wrap yarns	Branch of shed	P_S [cN]	P_{SURF} [cN]		P_{FZ} [cN]	P_{RZ} [cN]	$t_P \cdot 10^{-2}$ [seconds]	l_P [mm]	P_F [cN]
				Statics	Dynamics					
I-1	PL	1	192.2	61.2	142.8	264.0	249.6	2.5	15.9	73.4
		2	192.2			251.5	240.3			
		3	192.2			228.6	221.0			
	BIN	1	47.8			137.6	130.1			
		2	47.8			136.2				
	FL	3	102.1			213.7	199.1			
I-2	PL	1	164.7	42.8	139.3	239.0	226.7	3.08	22.3	56.3
		2	164.7			229.9	219.6			
		3	164.7			212.5	203.4			
	BIN	1	47.8			132.8	125.6			
		2	47.8			131.5				
	FL	3	42.2			168.7	97.2			
I-3	PL	1	178.3	52.9	140.0	253.7	239.8	2.53	16.7	71.1
		2	178.3			242.0	231.2			
		3	178.3			230.3	222.6			
	BIN	1	47.8			140.5	132.8			
		2	47.8			139.0				
	FL	3	69.5			203.1	149.2			
I-4	PL	1	208.3	67.8	147.8	277.9	262.7	2.35	15.0	93.0
		2	208.3			267.1	255.1			
		3	208.3			257.4	248.8			
	BIN	1	47.8			142.1	134.8			
		2	47.8			140.7				
	FL	3	125.4			231.1	245.3			
I-5	PL	1	223.4	72.3	152.5	289.6	273.8	2.09	12.6	94.2

	2	223.4			280.0	267.5			
	3	223.4			273.6	264.4			
BIN	1	47.8			139.1	131.5			
	2	47.8			137.6				
FL	3	150.3			244.2	287.5			

For multilayer technical fabrics MTF – 9 if threading tension of the ground/back wrap yarns increases from 125.8 cN (variant II-2) to 175.4 cN (variant II-5) the beat-up force increases from 72.5 cN to 118.7 cN by one yarn. At the same time the value of the beat strip decreases from 18.2 mm to 7.2 mm. Where threading tension increases, wrap tension at the fell of the fabric in the moment of beat increases as follows: ground/back wrap yarns from 217.7 cN (variant II-2) to 261.4 cN (variant II-5) and filling wrap yarns from 124.1 cN (variant II-2) to 206.3 cN (variant II-5).

Table 4.6

Results that determines influence of the input tension of wrap yarns of the protective layers on the beat-up force value for multilayer technical fabric MTF – 9

№.	Wrap yarns	Branch of shed	P_S [cN]	P_{SURF} [cN]		P_{FZ} [cN]	P_{RZ} [cN]	$t_P \cdot 10^{-2}$ [seconds]	l_P [mm]	P_F [cN]
				Statics	Dynamics					
II-1	PL	1	150.6	51.9	101.6	246.6	235.5	2.01	11.9	70.8
		2	150.6			256.7	241.0			
		3	150.6			172.8	169.5			
	FL	1	56.1			181.7	169.0			
		3	56.1			96.3	93.1			
II-2	PL	1	125.8	29.1	72.5	217.7	208.8	2.68	18.2	74.7
		2	125.8			225.7	211.9			
		3	125.8			145.8	143.1			
	FL	1	26.8			124.1	115.5			
		3	26.8			65.1	63.0			
II-3	PL	1	143.2	34.2	80.3	229.6	220.1	2.26	14.5	76.6

		2	143.2			239.7	225.0			
		3	143.2			157.9	154.9			
	FL	1	38.3			134.6	125.2			
		3	38.3			81.0	78.3			
	PL	1	162.0			255.8	245.3			
		2	162.0			272.3	255.7			
II-4		3	162.0	52.1	197.4	176.4	173.1	1.96	11.7	82.5
	FL	1	61.6			194.0	180.5			
		3	61.6			102.5	99.1			
	PL	1	175.4			261.4	250.5			
		2	175.4			275.1	258.3			
II-5		3	175.4	59.8	118.7	188.5	185.0	1.39	7.2	86.6
	FL	1	72.2			206.3	191.9			
		3	72.2			152.6	147.6			

Two plans of active carrying out of experiment (tables 4.7, 4.8) were realized to determine joint influence of spade value φ_Z and different tension of shed h. For multilayer technical fabric MTF – 1 the value of different tension of shed changed within limits from -10 mm to 10 mm with a step of 10 mm; the value of spade changed within limits from 350 to 550 with a step of 100. For multilayer technical fabric MTF – 9 the value of different tension of shed changed within limits from -10 mm to 10 mm with a step of 10 mm; the value of spade changed within limits from 60 to 220 with a step of 80. Such decrease in value of spade comparing to multilayer technical fabric MTF – 1 induces decrease in dynamic and static components of the wrap yarns tension in the 3rd branch of the shed. The backrest shall be installed 10mm lower with respect to neutral line; and that what corresponds to its optimal position.

Using data from tables 4.7, 4.8 for multilayer technical fabric MTF – 1 and MTF – 9, using well-known method of coefficient determination in the regression equation for orthogonal design of the 2nd order the following regression dependencies were obtained:

for MTF – 1

$$P = 2488.2 + 46.3h - 14.8\varphi_Z - 0.68h\varphi_Z - 1.4h^2 , \qquad (4.3)$$

for MTF – 9

$$P = 1511.2 + 16.7h - 31.4\varphi_Z - 0.7h\varphi_Z - 0.4h^2 + 0.7\varphi_Z^2 . \qquad (4.4)$$

Table 4.7

Results that determines joint influence of spade and different tension of shed on beat-up force value for multilayer technical fabric MTF – 1

№.	Wrap yarns	Branch of shed	P_{SURF} [cN]		P_{FZ} [cN]	P_{RZ} [cN]	P_F [cN]
			Statics	Dynamics			
I-9	PL	1	39.1	117.7	229.6	217.3	67.2
		2			219.5	209.6	
		3			200.0	193.2	
	BIN	1			153.8	145.4	
		2			152.2		
	FL	3			145.9	135.9	
I-7	PL	1	33.7	98.5	226.1	213.7	76.9
		2			215.3	205.6	
		3			194.8	188.3	
	BIN	1			148.5	140.4	
		2			146.9		
	FL	3			139.3	129.7	
I-8	PL	1	49.1	139.7	243.9	230.5	64.3
		2			232.6	222.2	
		3			209.6	202.5	
	BIN	1			166.4	157.3	

		2			164.6		
	FL	3			186.8	174.0	
I-6	PL	1	38.6	108.4	229.5	216.9	75.1
		2			219.0	209.2	
		3			198.2	191.4	
	BIN	1			153.5	145.1	
		2			151.9		
	FL	3			145.7	135.7	
I-12	PL	1	36.4	102.1	226.6	214.1	69.8
		2			216.1	206.4	
		3			192.5	186.0	
	BIN	1			150.5	142.3	
		2			148.9		
	FL	3			140.5	130.9	
I-13	PL	1	42.2	120.9	236.2	223.3	73.1
		2			225.2	215.1	
		3			204.3	197.4	
	BIN	1			164.1	155.1	
		2			162.3		
	FL	3			165.5	154.1	
I-10	PL	1	48.1	133.0	239.8	226.7	67.0
		2			230.7	220.4	
		3			205.6	198.7	
	BIN	1			164.3	155.3	
		2			162.5		
	FL	3			174.8	162.8	
I-11	PL	1	40.8	111.6	234.3	221.4	71.8
		2			223.1	213.1	

		3			208.1	201.1	
	BIN	1			159.3	150.6	
		2			157.6		
	FL	3			146.2	136.2	
	PL	1			236.0	223.1	
		2			224.3	214.3	
I-14		3	42.8	119.6	203.4	196.6	66.9
	BIN	1			163.7	154.8	
		2			162.0		
	FL	3			164.4	153.1	

Efficacy of obtained regression dependences were checked using SPSS program for statistical processing of experimental data [1, 6, 8-23]. Analysis of coefficient significance of regression dependences (3) and (4.4) allowed to drop insignificant [2, 3, 8, 22-23]. In regression dependences (4.3) and (4.4) value of spade φ_Z shall be inserted in degrees, and h value that characterizes different tension of shed shall be inserted in mm.

Table 4.8

Results that determines joint influence of spade and different tension of shed on beat-up force value for multilayer technical fabric MTF –9

№.	Wrap yarns	Branch of shed	P_{SURF} [cN]		P_{FZ} [cN]	P_{RZ} [cN]	P_F [cN]
			Statics	Dynamics			
	PL	1			153.5	147.2	
		2			161.3	151.4	
II-9		3	26.2	76.6	135.9	132.9	58.9
	FL	1			124.1	115.5	
		3			107.5	103.4	
II-7	PL	1	22.3	72.5	145.0	131.0	48.3

		2			152.2	143.5	
		3			128.7	125.8	
	FL	1			117.6	109/4	
		3			94.2	90.6	
II-8	PL	1	39.2	97.6	196.2	188.1	68.1
		2			205.5	192.9	
		3			169.0	166.7	
	FL	1			158.2	147.1	
		2			138.5	135.2	
II-6	PL	1	28.2	79.2	158.4	151.9	51.9
		2			166.8	155.6	
		3			137.9	136.0	
	FL	1			128.4	119.4	
		3			102.3	99.9	
II-12	PL	1	24.1	73.2	145.1	139.1	45.4
		2			154.2	144.8	
		3			126.6	124.2	
	FL	1			107.9	100.4	
		3			89.1	86.1	
II-13	PL	1	30.1	79.9	160.6	154.0	54.4
		2			168.3	158.0	
		3			141.1	138.5	
	FL	1			129.5	120.5	
		3			112.8	109.1	
II-10	PL	1	35.6	88.3	177.0	169.7	63.1
		2			186.0	174.6	
		3			154.1	152.0	
	FL	1			143.1	133.1	

		3			125.6	122.5	
II-11	PL	1	24.5	75.6	150.8	144.6	50.9
		2			159.2	149.4	
		3			135.7	132.6	
	FL	1			122.5	114.0	
		3			105.2	101.1	
II-14	PL	1	28.7	79.6	159.1	152.6	60.2
		2			167.6	157.4	
		3			140.8	138.1	
	FL	1			129.1	120.1	
		3			112.1	108.4	

Figure 4.8 shows comparative analysis of the manufacturing conditions for multilayer technical fabrics MTF – 1 and MTF – 9.
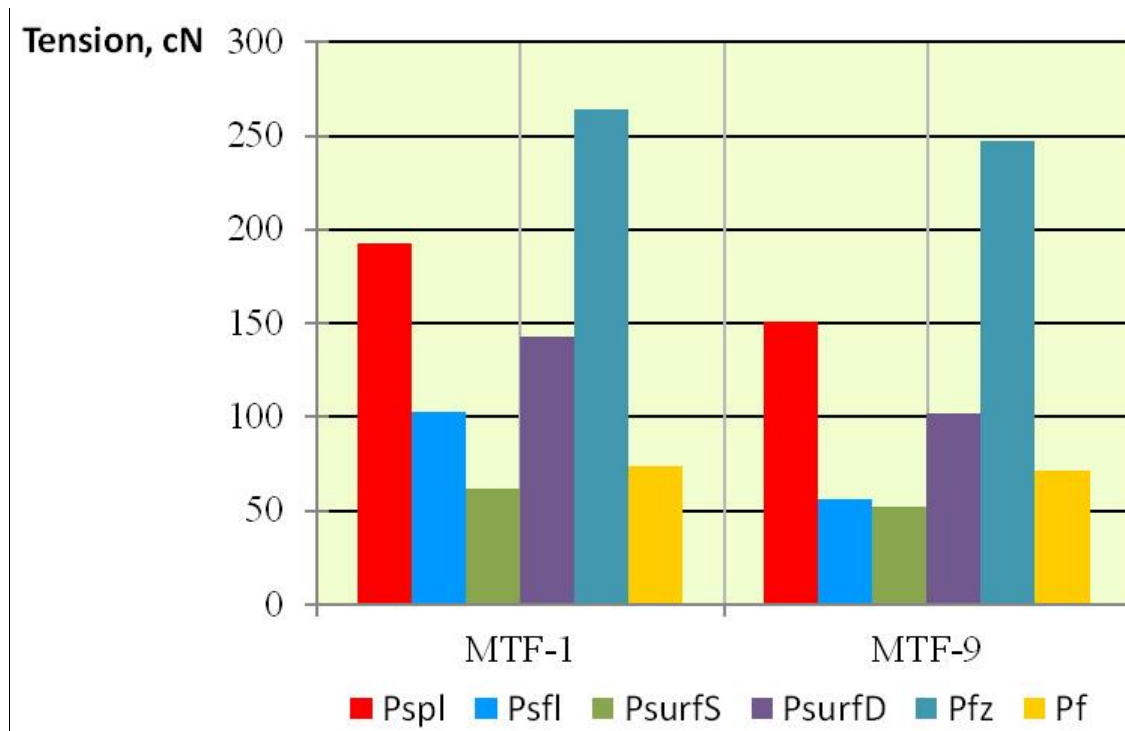
Figure 4.8 Comparative analysis of the manufacturing conditions for multilayer technical fabrics MTF – 1 and MTF – 9: ■ – tension of wrap yarns of the

external protective layers(PL) in static conditions P_{SPL}; ■ - tension of wrap yarns of the force layers(FL) in static conditions P_{SFL}; ■ – beat-up force equivalent to one wrap yarn in statics $P_{SURF}S$; ■ - beat-up force equivalent to one wrap yarn in dynamics $P_{SURF}D$; ■ – tension of wrap yarns of the external protective layers(PL) before the area of fabric formation P_{FZ}; ■ – tension of fabric equivalent to one wrap yarn P_F

Threading tension of the wrap yarns of the external protective layers (PL) decreased by 22% (from 192.2 cN to 150.6 cN), threading tension of the wrap yarns of the force layers (FL) decreased by 45% (from 102.1 cN to 56.1 cN), beat-up force, equivalent to one yarn, in static conditions decreased by 15% (from 61.2 cN to 51.9 cN), beat-up force, equivalent to one yarn, in dynamic conditions decreased by 29% (from 142.8 cN to 101.6 cN), tension of the wrap yarns of the external protective layers (PL) decreased by 7% (from 264.0 cN to 246.6 cN), tension of fabric at the moment of beat, equivalent to one yarn, decreased by 4%(from 73.4 cN to 70.8 cN). Value of beating strip decreased from 15.9 mm to 11.9 mm. Obtained results allow to state that multilayer technical fabric MTF – 9 manufactured on the machine at smaller technological loads. It allows to significantly cut yarn breakages, preserve their strength properties, and increase machine capacity.

Resulting from multi-method experimental researches in improvement of structure and technology of multilayer technical fabric manufacturing the new structure was obtained. Its use leads to 50% increased in strength of power grip for laying pipes with factory insulation coating of oil and gas pipelines. Realization of active planning of the experiment allowed to determine optimal parameters of threading for weaving machine, at which beat-up force of the filling yarn will have minimum necessary value for obtaining multilayer technical fabric of the defined structure. At the same time threading tension of the wrap yarns of the external protective layers (PL) decreased by 22%, threading

tension of the wrap yarns of the force layers (FL) decreased by 45%, beat-up force, equivaletn to one yarn, in static conditions decreased by 15%, beat-up force, equivaletn to one yarn, in dynamic conditions decreased by 29%, tension of the wrap yarns of the external protective layers (PL) before the fabric formation area decreased by 7%, tension of fabric at the moment of beat, equivalent to one yarn, decreased by 4%. Beat-up force value regressional dependences on spade value and different tension of shed were obtained. Obtained results may be used to improve the structure and technology of multilayer technical fabric manufacturing.

5. EFFECT OF THE YARN STRUCTURE ON THE TENSION DEGREE WHEN INTERACTING WITH HIGH-CURVED GUIDE WAYS

Modeling of the yarn processing process in weaving looms and knitting machines is made in order to study the process of yarn interaction with the operative part surfaces in the production equipment.   [1- 3, 8, 10, 23, 25]. The shape of the operative part surfaces is similar to the cylindrical surface [25]. Therefore, when carrying out the experiment, cylindrical rods of different diameters were used as guide way surfaces [8, 25].

Figure 5.1 shows the diagrams of yarn interaction with a cylindrical guide way.

In the first case (Figure 5.1 a), the diameter of the cylindrical guide way surface D substantially exceeds the yarn diameter $D >> d$, $D = 2R$, $d = 2r$, where D is the diameter of the cylindrical guide way surface; d is the yarn diameter; R, r are, respectively, the radius of the cylindrical guide way surface and the radius of the yarn cross section [2, 5]. In the second case (Figure 5.1 b), the diameter of the cylindrical guide way surface is comparable to the yarn diameter $D \approx d$ [1, 8].

a   b
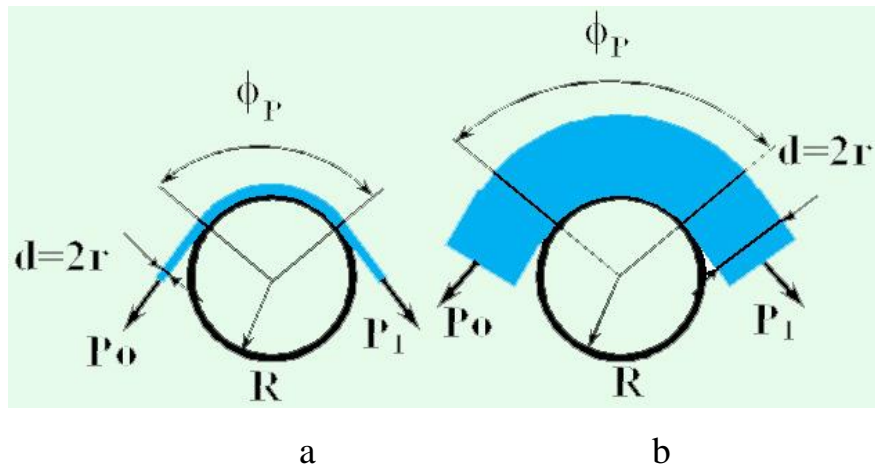
Figure 5.1 Diagrams of yarn interaction with a cylindrical guide way surface: a – the case when the diameter of the cylindrical guide way surface substantially exceeds the yarn diameter; b – the case when the diameter of the cylindrical guide way surface is comparable to the yarn diameter.

This type of interaction takes place when the yarn comes into contact with the heddle eye surfaces of weaving loom frames (Figure 5.2a), when it comes into contact with the surfaces of knitting machine needles (Figure 5.2 b – polyamide filament yarn 29 Tec; Figure 5.2 c – polyamide filament yarn 29x2 Tec).

a   b   c
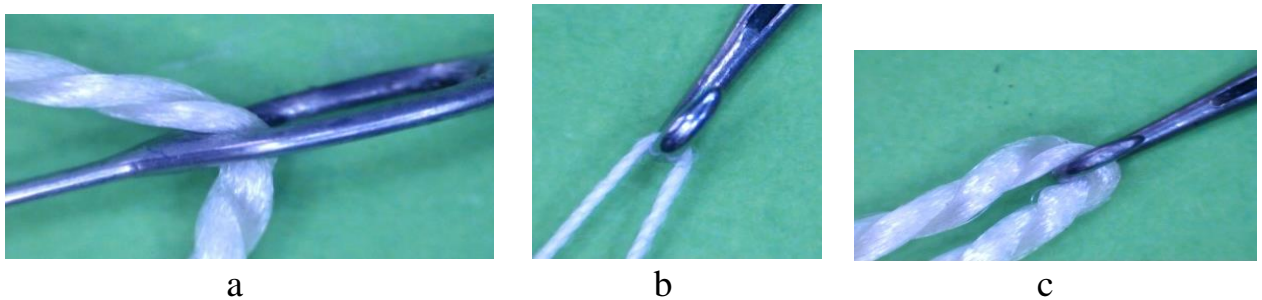
Figure 5.2 Yarn interaction with operative parts of weaving looms and knitting machines: a – yarn interaction with heddle eye surfaces of weaving loom frames; b – yarn interaction with the surface of knitting machine needles (polyamide filament yarn 29 Tex); c – yarn interaction with the surface of knitting machine needles (polyamide filament yarn 29x2 Tec).

Tension of fabric P after the cylindrical guide way for the case when $D \gg d$ is determined by the formula [1- 3]

$$P = P_0 e^{\mu \varphi_P} \tag{5.1}$$

where P is the tension of fabric behind the cylindrical guide way;

P_0 - is the tension of fabric in front of the cylindrical guide way [2];

μ - is the constant of friction [1, 3];

φ_P - is the nominal value of the braid angle between the yarn and the guide way [4, 5].

Figure 5.3 shows the diagram of how the tension of fabric behind the cylindrical guide way depends on the cylindrical guide way radius.

The formula (1) does not consider actual conditions of interaction between the yarn and the cylindrical guide way, when the diameter of the cylindrical guide way surface is comparable to the diameter of the yarn $D \approx d$ [4, 8, 25].

In this case, it is necessary to consider the yarn diameter deformation in the contact area. Furthermore, the tension degree has its impact on the flexural modulus. It is obvious that the increase in tension is explained by a change in the braid angle between the yarn and the high-curved guide way.
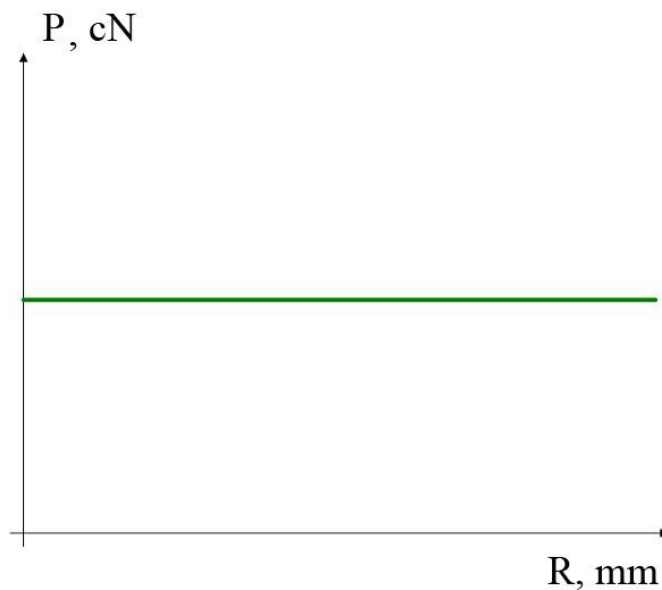
Figure 5.3 Dependence of the tension of fabric behind the cylindrical guide way depends on the cylindrical guide way radius.

At the same time, the actual braid angle for filament yarn and spun yarn will be higher than the nominal φ_P, due to the yarn diameter deformation in the contact area, while the braid angle for monofilament yarns will be less than the nominal φ_P due to the flexural modulus. The flexural modulus value for filament yarns and spun yarn depends on the degree of their twist [25]. When the yarn twist increases, its flexural modulus increases too. This can be explained by the fact that with an increase in twist, specific pressure between individual filaments increases, which leads to an increase in friction forces that prevent elementary fiber movements during flexure.

Thus, the challenge remains urgent as to determining the effect of the yarn structure on the tension degree behind the guide way surface, when the condition $D \approx d$ is met. When creating a design of the experiment, it is necessary to consider the direction of the relative shift of the friction surfaces [25], the tension of fabric before the guide way [8, 11, 22, 25], the structure of the yarn [5, 8, 9], the value of the nominal braid angle between the yarn and the guide way surface [1, 8, 24, 25]. The flexural modulus for monofilament yarns and filament yarns, which have different twists, is a crucial factor when determining the degree of tension [1, 3, 8].

Such restrictions required the development of a conceptually new experimental setup pattern, which differs from those designed earlier [2, 3, 25].

To date, the range of natural-fiber filter fabric produced by the textile industry does not always meet production requirements. In addition to filter fabrics, many industries use non-ferrous metal mesh as a filter material, which, like natural-fiber fabrics, are non-durable when used. This leads to reduction in the performance of equipment, increase in downtime associated with the replacement of used filters, and this, in turn, leads to an increase in the net cost of the products produced.

For the experiment, polyamide filaments were selected as raw materials. These filaments are the same as those used to produce filter fabric and mesh. Filter fabrics made of polyamide filament yarns and monofilament yarns have a number of advantages over natural-fiber fabrics and non-ferrous mesh. Mesh made with polyamide monofilament yarns, unlike mesh made with non-ferrous metals, has a stronger durability, is resistant to corrosion, can be cut more efficiently, and is much more cheaper.

For industrial testing, raw materials and equipment were used to carry out experiments in the production environment of "TECHNOFILTER" Mechanical Fabric Factory, Private Joint-Stock Company, filter mechanical fabrics and meshes of which are widely used in mining, sugar, dairy, and chemical industries.

For the first set of experiments (variant 1) polyamide monofilament yarn 36.3 Tex was chosen, with the diameter of d = 2r = 0.200 mm, the flexural modulus of B=14.0 cN mm^2. Figure 5.4a shows a general view. Figure 5.4 b shows diagrams of monofilament yarn interaction with a cylindrical guide way surface. The analysis of the interaction diagram (Figure 5.4 b) shows that the actual braid angle φ will be less than the nominal braid angle φ_P. This is explained by flexural resistance of the monofilament yarn. The degree of this resistance is determined by the value of the monofilament yarn flexural modulus,

$$B = EI, \, I = \pi d^4 / 64,$$ (5.2)

where E - is the stretching elastic modulus for polyamide monofilament yarn;

I - is the area moment of inertia for monofilament yarn.

One of the factors that influences the tension of fabric is its twist. When the yarn twist increases, its flexural modulus increases too. This can be explained by the fact that with an increase in twist, specific pressure between individual filaments increases, which leads to an increase in friction forces that prevent elementary fiber movements during flexure. So the minimum value of

the flexural modulus for polyamide filament yarn 29 Tex equals to $1.3 \cdot 10^{-5}$ cN·mm^2, when the twist tends to zero, and the maximum value equals to 11.2 cN·mm^2, when the twist reaches a critical value and the yarn breaks. The yarn flexural modulus value has its impact on the actual value of the braid angle of the guide way surface, the value of which determines the tension of fabric. That is why, three series of experiments for polyamide filament yarns of various twist were carried out.
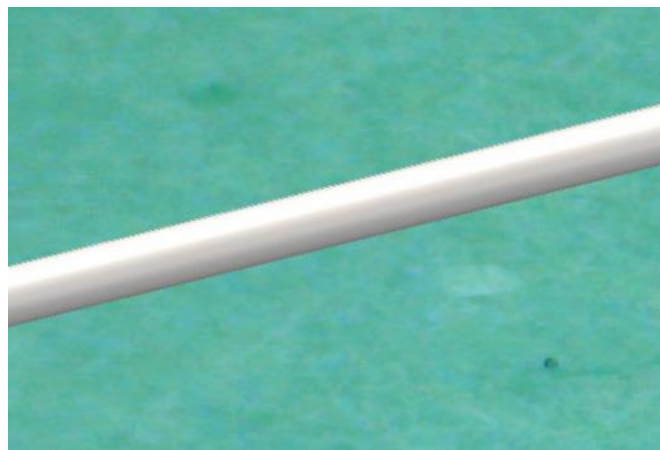
a
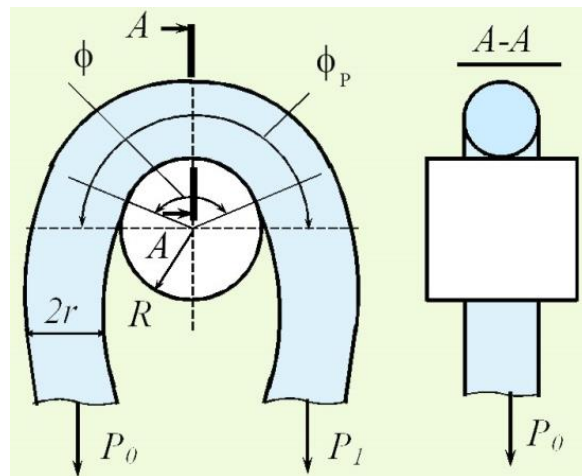
b

Figure 5.4 Information on polyamide monofilament yarn 36.3 Tex, with the diameter of d = 2r = 0.200 mm, the flexural modulus of B=14.0 cN mm^2: a – general view; b – diagram of interaction with the cylindrical guide way surface.

For the second series of experiments (variant 2), polyamide filament yarn 29 Tex was chosen, which consisted of 80 filaments, flat twist Kr = 100 twists/meter, the nominal diameter d = 2r = 0.199 mm, the flexural modulus B=2.6·10^{-5} cN·mm^2. Figure 5.5 a shows the general view of the yarn. Figure 5.5 b shows a diagram of polyamide filament yarn interaction with a cylindrical guide way surface. The analysis of the interaction diagram (Figure 5.5 b) shows that the actual braid angle φ will be significantly higher than the nominal braid angle φ_P. This is explained by deformation of the yarn's diameter in the contact area. The value of the flexural modulus for this polyamide filament yarn will be equal

$$B = EI, I = \sum_{i=1}^{80} \pi d_{fi}^4 / 64,$$ (5.3)

where E - is the stretching elastic modulus for flat-twisted polyamide filament yarn;

d_{fi} - is the diameter of polyamide filament yarn.

The simple summation of the area moments of inertia for polyamide filament yarn with a flat twist is explained by the fact that when the yarn surface deforms in the area of contact with the cylindrical guide way, they will be located on the lateral surface in the form of a layer with the thickness equal to the diameter d_{fi}. The flexural modulus for this yarn will be insignificant. The degree of tension will be affected only by an increase in the braid angle due to deformation of the yarn surface in the contact area.

For the third series of experiments (variant 3), polyamide filament yarn 29 Tex was chosen, which consisted of 80 filaments, flat twist Kr = 400 twists/meter, the nominal diameter d = 2r = 0.200 mm, the flexural modulus B=4.0·10^{-2} cN·mm^2. Figure 5.6 a shows the general view of the yarn. Figure 5.6 b shows a diagram of polyamide filament yarn interaction with a cylindrical guide way surface. The analysis of the interaction diagram (Figure 5.6 b) shows

that the actual braid angle φ will be higher than the nominal braid angle φ_P. However, its value will be less than for the flat-twisted yarn due to resistance to flexure of the polyamide filament yarn of medium twist.

a
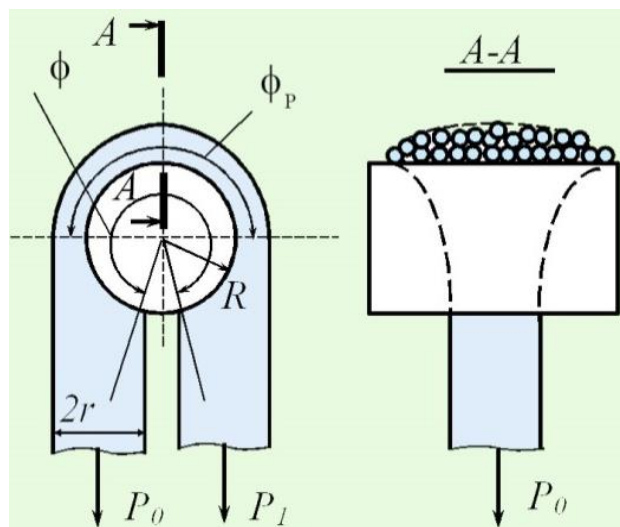
b

Figure 5.5 Information on the polyamide filament yarn 29 Tex, which consisted of 80 filaments, flat twist Kr = 100 twists/meter, the nominal diameter d = 2r = 0.199 mm, the flexural modulus B=2.6·10^{-5} cN·mm^2: a – general view; b – diagram of interaction with the cylindrical guide way surface.

The value of the flexural modulus for the polyamide yarn of medium twist is 1,000 times higher than that of the flat-twisted polyamide yarn [25].
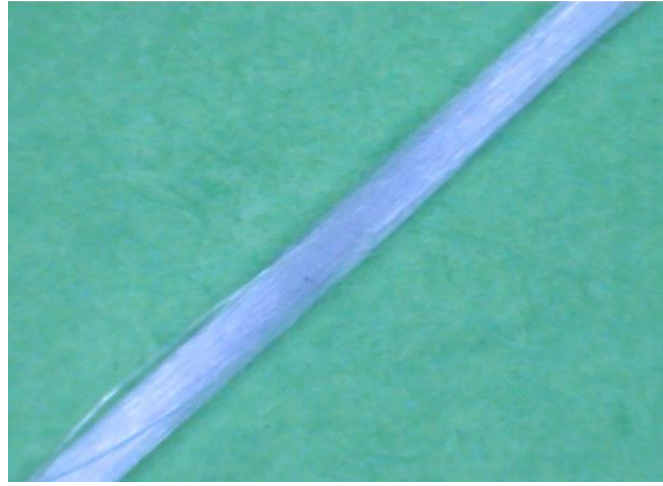
a
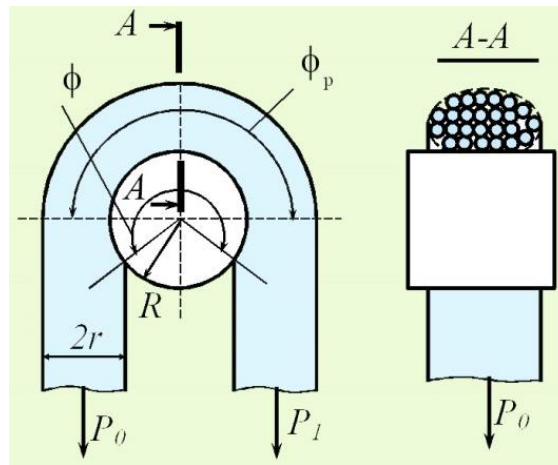
b

Figure 5.6 Information on the polyamide filament yarn 29 Tex, which consisted of 80 filaments, flat twist Kr = 400 twists/meter, the nominal diameter d = 2r = 0.200 mm, the flexural modulus B=4.0·10^{-2} cN·mm^2: a – general views; b – diagram of interaction with the cylindrical guide way surface

For the fourth series of experiments (variant 4), polyamide filament yarn 29 Tex was chosen, which consisted of 80 filaments, flat twist Kr = 800 twists/meter, the nominal diameter d = 2r = 0.208 mm, the flexural modulus B= 0.22 cN·mm^2. Figure 5.7 a shows the general view of the yarn. Figure 5.7 b shows a diagram of interaction between the hard-twisted polyamide filament yarn and a cylindrical guide way surface. The analysis of the diagram of interaction (Figure 5.7 b) shows that the degree of the actual braid angle φ is

influenced more by the flexural resistance of the hard-twisted polyamide filament yarn than the yarn surface deformation in the contact area. The value of the flexural modulus for this polyamide filament yarn will be equal

$$B = EI, I = k(\sum_{i=1}^{80} \pi d_{fi}^4 / 64), k(\sum_{i=1}^{80} \pi d_{fi}^4 / 64) \cong \pi d / 64 \qquad (5.4)$$

where k - is the ratio that takes into account the extent of preservation of the cross-sectional shape of the hard-twisted polyamide filament yarn.

This thread will have a cross-sectional shape close to the circumference (Figure 5.7 b). The reasons for this were indicated above. By the way it behaves, hard-twisted polyamide filament yarn is similar to polyamide monofilament yarn.

The four variants used yarns with almost equal diameter made of the same material (polyamide), but with a different structure: monofilament yarn; filament yarn.

For each of the 4 variants, an orthogonal second-order plan for three factors was designed and implemented in the paper [8, 25].

a

b
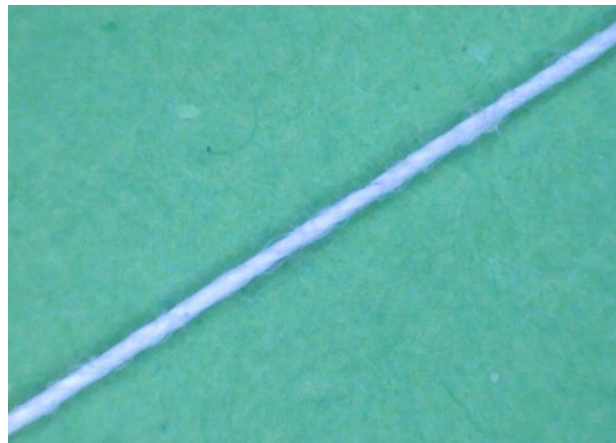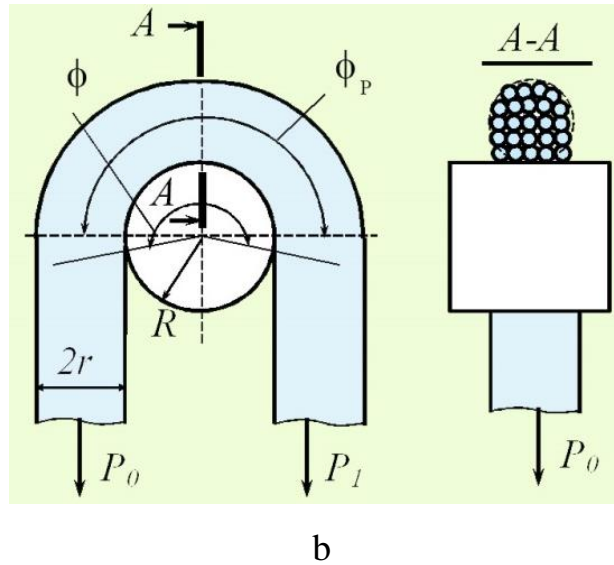
Figure 5.7 Information on the polyamide filament yarn 29 Tex, which consisted of 80 filaments, flat twist Kr = 800 twists/meter, the nominal diameter d = 2r = 0.208 mm, the flexural modulus B= 0.22 cN·mm^2: a – general view; b – diagram of interaction with the cylindrical guide way surface

The general view of the regression equation to determine the joint effect of the tension of fabric prior it goes to the cylindrical guide way P_0, the radius of the cylindrical guide way R and the nominal value of the braid angle φ_P on the tension of fabric behind the cylindrical guide way P, is as follows.

$$P = b_0 + b_1 x_1 + b_2 x_2 + b_3 x_3 + b_{12} x_1 x_2 + b_{13} x_1 x_3 + b_{23} x_2 x_3 +$$
$$+ b_{11} x_1^2 + b_{22} x_2^2 + b_{33} x_3^2. \tag{5.5}$$

The range of factor variation in the equation (5.5) was determined by the actual yarn processing conditions. In the blinded values: the tension of fabric before it goes to the cylindrical guide way P_0 was indicated as x_1; the cylindrical guide way radius R was indicated as x_2; the nominal value of the braid angle φ_P was indicated as x_3. Values and interval of variation of the tension of fabric before the fabric goes to the cylindrical guide way P_0 and the cylindrical guide way radius R are determined based on the conditions of interaction with the cylindrical guide way surface. Two main criteria may be distinguished here. Let's discuss them in more detail.

The first criterion refers to the choice of such an acceptable degree of the tension P_0 of flexure-resistant fabric before it reaches the guide way surface, which will ensure the necessary braid angle for the cylindrical guide way. Figure 5.8 shows the design diagram.
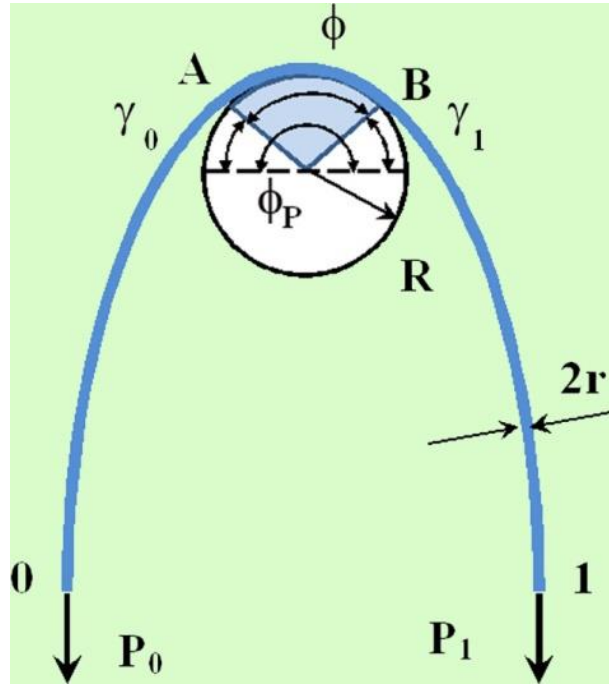
Figure 5.8 Design diagram to determine an acceptable degree of the tension P_0 of flexure-resistant fabric before the guide way surface

The equation that links the tension P_0 of fabric before the cylindrical guide way surface, the flexural modulus B, the radii of the cylindrical guide way surface R and the yarn r, the angle γ_0 by which the actual braid angle φ is reduced due to the flexural resistance of the yarn, is as follows [25]

$$\cos \gamma_0 = 1 - \frac{B}{2P_0(R+r)^2}.$$ (5.6)

Let's find the bottom limit of the degree of the tension P_0 of fabric before the cylindrical guide way surface. It is obvious that at the degree of $\gamma_0 = \pi / 2$, the

actual braid angle φ will equal to 0 (Figure 5.8). Then using the equation (5.6), the following inequality will be obtained:

$$P_0 > \frac{B}{2(R+r)^2}.$$

(5.7)

It is quite obvious that the degree of the tension P_0 of fabric before the cylindrical guide way surface should be selected with the equation (5.7) in mind. Figure 5.9 shows graphic dependences of the degree P_0 depending on R for polyamide monofilament yarn (variant 1), for polyamide filament yarn (variants 3 and 4). The highlighted area in Figure 5.9 corresponds to the range of radius variation R of cylindrical guide way surface, under which the condition $D \approx d$ is met. The analysis of these dependencies shows that to get into this interval, the tension degree P_0 should be higher than 20 cN for monofilament yarn (variant 1). For polyamide yarns (variants 3 and 4), the tension should be higher than 5 cN. For variant 2, the value of the nominal braid angle will be ensured by the tension less than 5 cN.
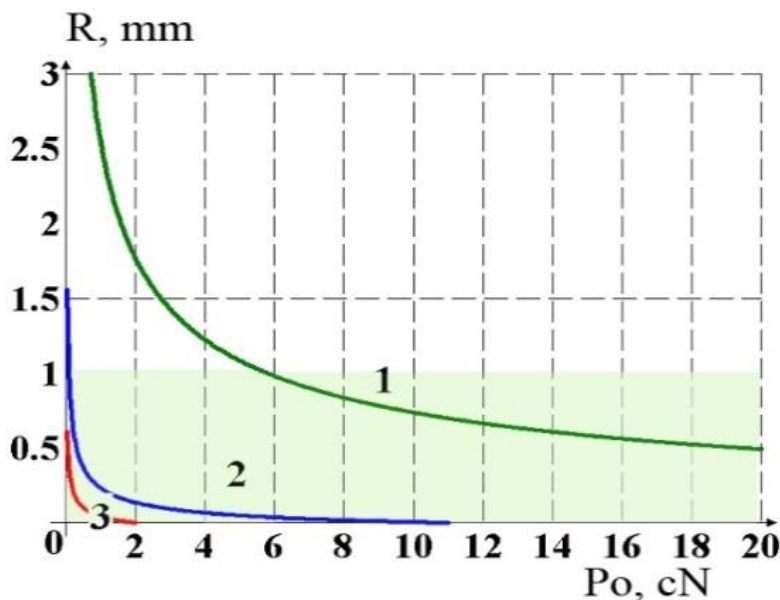
Figure 5.9 Dependences of the radius of the guide way curve R on the tension Po of fabric: 1 – polyamide monofilament yarn; 2 – hard-twisted polyamide filament yarn; 3 – medium-twisted polyamide filament yarn

Let's determine the acceptable values and intervals of radius R variation of the cylindrical guide way surface, taking into account the yarn surface deformation in the contact area for variants 2-4. Figure 10 a shows the design diagram.
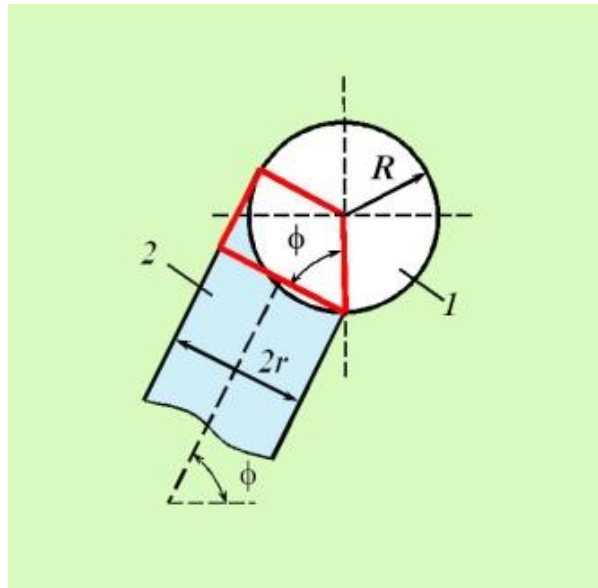
a
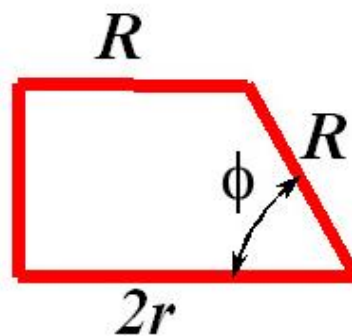
b

Figure 5.10 Determination of acceptable values of the guide way surface radii $R=D/2$ and yarn $r=d/2$ depending on the yarn's tilt angle φ to the horizontal to the guide way surface: a – design diagram; b – compliance trapeze

The equation which links the cross-sectional deformation and the radius R, taking into account the compliance trapeze (Figure 10 b), is as follows:

$$R+R\cos\varphi=2r,\ D=2R,\ d=2r \quad , \tag{5.8}$$

where φ is the tilt angle to the yarn side's horizontal to the cylindrical guide way. When deriving the equation (5.8), it was assumed that the yarn surface deformation would have the maximum value (variant 1). To ensure the condition of non-contact of yarn's sides before and after the guide way surface, with the equation (5.8) an inequality will be obtained that makes it possible to meet this condition:

$$\frac{D}{d} > \frac{2}{(1+\cos\varphi)} .$$

(5.9)

Based on the inequality (5.9), a graphical dependence of the ratio D/d from the tilt angle φ to the yarn side's horizontal to the cylindrical guide way was created, which is shown in Figure 5.11.
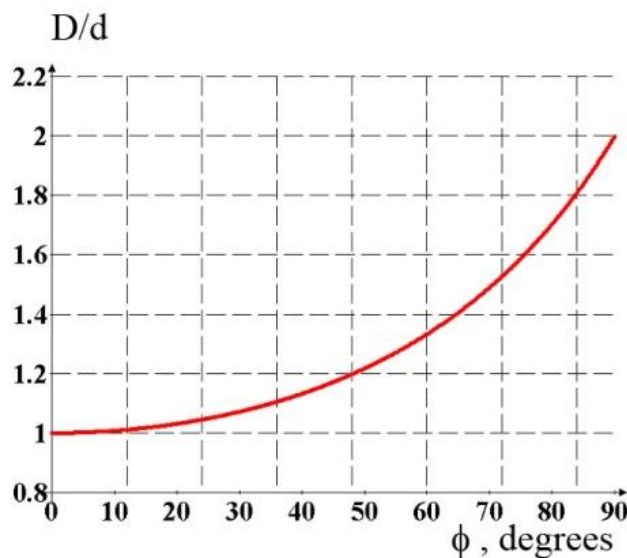
Figure 5.11 Dependence of the ratio of guide way surface diameter D and yarn's diameter d on the tilt angle φ of the yarn to the horizontal to the guide way surface

The analysis of the dependence of the ratio of the guide way surface diameter D and yarn's diameter d on the tilt angle φ showed that if $\varphi=0^0$ $D=d$, and if $\varphi=90^0$ $D=2d$. This is the only case when this condition of non-contact of yarn sides before and after the guide way surface will be met. Thus, the radius $R=D/2$ of the cylindrical surface must always exceed the diameter d of the yarn.

In view of the above, two series of experimental research were implemented. In the first series, for variants 1-4, the degree of tension P_0 of fabric before the cylindrical guide way surface in the middle of the experiment corresponded to 30 cN. In the second series, for variants 2-4, the degree of tension P_0 of fabric before the cylindrical guide way surface in the middle of the experiment corresponded to 10 cN. In the middle of the experiment, the radius of the cylindrical guide way surface curve for the first and second series was equal to 1 mm. In the middle of the experiment, the nominal value for the braid angle φ_P for the first and second series equaled to 135^0.

Table 1 shows a second-order orthogonal matrix for the first series of the experiments for polyamide yarns (variants 1-4).

Table 5.1

Second-order orthogonal matrix for the first series of the experiments for polyamide yarns (variants 1-4)

№	Factors					
	Input tension		Radius of the guide way curve		Value of spade	
	x_1	P_0, cN	x_2	R, mm	x_3	φ, degrees
1	+1	32	+1	1.3	+1	145
2	-1	28	+1	1.3	+1	145
3	+1	32	-1	0.7	+1	145
4	-1	28	-1	0.7	+1	145
5	+1	32	+1	1.3	-1	125
6	-1	28	+1	1.3	-1	125
7	+1	32	-1	0.7	-1	125
8	-1	28	-1	0.7	-1	125

9	-1.215	27.6	0	1.0	0	135
10	+1.215	32.4	0	1.0	0	135
11	0	30	-1.215	0.6	0	135
12	0	30	+1.215	1.4	0	135
13	0	30	0	1.0	-1.215	123
14	0	30	0	1.0	+1.215	147
15	0	30	0	1.0	0	135

The correlation between the open-label and blinded values for the first series of experiments for polyamide yarns (variants 1-4) is as follows:

$$x1 = \frac{P_0 - 30}{2}, \quad x2 = \frac{R - 1.0}{0.3}, \quad x3 = \frac{\phi - 135}{10}. \tag{5.10}$$

Table 5.2 shows a second-order orthogonal matrix for the second series of the experiments for polyamide yarns (variants 2-4).

Table 5.2

Second-order orthogonal matrix for the second series of the experiments for polyamide yarns.(variants 2-4)

№	Factors					
	Input tension		Radius of the guide way curve		Value of spade	
	x_1	P_0, cN	X_2	R, mm	X_3	φ, degrees
1	+1	12	+1	1.3	+1	145
2	-1	8	+1	1.3	+1	145
3	+1	12	-1	0.7	+1	145
4	-1	8	-1	0.7	+1	145
5	+1	12	+1	1.3	-1	125
6	-1	8	+1	1.3	-1	125
7	+1	12	-1	0.7	-1	125

8	-1	8	-1	0.7	-1	125
9	-1.215	7.6	0	1.0	0	135
10	+1.215	12.4	0	1.0	0	135
11	0	10	-1.215	0.6	0	135
12	0	10	+1.215	1.4	0	135
13	0	10	0	1.0	-1.215	123
14	0	10	0	1.0	+1.215	147
15	0	10	0	1.0	0	135

The correlation between the open-label and blinded values for the first series of experiments for polyamide yarns (variants 2-4) is as follows

$$x1 = \frac{P_0 - 10}{2}, \quad x2 = \frac{R - 1.0}{0.3}, \quad x3 = \frac{\phi - 135}{10}. \tag{5.11}$$

Figure 5.12 shows the diagram of the experimental unit. Its set-up is described in detail in the paper [8, 25]. The distinction is that unit 4 of modeling the conditions of interaction with guide ways and operative parts of textile machines includes a set of cylindrical rods, the diameter of which equals to the diameter of the guide ways and operative parts of textile machines.
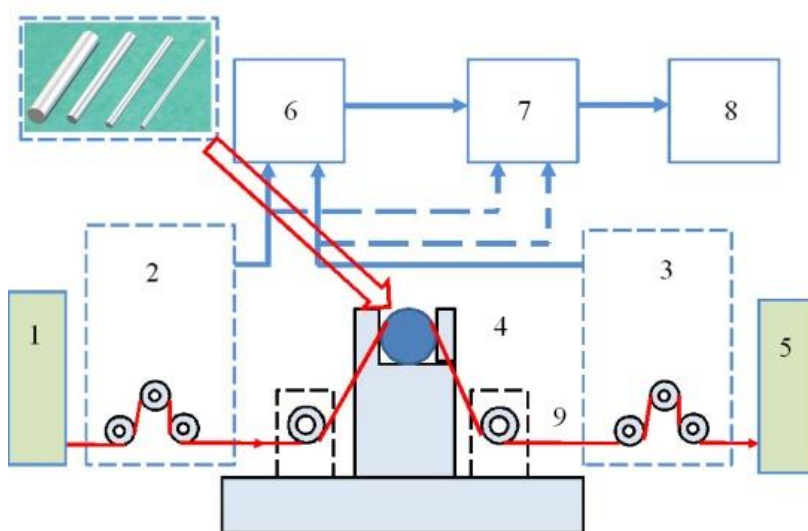
Figure 5.12 Diagram of the experimental unit: 1 – filament feeder unit; 2 – unit for measuring the tension of fabrics slack side; 3 – unit for measuring the tension of fabrics slack side; 4 – unit for modeling the conditions of interaction with guide ways and operative parts of textile machines; 5 – yarn receiver unit; 6 – driver; 7 – analog-to-digital converter ADC; 8 – personal computer; 9 – yarn

The value of the radii of the guide way and polyamide filament yarns, their structure was determined using USB Digital microscope Sigeta (Figure 5.13).

Figure 5.13 Set-up to determine the radii of the guide way and polyamide filament yarns

As a result of implementation of second-order orthogonal designs for three factors (Tables 5.1-5.2) for the first series (variants 1-4) and the second series (variants 2-4), about 10 parallel measurements were performed. Its mean values are shown in Tables 5.3 and 5.4.

Table 5.3

Results of the first series of the experimental research to determine the joint effect of the tension of fabric prior it goes to the cylindrical guide way P_0, the radius of the cylindrical guide way R and the nominal value of the braid angle φ_P on the tension of fabric behind the cylindrical guide way P

(variants 1 -4)

№	Factors			P_2, cN	P_3, cN	P_4, cN	P_1, cN
	Input tension	Radius of the guide way curve	Value of spade				
	x_1	x_2	x_3				
1	+1	+1	+1	88.53	87.10	85.13	50.35
2	-1	+1	+1	77.51	76.18	74.33	42.94
3	+1	-1	+1	107.17	104.11	99.81	38.26
4	-1	-1	+1	93.85	90.98	86.94	32.21
5	+1	+1	-1	78.57	77.31	75.55	45.47
6	-1	+1	-1	68.79	67.61	65.96	38.83
7	+1	-1	-1	54.48	91.77	87.97	35.41
8	-1	-1	-1	82.73	80.19	76.69	29.99
9	-1.215	0	0	76.80	75.09	72.72	36.06
10	+1.215	0	0	90.09	88.24	85.67	43.95
11	0	-1.215	0	101.21	97.77	92.92	31.65
12	0	+1.215	0	77.03	75.84	74.18	45.47
13	0	0	-1.215	77.57	75.91	73.61	37.79
14	0	0	+1.215	89.76	87.86	85.19	42.31
15	0	0	0	83.45	81.67	79.19	39.98

The first series for $27.6 \ cN \leq P_0 \leq 32.4 \ cN$

for polyamide monofilament yarn 36.3 Tex (variant1)

$$P_1 = 3.27 + 0.72P_0 - 9.29R - 0.14\varphi + 0.53P_0R +$$
$$+0.01P_0\varphi + 0.16R\varphi - 0.02P_0^2 - 6.44R^2 - 0.001\varphi^2, \qquad (5.12)$$

for polyamide filament yarn 29 Tex, of flat twist Kr = 100 twists/meter (variant 2)

$$P_2 = 112.35 - 2.13P_0 - 19.77R - 0.63\varphi - 0.88P_0R +$$
$$+0.02P_0\varphi - 0.21R\varphi + 0.05P_0^2 + 24.67R^2 + 0.003\varphi^2, \qquad (5.13)$$

for polyamide filament yarn 29 Tex, medium twist Kr = 400 twists/meter (variant 3)

$$P_3 = 101.06 - 1.83P_0 - 15.98R - 0.59\varphi - 0.85P_0R +$$
$$+0.02P_0\varphi - 0.19R\varphi + 0.05P_0^2 + 22.33R^2 + 0.003\varphi^2, \qquad (5.14)$$

for polyamide filament yarn 29 Tex, hard twist Kr = 800 twists/meter (variant 4)

$$P_4 = 91.14 - 1.62P_0 - 10.12R - 0.57\varphi - 0.80P_0R +$$
$$+0.02P_0\varphi - 0.18R\varphi + 0.04P_0^2 + 19.0R^2 + 0.003\varphi^2. \qquad (5.15)$$

For the nominal value of the braid angle in the middle of the experiment $\varphi_P = 135^0$, with the change in the tension of fabric before the cylindrical guide way $27.6 \ cN \leq P_0 \leq 32.4 \ cN$, the equations (12)-(15) are converted as follows:

for polyamide monofilament yarn 36.3 Tex (variant 1)

$$P_1 = 1.94P_0 + 12.75R - 0.02P_0^2 - 6.44R^2 + 0.53P_0R - 24.65, \qquad (5.16)$$

for polyamide filament yarn 29 Tex, flat twist и Kr = 100 twists/meter (variant 2)

$$P_2 = 79.67 + 0.23P_0 - 48.12R - 0.88P_0R + 0.05P_0^2 + 24.67R^2, \qquad (5.17)$$

for polyamide filament yarn 29 Tex, medium twist Kr = 400 twists/meter (variant 3)

$$P_3 = 70.62 + 0.47P_0 - 42.44R - 0.85P_0R + 0.05P_0^2 + 22.33R^2, \qquad (5.18)$$

for polyamide filament yarn 29 Tex, hard twist Kr = 800 twists/meter (variant 4)

$$P_4 = 59.48 + 0.68P_0 - 33.96R - 0.80P_0R + 0.04P_0^2 + 19.0R^2. \qquad (5.19)$$

Figure 5.14 shows the response surfaces for the first series of experiments for variants 1-4. The relevance of the regression dependencies obtained was checked with the SPSS program for statistical processing of experimental data [5].

Figure 5.14 Response surfaces for the first series of experiments for variants 1-4: ■ - for polyamide filament yarn 29 Tex, flat twist; ■ – for polyamide filament yarn 29 Tex, medium twist; ■ – for polyamide filament yarn 29 Tex, hard twist; ■ – for polyamide monofilament yarn 36.3 Tex

For the nominal value of the braid angle $\varphi_P = 135^0$, tension of fabric before the cylindrical guide way $P_0 = 30\ cN$, the equations (5.16)-(5.19) are converted as follows in the middle of the experiment:

for polyamide monofilament yarn 36.3 Tex (variant 1)

$$P_1 = 15.55 + 28.65R - 6.44R^2, \qquad (5.20)$$

for polyamide filament yarn 29 Tex, flat twist (variant 2)

$$P_2 = 133.89 - 74.52R + 24.67R^2 \, , \qquad (5.21)$$

for polyamide filament yarn 29 Tex, medium twist (variant 3)

$$P_3 = 127.47 - 67.94R + 22.33R^2 \, , \qquad (5.22)$$

for polyamide filament yarn 29 Tex, hard twist (variant 4)

$$P_4 = 118.13 - 57.96R + 19.0R^2 \, . \qquad (5.23)$$

Figure 5.15 shows graphic dependences of the change in the tension of fabric after the cylindrical guide way (the first series of experiments), which were obtained using the dependences (5.20)-(5.23). For variants 2-4, for polyamide filament yarns, the tension P decreases when the radius R of the cylindrical guide way is increased. This is explained by the fact that the yarn surface deformation is decreased in the contact area and, therefore, the value of the braid angle for the cylindrical guide way also decreases. For variant 1, for monofilament yarns, the tension P increases as the radius R of the cylindrical guide way increases, which is explained by an increase in the braid angle. The line 5 is an asymptote for dependencies 1-5, which corresponds to the case when $D \gg d$, formula (5.1).
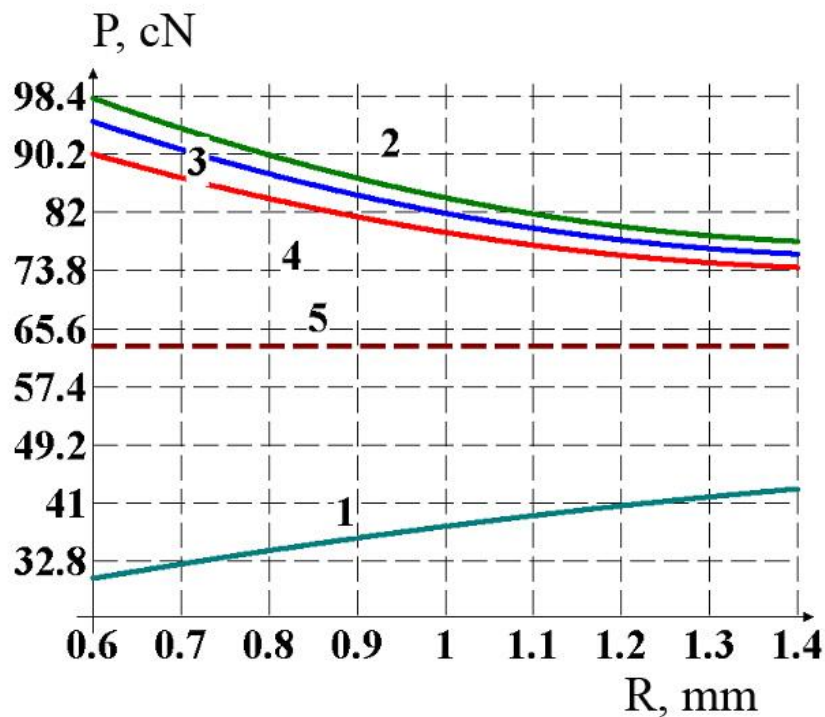
Figure 5.15 Graphic dependences of the change in the tension of fabric after the cylindrical guide way (the first series of experiments): 1 – for polyamide filament yarn 36.3 Tex; 2 – for polyamide filament yarn 29 Tex, flat twist; 3 – for polyamide filament yarn 29 Tex, medium twist; 4 – for polyamide filament yarn 29 Tex, hard twist; 5 – the dependence for polyamide yarn

$$D \gg d,\ D = 2R,\ d = 2r$$

Table 5.4

Results of the second series of the experimental research to determine the joint effect of the tension of fabric prior it goes to the cylindrical guide way P_0, the radius of the cylindrical guide way R and the nominal value of the braid angle φ_P on the tension of fabric behind the cylindrical guide way P (variants 2-4)

№	Factors			P_2, cN	P_3, cN	P_4, cN
	Input tension	Radius of the guide way curve	Value of spade			
	x_1	x_2	x_3			
1	+1	+1	+1	33.93	33.03	31.78
2	-1	+1	+1	21.56	20.86	19.89
3	+1	-1	+1	48.44	46.11	42.86
4	-1	-1	+1	28.58	26.91	24.56
5	+1	+1	-1	30.07	29.28	28.16
6	-1	+1	-1	19.15	18.53	17.67
7	+1	-1	-1	42.38	40.32	37.43
8	-1	-1	-1	25.11	23.64	21.57

9	-1.215	0	0	20.91	20.02	18.77
10	+1.215	0	0	37.15	35.89	34.14
11	0	-1.215	0	40.64	38.17	34.72
12	0	+1.215	0	25.46	24.77	23.82
13	0	0	-1.215	26.71	25.71	24.31
14	0	0	+1.215	30.98	29.83	28.20
15	0	0	0	28.77	27.69	26.19

The second series for $7.6 \ cN \le P_0 \le 12.4 \ cN$

for polyamide filament yarn 29 Tex, of flat twist Kr = 100 twists/meter (variant 2)

$$P_2 = 38.96 + 1.3P_0 - 6.21R - 0.49\varphi - 2.88P_0R +$$
$$+0.03P_0\varphi - 0.14R\varphi + 0.07P_0^2 + 18.77R^2 + 0.002\varphi^2, \qquad (5.24)$$

for polyamide filament yarn 29 Tex, of middle twist Kr = 400 twists/meter (variant 3)

$$P_3 = 35.41 + 1.27P_0 - 3.56R - 0.47\varphi - 2.7P_0R +$$
$$+0.02P_0\varphi - 0.12R\varphi + 0.06P_0^2 + 16.55R^2 + 0.002\varphi^2, \qquad (5.25)$$

for polyamide filament yarn 29 Tex, of hard twist Kr = 800 twists/meter (variant 4)

$$P_4 = 29.07 + 1.08P_0 + 0.03R - 0.41\varphi - 2.45P_0R +$$
$$+0.02P_0\varphi - 0.11R\varphi + 0.06P_0^2 + 13.66R^2 + 0.002\varphi^2.$$

(5.26)

For the nominal value of the braid angle in the middle of the experiment $\varphi_P = 135^0$, with the change in the tension of fabric before the cylindrical guide way $7.6 \ cN \le P_0 \le 12.4 \ cN$, the equations (5.24)-(5.26) are converted as follows:

$$P_2 = 9.22 + 4.74P_0 - 24.65R + 0.07P_0^2 + 18.77R^2 - 2.88P_0R , \quad (5.27)$$

$$P_3 = 6.23 + 4.58P_0 - 20.21R + 0.06P_0^2 + 16.55R^2 - 2.7P_0R , \qquad (5.28)$$

$$P_4 = -2.48 + 4.32P_0 - 14.28R + 0.06P_0^2 + 13.66R^2 - 2.45P_0R. \qquad (5.29)$$

Figure 5.16 shows the response surfaces for the second series of experiments for variants 2-4. Dependences of the tension of fabric after the cylindrical guide way on the tension P_0 and the radius of the cylinder R were established at the fixed value of nominal braid angle for the cylinder φ. This value corresponded to the focus point of the experiment (Table 5.2). The relevance of the regression dependencies obtained was checked with the SPSS program for statistical processing of experimental data [25].
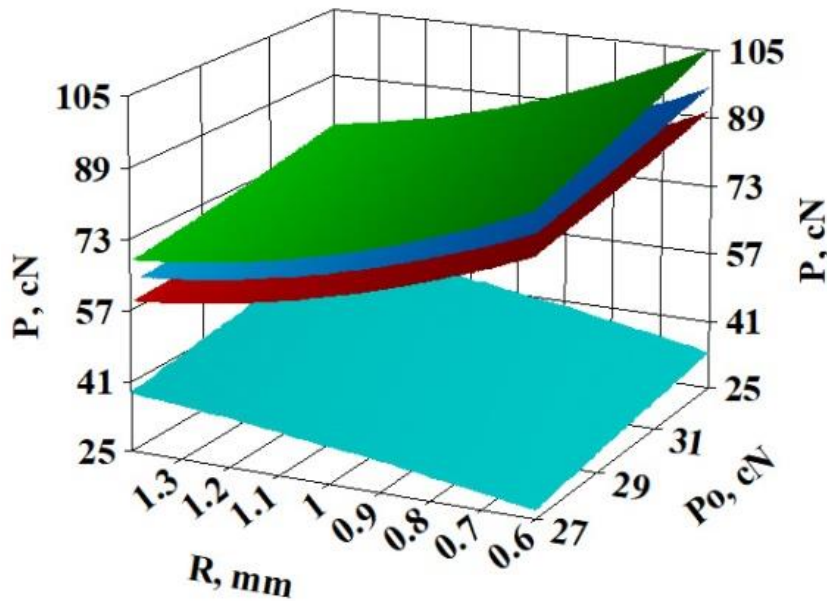

a   b   c
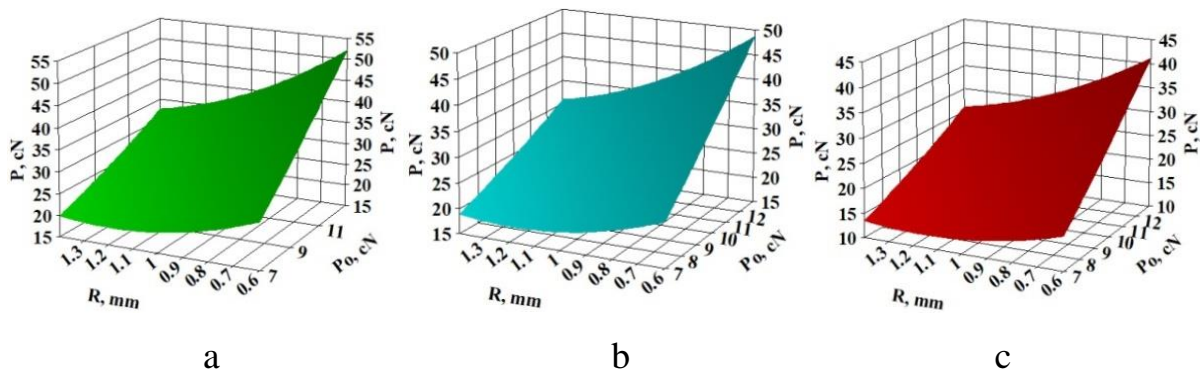
Figure 5.16 Response surfaces for the second series of experiments for variants 2-4: a – for polyamide filament yarn 29 Tex, flat twist Kr = 100 twists/meter (variant 2); b – for polyamide filament yarn 29 Tex, middle twist Kr = 400 twists/meter (variant 3); c – for polyamide filament yarn 29 Tex, hard twist Kr = 800 twists/meter (variant 4)

For the nominal value of the braid angle $\varphi_P = 135^0$, tension of fabric before the cylindrical guide way $P_0 = 10\ cN$, the equations (5.27)-(5.29) are converted as follows in the middle of the experiment:

for polyamide filament yarn 29 Tex, flat twist (variant 2)

$$P_2 = 63.62 - 53.45R + 18.77R^2 \qquad (5.30)$$

for the polyamide yarn of medium twist 29 Tex (variant 3)

$$P_3 = 58.03 - 47.21R + 16.55R^2 \, , \qquad (5.31)$$

for the flat-twisted polyamide yarn 29 Tex (variant 4)

$$P_4 = 46.72 - 38.78R + 13.66R^2 \, . \qquad (5.32)$$

Figure 5.17 shows graphic dependences of the change in the tension of fabric after the cylindrical guide way (the second series of experiments), which were obtained using the dependences (5.30)-(5.32). For variants 2-4, for polyamide filament yarns, the tension P decreases when the radius R of the cylindrical guide way is increased. This is explained by the fact that the yarn surface deformation is decreased in the contact area and, therefore, the value of the braid angle for the cylindrical guide way also decreases.
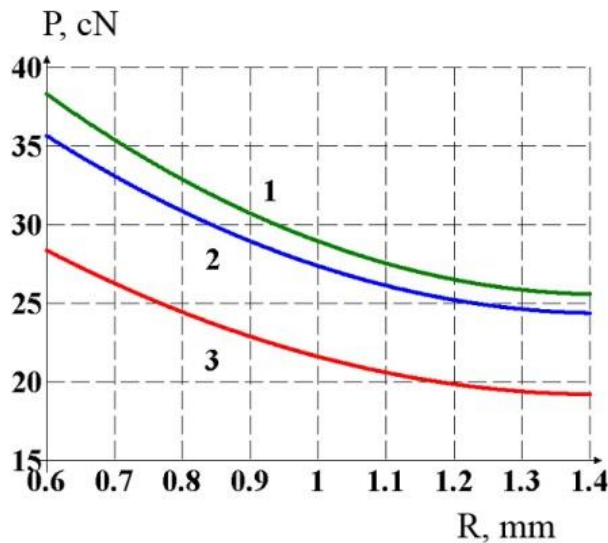
Figure 5.17 Graphic dependences of the change in the tension of fabric after the cylindrical guide way (the second series of experiments, variants 2-4)

The results obtained can be used to optimize the technological process of manufacturing filter fabrics from polyamide filament yarns and monofilament yarns, when it is possible, at the initial stage, to determine the intensity of the fabric formation process.

As a result of the comprehensive experimental research to determine the effect of the yarn structure on the tension degree when interacting with high-

curved guide ways, regression dependencies were obtained for polyamide monofilament yarns and filament yarns that made it possible to determine the effect of their structure, tension before the guide way surface, radius of the high-curved cylindrical guide way surface and the nominal braid angle for the guide way on the tension degree after the guide way.

Two series of experimental research were implemented: for the change in the tension of fabric P_0 before the cylindrical guide way in the range from $27.6 \ cN \le P_0 \le 32.4 \ cN$ (the first series); for the change in the tension of fabric P_0 before the cylindrical guide way in the range from $7.6 \ cN \le P_0 \le 12.4 \ cN$ (the second series). In the first series, for four types of polyamide yarns (variant 1 – polyamide monofilament yarn 36.3 Tex, variant 2 – polyamide filament yarn 29 Tex of flat twist, variant 3 – polyamide filament yarn 29 Tex of medium twist, variant 4 – polyamide filament yarn 29 Tex of hard twist) patterns in the change of the output tension were determined depending on the radius of the cylindrical guide way curve. In the second series, for variants 2-4, regression dependencies were obtained to determine the joint effect of the tension of fabric before the cylindrical guide way P_0, the radius of the cylindrical guide way R and the nominal value of the braid angle φ_P on the tension of fabric behind the cylindrical guide way P.

The results obtained enable optimization of yarn processing using production equipment, to reduce yarn breakage and to improve performance.

The results obtained can be used to improve technological processes in the textile and knitwear production.

6. DETERMINING TENSION OF YARNS WHEN INTERACTING WITH GUIDES AND OPERATIVE PARTS OF TEXTILE MACHINERY HAVING THE TORUS FORM

Improvement of technological processes for weaving and knitting production shall mean optimization of technological efforts based on minimization of yarn tension in the area of fabric and knit formation [8]. Determining of yarn tension degree in the working area of technological machine when rewinding spun yarn [2-4], of weaving loom [5-6], knitting machine [27] makes it possible to evaluate intensity of running technological process. Main characteristic property of most Technological processes in textile industry is interaction between yarns and guide and operative parts, when guide's surface curvature radius in the area of contact is comparable to the yarn or spun yarn diameter [8]. Figure 6.1a represents cases of interaction between the yarn and guide and operative parts of knitting machines. Figure 6.1b represents cases of interaction between the yarn and operative parts of weaving looms.
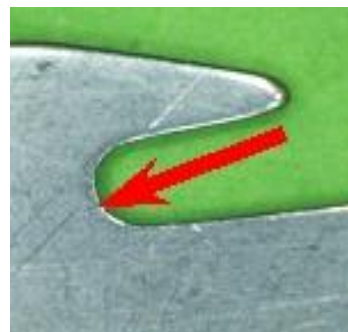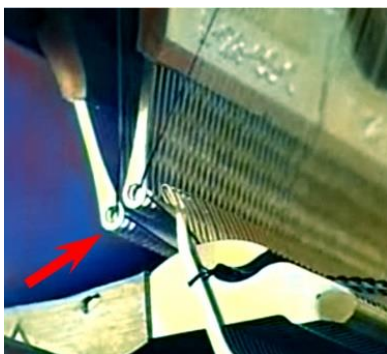
a
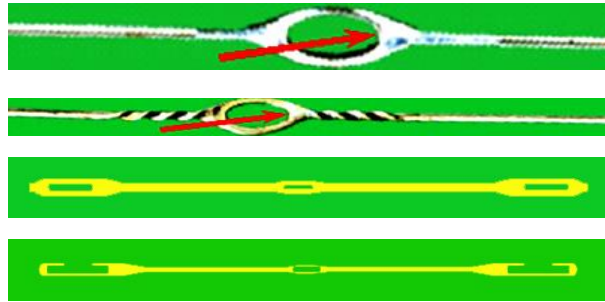
b
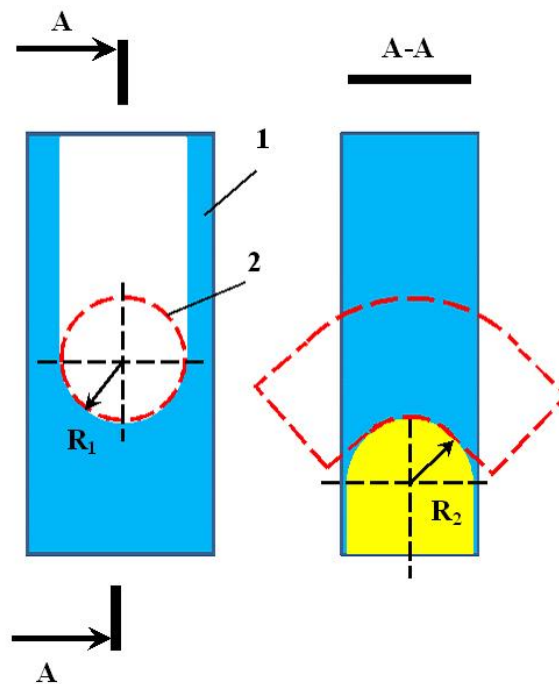
c

Figure 6.1 interaction of yarn with high-curved guides at the textile machinery: a – c with guides and operative parts of knitting machines; b – c with operative parts of weaving looms; c – designed diagram of interaction between yarn and guide having the form of torus; 1 – fragment of guide surface; 2 – yarn; R_1 -

radius of internal circumference of torus; R_2 - radius of working circumference of torus

Figure 6.1c represents designed diagram of interaction between a yarn and guide surface having the form of torus when guide's curve radius and yarn diameter radius are comparable with each other. Analysis of interaction diagram shows that ratio of the radius of internal circumference of torus R_1 to the radius of the working circumference R_2, contact angle between the yarn and the working surface of torus' circumference, radial contact angle between the yarn and internal surface of torus [8] are of great significance. Interaction between the yarn and guide surface, if there exists a radial contact with that surface, occur during fabric element and new course of knitted fabric formation [27].

Such a complex type of interaction requires taking into account the direction of the yarn's friction surfaces and guide surface [11], as well as relative motion of moved material [8]. In our paper [1-2] we underline the necessity to take into account twists of multifilament and spun yarn and value of its bending modulus. Bending modulus has significant effect on the value of the actual contact angle between the yarn and the guide surface. The above has been proved in our paper [27] during research of conditions of interaction between polyamide multifilament or polyamide monofilament and guide surface. The mentioned papers consider cases of interaction between the yarn and high curved guide surfaces regardless of radial contact with the yarn surface in the contact area.

Our papers show the results of experimental determining of the yarn tension with a help of special units [23, 27]. It is impossible to use the obtained results when performing research of interaction between the yarn and high-curved guide, in case there is a radial contact with the yarn surface in the contact area. To contribute to increase accuracy of dimensions and possibilities to ensure metrological self-control in is better to use the redundant measurements method, which makes the measurements result independent of conversion function parameters and their deviation from nominal values [27]. Design of experimental

unit determines the accuracy of results receives when determining the yarn tension. The paper [8] shows the diagram for determination of the yarn tension, which uses cylinders with big radii as guides. The mentioned diagram has its disadvantages. Using this diagram, it is impossible to simulate actual conditions of interaction between the yarn and guide and operative parts of weaving looms and knitting machines. The experimental unit with rotating cylinder has similar disadvantages [27]. The paper [8] represents results of determining tension value for wide spectrum of guide surfaces having the form of cylinder. During the experiment, however, there was no radial contact between the yarn and guide surface. Absence of such contact limits the use of obtained results in terms of analysis of conditions pf interaction between the yarn and the actual guide and operative parts of weaving looms and knitting machines.

Four types of yarn have been chosen for experiment. SN1 series: carded cotton spun yarn 29x2 Tex. It is used as warp yarns for production of tartan (spring-autumn twill fabric), and knitted fabric (for outer garments and body linen). SN2 series: woolen spun yarn 31x2 Tex. It is used as warp yarns to produce pure-wool twill suiting (for knitted outer garments, small part also for winter and sports hosiery, as well as hand-wear). SN3 series: linen wet-spun yarn made of bleached roving 41 Tex, obtained from dressed flax. It is used as warp yarns to produce sindon, knitted fabric LN-1 and LN-2 for outer garment. SSA series: polyamide multifilament 29x2 Tex. It is used as warp yarns of outer protective layers of multilayer technical fabrics (MTF) for laying yard-coated pipes, as well as for knitting of outer knitwear and sportswear.

For four series SN1, SN2, SN3 and SSA an orthogonal second-order plan for three factors was designed and implemented in the paper [9, 20]. The general view of the regression equation to determine the joint effect of the yarn tension prior it goes to the guide having the form of torus P_0, ratios of radius of internal circumference of torus R_1 to working circumference radius R_2, and the nominal

value of the contact angle φ_p on the yarn tension behind the guide having the form of torus P, is as follows

$$P = b_0 + b_1 x_1 + b_2 x_2 + b_3 x_3 + b_{12} x_1 x_2 + b_{13} x_1 x_3 + b_{23} x_2 x_3 +$$
$$+ b_{11} x_1^2 + b_{22} x_2^2 + b_{33} x_3^2.$$

(6.1)

The range of factor variation in the equation (6.1) was determined by the actual yarn processing conditions. In the blinded values: yarn tension before it goes to the guide having the form of torus P_0 was indicated as x_1; ratio of the radius of internal circumference of torus R_1 to working circumference radius R_2 was indicated as x_2; the nominal value of the contact angle φ_p was indicated as x_3. While determining ratio of radius of internal circumference of torus R_{1S1} to working circumference radius R_{2S1} the diameter of carded cotton spun yarn 29x2 Tex, which is 0.31 mm is taken into account. Therefore, in the middle of the experiment, radius of working circumference of torus R_{2S1} takes on the value of 0.35 mm. Radius of internal circumference of torus R_{1S1} is determined by geometrical dimensions of the operative parts of weaving looms, knitting machines, and textile looms (needles and sinkers of knitting machines, heddles of the textile looms). Radii values were determined using USB Digital microscope Sigeta (Figure 6.2). In the middle of the experiment, to exclude the yarn jamming the R_{1S1} takes on the value of 0.6 mm. Table 1 shows values of ratio of radius of internal circumference of torus R_{1S1} to radius of working circumference R_{1S1} in the blinded values.

Factor x_3 is a nominal value of contact angle for knitting machines when producing knitted fabric for outer garments and body linen, for needles and sinkers it changes within the range from $\varphi_{pS1} = 60^0$ to $\varphi_{pS1} = 180^0$. When producing tartan (spring-autumn twill fabric) the maximum nominal value of contact angle (heddle eye) for shuttle looms is $\varphi_{pS1} = 29^0$ in case of open shed. The same for shuttleless looms will be $\varphi_{pS1} = 22^0$; and pneumatic type rapier looms it will be $\varphi_{pS1} = 41^0$. Taking into account the above values it takes up in the

middle of the experiment the value of nominal contact angle of guide surface having the form of torus 95^0.

Table 6.1

Second-order orthogonal matrix for series SN1 for carded cotton spun yarn 29x2 Tex

№	Factors					
	Input tension		Torus radii ratio		Contact angle	
	x_1	$P_{0S1, cN}$	x_2	R_{1S1}/R_{2S1}	x_3	φ_{pS1}, degrees
1	+1	27	+1	2	+1	105
2	-1	23	+1	2	+1	105
3	+1	27	-1	1.4	+1	105
4	-1	23	-1	1.4	+1	105
5	+1	27	+1	2	-1	85
6	-1	23	+1	2	-1	85
7	+1	27	-1	1.4	-1	85
8	-1	23	-1	1.4	-1	85
9	-1.215	22.6	0	1.7	0	95
10	+1.215	27.4	0	1.7	0	95
11	0	25	-1.215	1.3	0	95
12	0	25	+1.215	2.1	0	95
13	0	25	0	1.7	-1.215	83
14	0	25	0	1.7	+1.215	107
15	0	25	0	1.7	0	95

The correlation between the open-label and blinded values of series SN1 for carded cotton spun yarn 29x2 Tex is as follows

$$x1 = \frac{P_{0S1} - 25}{2}, \quad x2 = \frac{R_{1S1} / R_{2S1} - 1.7}{0.3}, \quad x3 = \frac{\phi_{PS1} - 95}{10}. \tag{6.2}$$

Table 6.2 shows a second-order orthogonal matrix for series SN2. Factor x_1 is a yarn tension prior the yarn goes to the guide having the form of torus, in the middle of the experiment for woolen spun yarn 31x2 Tex it is taken up as relatively equal to filling tension of warp yarns. During production of pure-wool twill suiting, outer knitted garments, hosiery of winter and spots assortment, as well as handwear this value will be $P_{0S2} = 22$ cN.

When determining ratio of radius of internal circumference of torus R_{1S2} to radius of working circumference R_{2S2} the diameter of woolen spun yarn 31x2 Tex, which is 0.34 mm shall be taken into account. Therefore, in the middle of the experiment, the radius of working circumference of torus R_{2S2} is taken up as equal to 0.35 mm. The radius of internal circumference of torus R_{1S2} is determined by geometrical dimensions of operative parts of knitting machines and textile looms. Values of radii were determined using USB Digital microscope Sigeta (figure 2). In the middle of the experiment, to exclude yarn jamming the value of R_{1S2} was taken up as equal to 0.8 mm. Table 6.2 shows values of ratio of radius of internal circumference of torus R_{1S2} to the radius of working circumference R_{2S2} in blinded values.

Table 6.2

Orthogonal matrix for series SN2 for woolen spun yarn 31x2 Tex

№	Factors					
	Input tension		Torus radii ratio		Contact angle	
	x_1	$P_{0S2, cN}$	x_2	R_{1S2}/R_{2S2}	x_3	φ_{pS2}, degrees
1	+1	24	+1	2.9	+1	105
2	-1	20	+1	2.9	+1	105
3	+1	24	-1	1.7	+1	105
4	-1	20	-1	1.7	+1	105

5	+1	24	+1	2.9	-1	85
6	-1	20	+1	2.9	-1	85
7	+1	24	-1	1.7	-1	85
8	-1	20	-1	1.7	-1	85
9	-1.215	19.6	0	2.3	0	95
10	+1.215	24.4	0	2.3	0	95
11	0	22	-1.215	1.6	0	95
12	0	22	+1.215	3	0	95
13	0	22	0	2.3	-1.215	83
14	0	22	0	2.3	+1.215	107
15	0	22	0	2.3	0	95

The correlation between the open-label and blinded values of series SN2 for woolen spun yarn 31x2 Tex is as follows

$$x1 = \frac{P_{0S2} - 22}{2}, \quad x2 = \frac{R_{1S2} / R_{2S2} - 2.3}{0.6}, \quad x3 = \frac{\phi_{PS2} - 95}{10}. \tag{6.3}$$

Table 6.3 shows a second-order orthogonal matrix for series SN3. Factor x_1 is yarn tension prior the yarn goes to the guide having the form of torus, in the middle of the experiment for linen wet-spun yarn made of bleached roving 41 Tex it is taken up as relatively equal to filling tension of warp yarns. During production of sindon, knitted fabric LN-1 and LN-2 for outer garments this value will be equal to $P_{0S3} = 28$ cN.

When determining the ratio of radius of internal circumference of torus R_{1S3} to radius of working circumference R_{2S3} the diameter of linen wet-spun yarn made of bleached roving 41 Tex which equals 0.28 mm is taken into account. Therefore, in the middle of experiment, radius of working circumference of torus R_{2S3} is taken up as 0.35 mm. The radius of internal circumference of torus R_{1S3} is determined due to geometrical dimensions of operative parts of knitting machines and textile looms. In the middle of experiment, to exclude yarn

jamming the value of R_{1S3} is taken up as 0.5 mm. Table 3 shows the ratios of radius of internal circumference of torus R_{1S3} to radius of working circumference R_{2S3} in blinded values.

Table 6.3

Orthogonal matrix for series SN3 for linen wet-spun yarn made of bleached roving 41 Tex

№	Factors					
	Input tension		Torus radii ratio		Contact angle	
	x_1	$P_{0S3, cN}$	x_2	R_{1S3}/R_{2S3}	x_3	φ_{pS3}, degrees
1	+1	30	+1	1.7	+1	105
2	-1	26	+1	1.7	+1	105
3	+1	30	-1	1.1	+1	105
4	-1	26	-1	1.1	+1	105
5	+1	30	+1	1.7	-1	85
6	-1	26	+1	1.7	-1	85
7	+1	30	-1	1.1	-1	85
8	-1	26	-1	1.1	-1	85
9	-1.215	25.6	0	1.4	0	95
10	+1.215	30.4	0	1.4	0	95
11	0	28	-1.215	1	0	95
12	0	28	+1.215	1.8	0	95
13	0	28	0	1.4	-1.215	83
14	0	28	0	1.4	+1.215	107
15	0	28	0	1.4	0	95

The correlation between the open-label and blinded values of series SN3 for linen wet-spun yarn made of bleached roving 41 Tex is as follows

$$x1 = \frac{P_{0S3} - 28}{2}, \quad x2 = \frac{R_{1S3} / R_{2S3} - 1.4}{0.3}, \quad x3 = \frac{\phi_{PS3} - 95}{10}. \tag{6.4}$$

Table 6.4 shows a second-order orthogonal matrix for series SSA. Factor x_1 is yarn tension prior the yarn goes to the guide having the form of torus, in the middle of the experiment for polyamide multifilament 29x2 Tex it is taken up as relatively equal to filling tension of warp yarns. When producing multilayer technical fiber MTF for laying yard-coated pipes, knitting outer knitted and sports garments this value will be $P_{0SA} = 35$ cN.

When determining the ratio of radius of internal circumference of torus R_{1SA} to radius of working circumference R_{2SA} the diameter of polyamide multifilament 29x2 Tex, which is 0.29 mm, is taken into account. Therefore, in the middle of experiment, the radius of working circumference R_{2SA} is taken up as 0.35 mm. The radius of internal circumference of torus R_{1SA} shall be determined based on geometrical dimensions of operative parts of knitting machines and textile looms. Values of radii were determined using USB Digital microscope Sigeta (figure 2). In the middle of the experiment, to exclude yarn jamming, the value R_{1SA} is taken up as 0.55 mm. Table 4 shows values of ratio of radius of internal circumference of torus R_{1SA} to radius of working circumference R_{2SA} in blinded values.

Table 6.4

Orthogonal matrix for series SSA for polyamide multifilament 29x2 Tex

№	Factors					
	Input tension		Torus radii ratio		Contact angle	
	x_1	$P_{0SA, cN}$	x_2	R_{1SA}/R_{2SA}	x_3	φ_{pSA}, degrees
1	+1	37	+1	1.9	+1	105
2	-1	33	+1	1.9	+1	105
3	+1	37	-1	1.3	+1	105

4	-1	33	-1	1.3	+1	105
5	+1	37	+1	1.9	-1	85
6	-1	33	+1	1.9	-1	85
7	+1	37	-1	1.3	-1	85
8	-1	33	-1	1.3	-1	85
9	-1.215	32.6	0	1.6	0	95
10	+1.215	37.4	0	1.6	0	95
11	0	35	-1.215	1.2	0	95
12	0	35	+1.215	2	0	95
13	0	35	0	1.6	-1.215	83
14	0	35	0	1.6	+1.215	107
15	0	35	0	1.6	0	95

The correlation between the open-label and blinded values of series SSA for polyamide multifilament 29x2 Tex is as follows

$$x1 = \frac{P_{0SA} - 35}{2}, \quad x2 = \frac{R_{1SA}/R_{2SA} - 1.6}{0.3}, \quad x3 = \frac{\phi_{PSA} - 95}{10}. \tag{6.5}$$

Values of radii of guide having the form of torus were determined using USB Digital microscope Sigeta (figure 6.2).

Figure 6.2 Installation to determine radii of guide having the form of torus

yarns/decimetre); 5 - MTF – 9 (density of weft yarns 140 yarns/decimetre)

Figure 6.3 shows the diagram of experimental unit. Its set-up is described in detail in the paper [8, 27]. The distinction is that unit 4 of modelling the conditions of interaction between guides and operative parts of textile looms and knitting machines, which have the form of torus in the contact area with a yarn, includes a set of needles and sinkers, and heddles of knitting loom. The diameter of the working surface of torus commensurate with diameter of the processed yarns.
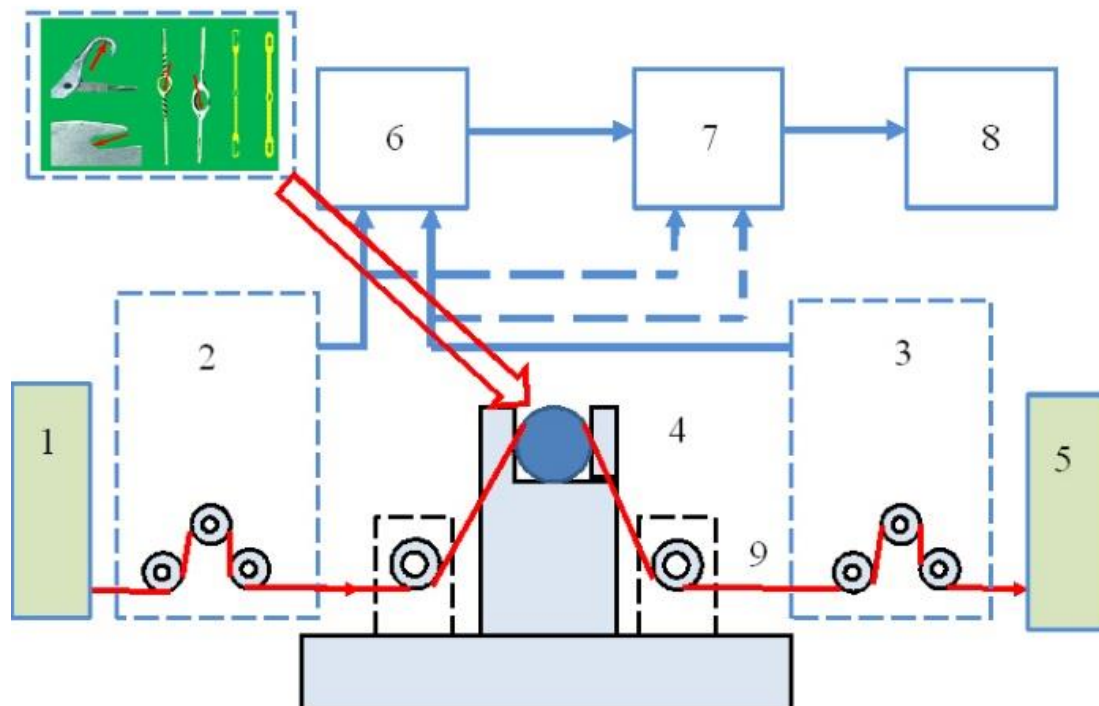
Figure 6.3 installation to determine radii of guide having the form of torus

yarns/decimetre); 5 - MTF – 9 (density of weft yarns 140 yarns/decimetre)

The diagram of the experimental unit: 1 - yarn feeder unit; 2 - unit for measuring the yarn tension's slack side; 3 - unit for measuring the yarn tension's slack side; 4 - unit for modelling the conditions of interaction with guides and operative parts of textile machines; 5 – yarn receiver unit; 6 – driver; 7 – analog-to-digital converter ADC; 8 – personal computer; 9 – yarn.

As a result of implementation of second-order orthogonal designs for three factors (tables 1-4) for series SN1-SN3 and SSA about 10 parallel measurements were performed. Its mean values are shown in Table 6.5.

Table 6.5

Results of the series of the experimental research to determine the joint effect of the yarn tension prior it goes to the guide having the form of torus P_0, the ratios of radius of internal circumference of torus R_1 to the radius of working circumference R_2, and nominal values of the contact angle φ_P to the yarn tension P behind the guide having the form of torus (series SN1-SN3 and SSA)

№	Factors			P_1, cN	P_2, cN	P_3, cN	P_{SA}, cN
	x_1	x_2	x_3				
1	+1	+1	+1	49.6	36.3	31.9	70.5
2	-1	+1	+1	40.5	29.4	27.7	60.8
3	+1	-1	+1	50.3	36.8	32.1	71.7
4	-1	-1	+1	41.1	29.8	27.8	61.8
5	+1	+1	-1	44.8	33.8	31.6	63.6
6	-1	+1	-1	36.9	27.4	27.4	55.1
7	+1	-1	-1	45.4	34.2	31.7	64.5
8	-1	-1	-1	37.3	27.8	27.4	55.9
9	-1.215	0	0	38.1	27.9	27.1	57.5
10	+1.215	0	0	48.3	35.9	32.2	68.4
11	0	-1.215	0	43.6	32.1	29.9	63.7
12	0	+1.215	0	42.8	31.6	29.6	62.3
13	0	0	-1.215	40.6	30.5	29.5	59.1
14	0	0	+1.215	45.7	33.2	29.9	66.8
15	0	0	0	43.1	31.8	29.7	62.9

Using the known method of determining the coefficients in the regression equation (6.1) for the second-order orthogonal plan [8, 27], taking into account the relationships (6.2)-(6.5), the following regression relationships were determined.

Series SN1, for carded cotton spun yarn 29x2 Tex, the range of change in input tension $22.6\ cN \le P_{0S1} \le 27.4\ cN$:

$$
\begin{aligned}
P_{S1} = &15.07 + 0.081 P_{0S1} - 0.3Z1 - 0.17 \varphi_{PS1} + 0.02 P_{0S1} \varphi_{PS1} - 0.07 P_{0S1} Z1 - \\
&-0.01 Z1 \varphi_{PS1} + 0.02 P_{0S1}^2 + 0.7 Z1^2 + 0.0002 \varphi_{PS1}^2, \quad Z1 = R_{1S1} / R_{2S1}.
\end{aligned}
\tag{6.6}
$$

Series SN2, for woolen spun yarn 31x2 Tex, the range of change in input tension $19.6\ cN \le P_{0S2} \le 24.4\ cN$:

$$
\begin{aligned}
P_{S2} = &12.6 + 0.22 P_{0S2} - 0.52Z2 - 0.12 \varphi_{PS2} + 0.007 P_{0S2} \varphi_{PS2} - 0.01 P_{0S2} Z2 - \\
&-0.002 Z2 \varphi_{PS2} + 0.02 P_{0S2}^2 + 0.1 Z2^2 - 0.0004 \varphi_{PS2}^2, \quad Z2 = R_{1S2} / R_{2S2}.
\end{aligned}
\tag{6.7}
$$

Series SN3, for linen wet-spun yarn made of bleached roving 41 Tex, the range of change in input tension $25.6\ cN \le P_{0S3} \le 30.4\ cN$:

$$
\begin{aligned}
P_{S3} = &1.52 P_{0S3} + 0.79Z3 + 0.029 \varphi_{PS3} - 0.04 P_{0S3} Z3 - \\
&-0.008 Z3 \varphi_{PS3} - 0.007 P_{0S3}^2 + 0.3 Z3^2 - 8.68, \quad Z3 = R_{1S3} / R_{2S3}.
\end{aligned}
\tag{6.8}
$$

Series SSA, for polyamide multifilament 29x2 Tex, the range of change in input tension $32.6\ cN \le P_{0SA} \le 37.4\ cN$:

$$
\begin{aligned}
P_{SA} = &9.69 + 0.57 P_{0SA} + 0.79 Z_{SA} - 0.22 \varphi_{PSA} + 0.015 P_{0SA} \varphi_{PSA} - 0.07 P_{0S2} Z_{SA} - \\
&-0.02 Z_{SA} \varphi_{PSA} + 0.01 P_{0SA}^2 + 0.56 Z_{SA}^2 + 0.0002 \varphi_{PSA}^2, \quad Z_{SA} = R_{1SA} / R_{2SA}.
\end{aligned}
\tag{6.9}
$$

For nominal value of contact angle in the middle of experiment $\varphi_P = 95^0$, when determining changes in yarn tension behind the guide surface having the form of torus, the equations (6.6)-(6.9) are converted as follows:

series SN1, for carded cottong spun yarn 29x2 Tex, the range of change in input tension $22.6\ cN \le P_{0S1} \le 27.4\ cN$:

$$
\begin{aligned}
&P_{S1} = 0.73 + 1.98 P_{0S1} - 1.25Z1 - 0.07 P_{0S1} Z1 + 0.02 P_{0S1}^2 + 0.7 Z1^2, \\
&Z1 = R_{1S1} / R_{2S1},
\end{aligned}
\tag{6.10}
$$

series SN2, for woolen spun yarn 31x2 Tex, the range of change in input tension $19.6 \; cN \le P_{0S2} \le 24.4 \; cN$:

$$P_{S2} = 4.81 + 0.89 P_{0S2} - 0.71 Z2 - 0.01 P_{0S2} Z2 + 0.02 P_{0S2}^2 + 0.1 Z2^2,$$
$$Z2 = R_{1S2} / R_{2S2},$$

(6.11)

series SN3, for linen wet-spun yarn made of bleached roving 41 Tex, the range of change in input tension $25.6 \; cN \le P_{0S3} \le 30.4 \; cN$:

$$P_{S3} = 1.52 P_{0S3} + 0.03 Z3 - 0.04 P_{0S3} Z3 - 0.0075 P_{0S3}^2 + 0.3 Z3^2 - 5.93,$$
$$Z3 = R_{1S3} / R_{2S3},$$

(6.12)

series SSA, for polyamide multifilament 29x2 Tex, the range of change in input tension $32.6 \; cN \le P_{0SA} \le 37.4 \; cN$:

$$P_{SA} = 1.99 P_{0SA} - 1.11 Z_{SA} - 0.067 P_{0S2} Z_{SA} + 0.005 P_{0SA}^2 + 0.56 Z_{SA}^2 - 9.03,$$
$$Z_{SA} = R_{1SA} / R_{2SA}.$$

(6.13)

Figure 6.4 shows the response surfaces for series SN1-SN3 and SSA. Yarn tension behind the guide surface having the form of torus is represented by functions, that take into account joint effect of yarn tension before the yarn goes to the guide having the form of torus P_0, ratios Z of radius of internal circumference of torus R_1 to radius of working circumference R_2. Nominal value of the contact angle φ_p was fixed value. Such value corresponded to the middle of the experiment (tables 6.1-6.4). Adequacy of the obtained regression relationships was tested using SPSS program for statistical processing of experimental data [8, 22, 23, 27].

For nominal value of contact angle $\varphi_P = 95^0$, having fixed value of the input tension, the equations (10)-(13) are converted as follows:

series SN1, for carded cotton spun yarn 29x2 Tex, with the value of input tension in the middle of experiment $P_{0S1} = 25$ cN:

$$P_{S1} = 62.75 - 3 Z1 + 0.7 Z1^2, \quad Z1 = R_{1S1} / R_{2S1},$$

(6.14)

series SN2, for woolen spun yarn 31x2 Tex, with the value of input tension in the middle of experiment $P_{0S2} = 22$ cN:

$$P_{S2} = 33.96 - 0.93Z2 + 0.1Z2^2, \quad Z2 = R_{1S2} / R_{2S2}, \tag{6.15}$$

series SN3, for linen wet-spun yarn made of bleached roving 41 Tex, with the value of input tension in the middle of experiment $P_{0S3} = 28$ cN:

$$P_{S3} = 30.76 - 1.09Z3 + 0.3Z3^2, \quad Z3 = R_{1S3} / R_{2S3}, \tag{6.16}$$

series SSA, for polyamide multifilament 29x2 Tex, with the value of input tension in the middle of experiment $P_{0SA} = 35$ cN:

$$P_{SA} = 66.93 - 3.46Z_{SA} + 0.56Z_{SA}^2, \quad Z_{SA} = R_{1SA} / R_{2SA}. \tag{6.17}$$

a

b

c

d
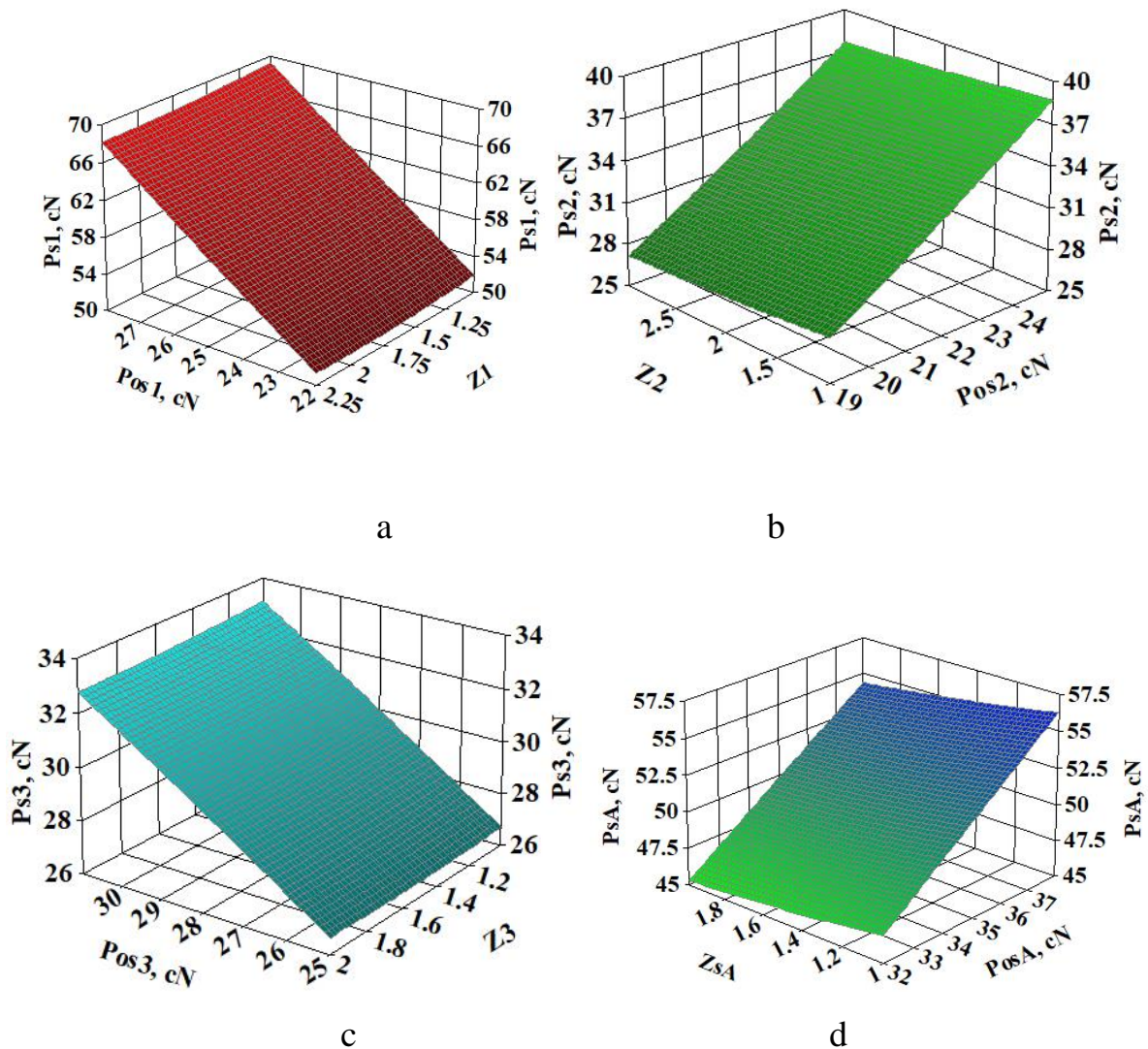
Figure 6.4 response surfaces for series SN1-SN3 and SSA: a - for cotton carded spun 29x2 Tex (series SN1); b – for woolen spun yarn 31x2 Tex (series SN2); c - for linen wet-spun yarn made of bleached roving 41 Tex (series SN3); d - for polyamide multifilament 29x2 Tex (series SSA)

Equations (6.14)-(6.17) were used to obtain values for yarn tension behind guide surface having the form of torus depending upon ratio Z of radius of internal circumference of torus R_1 to radius of working circumference R_2, which are represented in table 6.6.

Table 6.6

Values of yarn tension behind the guide surface having the form of torus depending on ratio *Z* of radius of internal circumference of torus *R₁* to radius of working circumference *R₂*

Z	Yarn tension values behind the guide surface having the form of torus			
	SN1	SN2	SN3	SSA
1	60.45	33.13	29.97	64.03
1.1	60.29	33.05	29.92	63.80
1.2	60.15	32.98	29.88	63.58
1.3	60.03	32.92	29.85	63.37
1.4	59.92	32.85	29.82	63.18
1.5	59.82	32.79	29.80	63.00
1.6	59.74	32.72	29.78	62.82
1.7	59.67	32.66	29.79	62.67
1.8	59.61	32.61	29.75	62.51
1.9	59.57	32.55	29.76	62.37
2.0	59.55	32.50	29.78	62.25

Figure 6.5 shows curves reflecting the changes in yarn tension behind guide surface having the form of torus depending on ratio *Z* of radius of internal circumference of torus R_1 to radius of working circumference R_2. These curves were fitted according to the data from Table 6.6.
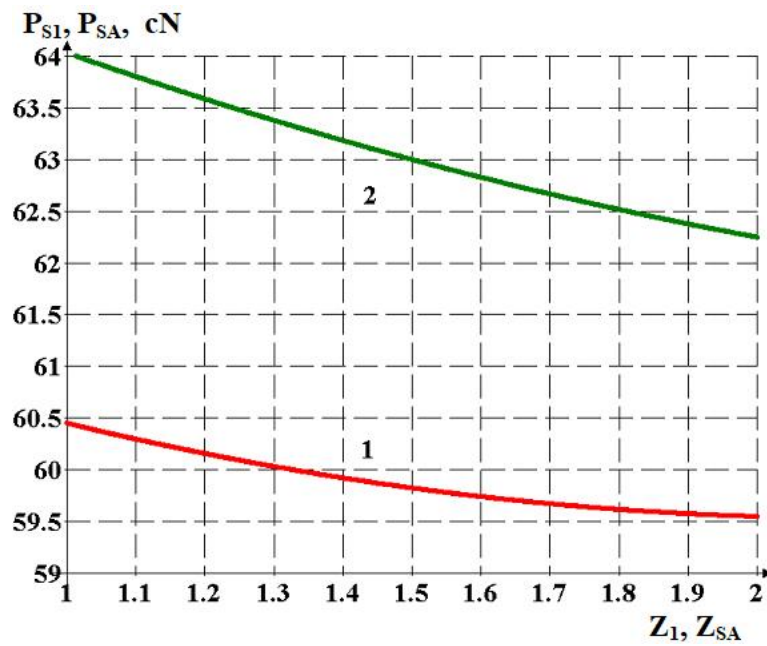
a
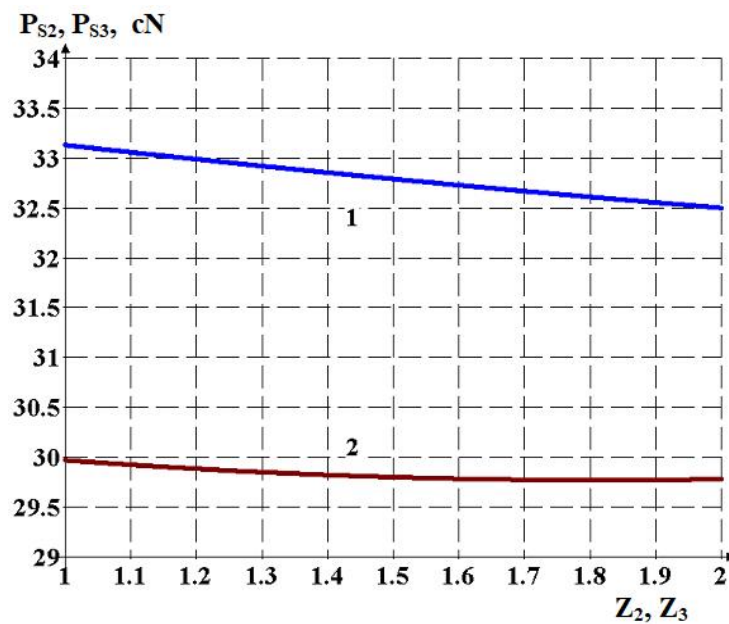
b

Figure 6.5 Curves reflecting the changes in yarn tension behind guide surface
having the form of torus depending on ratio of radius of internal circumference of
torus to radius of working circumference: a - series SN1(1), series SSA(2); b -
series SN2(1), series SN3(2)

Analysis of the above curves (figures 6.5a, 6.5b) shows that value of tension behind the guide surface having the form of torus decreases with the value of ratio Z of radius of internal circumference of torus R_1 to radius of working circumference R_2 (figure 6.1c) increase. It can be explained by decrease of value of contact angle of the lateral surface of yarn in the contact are with guide surface having the form of.

Obtained results may be used for optimization of technological processes in weaving and knitting productions with relation to minimization of the yarn tension in the working area, where knitted fabric and fabric are formed.

Improvement of a technological process in weaving and knitting production means optimization of technological efforts based on minimizing of yarn tension in the fabric and knitted fabric formation area. The research related to determining of the yarns tension when interacting with guide and operative parts of weaving looms and knitting machines having the form of torus in the area of contact with yarn established the mechanism of yarn tension increase behind the guide having the torus form due to change in geometrical dimensions and friction forces within contact area.

The regression relationships were obtained resulting from delivery of series of experimental researches to determine joint effect of yarn tension prior it goes to guide having the form of torus P_0, ratio of radius of internal circumference of torus R_1 to radius of working circumference R_2, and nominal value of contact angle φ_P on yarn tension P behind the guide having the form of torus for carded cotton spun yarn 29x2 Tex (input tension variation range $22.6\ cN \le P_{0S1} \le 27.4\ cN$ - series SN1), for woolen spun yarn 31x2 Tex (input tension variation range $19.6\ cN \le P_{0S2} \le 24.4\ cN$ - series SN2), for linen wet-spun yarn made of bleached roving 41 Tex (input tension variation range $25.6\ cN \le P_{0S3} \le 30.4\ cN$ - series SN3), for polyamide multifilament 29x2 Tex (input tension variation range $32.6\ cN \le P_{0SA} \le 37.4\ cN$ - series SSA). It was

established that tension degree behind the guide surface having the form of torus becomes less while value of ratio Z of radius of internal circumference of torus R_1 to radius of working circumference R_2 increases. It can be explained by decrease of contact angle value for lateral surface of yarn in the area of contact with guide surface having the form of torus.

Obtained results and their usage make it possible to optimize yarn manufacturing process at the Texnological equipment in view of minimization of yarn tension in the working area, where fabric and knittedfabric are formed, to reduce yarn breakage, and to improve performance of weaving and knitting machines.

Obtained results can be used to improve Texnological processes in the fabric and knitted fabric production.

MAIN CONCLUSIONS

1. Tension of warp yarn, before it enters the weaving area, is the value which determines intensity of the weaving process and cloth structure. Increased value of warp yarn tension, before entering the fabric formation area, causes a spiralling number of breaks, and decreased value does not allow to ensure shed cleanliness. Tension of warp yarns, before they enter the fabric formation area, includes input tension and additional tension, arising by virtue of frictional forces between warp yarns and surfaces of guiding and working components of cylinder form or one close to it.

This work represents experimental research in interation between different in itself natural warp yarns and cylindrical surfaces imitating separating rod of yarn break detector, as well as heddle eye for automatic shuttleless pneumatic rapier looms. As a result of the experiment regression dependences were obtained between warp yarns and value of the cylinder radius, as well as between contact angle and warp yarn tension just before the guide. Consistent application of the data of regression dependences allows to determine warp yarns tension before

they enter the fabric formation area for different kinds of natural raw material of warp yarns for wide range of looms.

2. Yarn tension in looms is a value defining intensity of formation process, structure of knitted fabric. Increased value of yarn tension before it enters knitting area causes a spiraling number of breaks, and decreased value causes troubles for the process of lapping the yarn under the needle of the loom. Tension of yarns before they enter knitting area include its tension when going off the bobbin and additional tension arising by virtue of frictional forces between yarns and surfaces of guiding and working components of the loom having the torus form.

It is very difficult to determine yarn tension in the loom within the area of textile fabric formation from experiments. It's appropriate to apply recursive approach and to determine tension within the threading areas in the loom from going off the bobbin to knitting area. Our work presents experimental research of interaction between different in their nature natural, synthetic and artificial yarns and spun yarn and surfaces in the form of torus, simulating surfaces of the yarn guides, yarn break detectors, needles and push downs of the looms with two types of tackings: an umbrella tacking, which is placed above knitting area; a tacking which is placed on the floor. As a result of the experiment regression dependences were obtained between tension and guide curvature radius, contact angle and tension of yarn and spun yarn before the guide in the form of torus. Consistent application of regression dependences data allows determining tension of yarn and spun yarn within the knitting area for different types of natural yarns, for wide range of looms.

3. At present during construction and operational commissioning of main oil and gas lines pipes with external factory polyethylene coating are used. Comparing to field coating of pipelines with insulation material introduction of factory insulation of pipes technology allowed for both getting a boost of pipes construction and significantly improve efficiency of its anticorrosive protection.

In both, the first and the second, cases for backing up and laying pipes with external factory insulation coating the chains and cords cannot be used. Extreme pressure in the contact area leads to damage of insulation coating, inducing metal corrosion where sections with damaged insulation contact with water and soil.

Woven power grips are used for laying pipes with factory insulation coating. These grips are manufactured of multilayer technical fabrics. Structure of multilayer technical fabrics and conditions of its formation on a weaving machine determine effectiveness of the woven power grips manufacturing process.

In this work the improvement of multilayer technical fabric was conducted and experimental researches of its formation on the weaving machine were carried out. The influence was determined of wrap yarn input tension, value of different tension of shed and value of spade on value of beat-up force, main technological parameter determining intensity of fabric formation process.

The researches that were carried out allowed to improve the structure of the multilayer technical fabric. Comparative analysis of conditions of prototype formation and formation of proposed multilayer technical fabric on the weaving machine was carried out. Resulting from the experiment beat-up force value regression dependences on value of input tension of wrap yarns, different tension of shed and value of spade were obtained. Analysis of regression dependences allowed to determine optimal parameters of weaving machine threading.

4. The research of the yarn structure effect on the tension degree when interacting with guide ways and operative parts of weaving looms and knitting machines, which have a high curve in the area of contact with the yarn, has established the mechanism of fabric tension increase after it passes the guide way due to a change in the guide way's curve radius and friction forces in the contact area. It has been proved that the increase in tension is explained by a

change in the braid angle between the yarn and the high-curved guide way. At the same time, the actual braid angle for filament yarn and spun yarn will be higher than the nominal one due to yarn diameter deformation in the contact area, while the braid angle for monofilament yarns will be less than the nominal one due to the flexural modulus. Based on the experimental research, regression dependences of the output tension on the radius of guide way surface curve were obtained for polyamide filament yarns of various twists and monofilament yarns. The analysis of the research results made it possible to establish ultimate values of the guide way curve radius at which tension will have minimal degree. This will enable minimization of the tension of fabric during its processing on the production equipment. This leads to a decrease in yarn breakages, an increase in the production equipment performance by reducing its downtime, improving the quality of the fabric and knitted garments produced. This suggests a practical value of the proposed technology solutions. The latter, in particular, are related to determining optimal geometric dimensions of guide ways and operative parts of weaving looms and knitting machines, at which the output tension will have the minimal required degree.

Therefore, there is a good reason to claim the possibility of guided management of the process of changing the tension of fabric in weaving looms and knitting machines by choosing geometrical dimensions of high-curved guide ways for specific yarn types.

5. The research related to determining of the yarns tension when interacting with guide and operative parts of weaving looms and knitting machines having the form of torus in the area of contact with yarn established the mechanism of yarn tension increase behind the guide having the torus form due to change in geometrical dimensions and friction forces within contact area. It was proved that yarn tension increase behind the guide is effected by ratio of radius of internal circumference of torus to radius of working circumference; contact angle between yarn and working circumference of torus; radial contact angle

between the yarn and internal surface of torus; physico-mechanical and structural properties of yarn. For multifilament and spun yarn, the actual contact angle is more than nominal one due to yarn diameter distortion in the contact area with surface of torus. Values of contact angles between yarns and working circumference and values of radial contact angles between yarns and internal torus surface shall be determined according to geometrical dimensions and design of guide and operative parts of weaving looms and knitting machines.

The paper includes experimental research of interaction between different by its nature yarns and spun yarn (natural, synthetic, and man-made) and surfaces having the torus form imitating guide and operative parts of weaving looms and knitting machines. Based on experimental research the regression relationships between tension values behind the guide and ratio of radius of internal circumference of torus to working circumference radius, yarn tension prior it goes to guide and nominal value of contact angle were obtained for cotton, woolen, linen spun yarn, and polyamide multifilament. The analysis of the regression relationships made it possible to establish ultimate values of geometrical dimensions for guide having the form of torus when tension has its minimum value. This will enable minimization of the yarn tension during its processing on the weaving looms and knitting machines. This leads to a decrease in yarn breakages, an increase in the production equipment performance by reducing its downtime, improving the quality of the fabric and knitted garments produced. This suggests a practical value of the proposed technology solutions. These latter are related, in particular, to determining optimal geometric dimensions of guides and operative parts of weaving looms and knitting machines having the form of torus in the area of contact with yarn, at which the output tension will have the minimal required degree.

Therefore, there is a good reason to claim the possibility of guided management of the process of changing the yarn tension in weaving looms and knitting

machines by choosing geometrical dimensions of high-curved guide for specific yarn types.

REFERENCES

1. Ресурсоощадні технології виробництва текстилю, одягу та взуття: монографія: в 2 т. Т.1/Теоретичні основи та методи розроблення ресурсоощадних технологій та обладнання для виробництва текстилю, одягу та взуття/ В.Ю.Щербань, Б.Ф.Піпа, В.В.Чабан та ін. – К.:КНУТД, 2016. – 373 с.

2. Ресурсоощадні технології виробництва текстилю, одягу та взуття: монографія: в 2 т. Т.2/Підвищення надійності ресурсоощадних виробництв текстилю, одягу і взуття на основі новітніх технологій та системного управління/ В.Ю.Щербань, Б.Ф.Піпа, В.В.Чабан та ін. – К.:КНУТД, 2016. – 214 с.

3. Ресурсоощадні технології та обладнання швейної та текстильної промисловості: монографія: в 2 ч. Ч.1/Наукові основи та інженерні методи проектування ресурсоощадних технологій і обладнання швейної та текстильної промисловості/ В.Ю.Щербань, Г.Б.Параска, Б.В.Орловський та ін. – К.:КНУТД, 2015. – 339 с.

4. Ресурсоощадні технології та обладнання швейної та текстильної промисловості: монографія: в 2 ч. Ч.2/Шляхи підвищення ефективності швейної та текстильної галузей України на базі новітних технологій та управління/ В.Ю.Щербань, Г.Б.Параска, Б.В.Орловський та ін. – К.:КНУТД, 2015. – 270 с.

5. Прогнозування фізико-механічних властивостей текстильних матеріалів побутового призначення/А.М. Слізков , В.Ю. Щербань ,С.М. Краснитський , О.Б. Демківський. –К.:КНУТД, 2013. – 223 с.

6. Щербань В.Ю. Алгоритмічні, програмні та математичні компоненти САПР в індустрії моди/ В.Ю.Щербань, О.З.Колиско, М.І.Шолудько, В.Ю.Калашник. – К.:Освіта України, 2017. – 745 с.

7. Прогнозування процесів на основі моделювання часових рядів: навч. Посіб./П.І.Бідюк, В.Ю.Щербань, Є.О.Демківський, Т.І.Демківська.-К.:КНУТД, 2017.-324 с.

8. Щербань В.Ю. Механіка нитки/В.Ю.Щербань. – К.:Видавництво «Укрбланковидав». – 2018. – 533 с.

9. Щербань В.Ю. Базове проектуюче забезпечення САПР в індустрії моди/ В.Ю.Щербань, Ю.Ю.Щербань, О.З.Колиско, Г.В.Мельник, М.І.Шолудько, В.Ю.Калашник. – К.:Освіта України, 2018. – 902 с.

10. Щербань В.Ю. САПР складних систем: математичні, алгоритмічні та комп'ютерні програмні компоненти /В.Ю.Щербань, О.З.Колиско, Ю.Ю.Щербань, Г.В.Мельник, М.І.Шолудько, В.Ю.Калашник. – К.:Освіта України: ФОП Маслаков, 2020. – 923 с.

11. Vasilchenko V.N. Steady motion of a textile yarn with two anchoring points over a rough surface / V.N. Vasilchenko, V.Yu. Shcherban, Ts.V. Apokin // Technology of the textile industry. - 1985. - № 4. - P.54-56.

12. Vasilchenko V.N. Equilibrium of a filament of a root base in the zone of formation of a multilayer technical fabric / V.N. Vasilchenko, V.Yu. Shcherban // Technology of the textile industry. - 1986. - № 5. - P.44-47.

13. Vasilchenko V.N. Influence of the twist of a capron complex filament on the value of its flexural rigidity / V.N. Vasilchenko, V.Yu. Shcherban // Technology of the textile industry. - 1986. - №4. - P.8-9.

14. Scherban V.Yu. Determination of the geometric characteristics of the shape of the filament axis moving along the deformable guide surface / V.Yu. Shcherban // Technology of the textile industry. - 1990. - №6. - P.52-55.

15. Scherban V.Yu. Determination of technological efforts in the process of surf during the formation of multilayer technical fabric / V.Yu. Shcherban // Technology of the textile industry. - 1990. - №3. - P.44-47.

16. Scherban V.Yu. Investigation of the process of duck surf during the formation of multilayer technical fabric / V.Yu. Shcherban // Technology of the textile industry. - 1990. - №4. - P.41-44.

17. Yakubitskaya I.A. Dynamic analysis of layout conditions on the end sections of the groove of the winding drum / I.A. Yakubitskaya, V.V. Chugin, V.Yu. Shcherban // Technology of the textile industry. - 1997. - №5. - P.33-37.

18. Yakubitskaya I.A. Differential equations of the relative motion of the filament element on the end sections of the coil of the winding drum / I.A. Yakubitskaya, V.V. Chugin, V.Yu. Shcherban // Technology of the textile industry. - 1997. - №6. - P.50-54.

19. Shcherban' V.Yu. Interaction of stiff yarns with the working parts of knitting and sewing machines/V.Yu.Shcherban' // Textile industry. -1988. - № 10. - pp.53.

20. Vasil'chenko V.N., Shcherban' V.Yu., Apokin Ts.V. Attachment for holding multilayer fabrics in the clamps of a universal tensile tester/ V.N.Vasil'chenko , V.Yu.Shcherban' , Ts.V.Apokin // Textile industry. – 1987. - №8. - pp.62.

21. Shcherban' V., Melnyk G. , Sholudko M. and Kalashnyk V. Warp yarn tension during fabric formation/V.Shcherban' , G.Melnyk , M.Sholudko, V.Kalashnyk // Fibres and Textiles. – 2018. – volume 25. - №2. – pp.97-104.

22. Shcherban' V., Melnyk G. , Sholudko M., Kolysko O. and Kalashnyk V. Yarn tension while knitting textile fabric/V.Shcherban' , G. Melnyk , M.Sholudko , O.Kolysko, V.Kalashnyk// Fibres and Textiles. – 2018. - volume 25. - №3. - pp. 74-83.

23. Shcherban' V., Melnyk G. , Sholudko M., Kolysko O. and Kalashnyk V. Improvement of structure and technology of manufacture of multilayer technical

fabric/V.Shcherban' , G. Melnyk , M.Sholudko , O.Kolysko, V.Kalashnyk// Fibres and Textiles. – 2019. - volume 26 - № 2 - pp. 54-63.

24. Shcherban' V., Korogod G., Chaban V., Kolysko O., Shcherban' Yu., Shchutska G. Computer simulation methods of redundant measurements with the nonlinear transformation function / V. Shcherban', G. Korogod, V. Chaban, O. Kolysko, Yu. Shcherban', G. Shchutska // Eastern-European Journal of Enterprise Technologies. -   2019. - volume 98. -№2/5. – pp.16-22.

25. Shcherban' V., Makarenko J., Melnyk G., Shcherban' Y., Petko A., Kirichenko A. Effect of the yarn structure on the tension degree when interacting with high-curved guides/ V. Shcherban', J. Makarenko, G. Melnyk, Y. Shcherban', A. Petko, A. Kirichenko // Fibres and Textiles. – 2019. - volume 26 - № 4 - pp. 59-68.

26. Shcherban' V., Makarenko J., Petko A., Melnyk G., Shcherban' Yu., Shchutska G. Computer implementation of a recursion algorithm for determining the tension of a thread on technological equipment based on the derived mathematical dependences / V.Shcherban', J.Makarenko, A.Petko, G.Melnyk, Yu.Shcherban', G.Shchutska // Eastern-European Journal of Enterprise Technologies. -   2020. - volume 104. -№2/1. – pp.41-50.

27. Shcherban' V., Kolysko O., Melnyk G., Sholudko M., Shcherban' Y. and Shchutska G. Determining tension of yarns when interacting with guides and operative parts of textile machinery having the torus form / V. Shcherban', O. Kolysko, G. Melnyk, M. Sholudko, Y. Shcherban' and G. Shchutska // Fibres and Textiles. – 2020. - volume 27 - № 4 - pp. 87-95.

28. Shcherban' V., Korogod G., Kolysko O., Kolysko M., Shcherban' Yu., Shchutska G. Computer simulation of multiple measurements of logarithmic transformation function by two approaches / V. Shcherban', G. Korogod, O. Kolysko, M. Kolysko, Yu. Shcherban', G. Shchutska // Eastern-European Journal of Enterprise Technologies. -   2020. - volume 6. -№4 (108). – pp. 6-13.

APPLICATION

The dependence of the thread tension after the guide in the form of a torus depending on the input tension and the radius of curvature of the torus surface in the contact zone

R, mm	Thread tension after the guide in the form of a torus P, cN $\delta = 8^0$								
	Input tension $P_O=5$ cN			Input tension $P_O=10$ cN			Input tension $P_O=15$ cN		
	PAT	WL	CY	PAT	WL	CY	PAT	WL	CY
2.01	8.6	7.54	8.19	17.29	15.1	16.84	26.24	22.79	25.8
2.41	8.59	7.53	8.2	17.07	15	16.68	25.68	22.51	25.35
2.81	8.6	7.54	8.22	16.97	14.95	16.6	25.38	22.37	25.11
3.21	8.62	7.55	8.24	16.93	14.93	16.57	25.22	22.29	24.97
3.61	8.65	7.57	8.26	16.92	14.93	16.55	25.14	22.26	24.88
4.01	8.69	7.59	8.29	16.93	14.94	16.55	25.1	22.24	24.83
4.41	8.72	7.6	8.31	16.96	14.95	16.56	25.09	22.24	24.81
4.81	8.76	7.62	8.33	16.99	14.97	16.58	25.11	22.25	24.8
5.21	8.79	7.64	8.35	17.03	14.99	16.59	25.13	22.27	24.8
5.61	8.82	7.66	8.38	17.07	15.01	16.61	25.17	22.29	24.81
6.01	8.86	7.67	8.39	17.11	15.04	16.63	25.21	22.31	24.82
6.41	8.89	7.69	8.41	17.16	15.06	16.65	25.26	22.34	24.84
6.81	8.92	7.7	8.43	17.2	15.08	16.67	25.3	22.36	24.86
7.21	8.95	7.72	8.45	17.24	15.1	16.7	25.35	22.39	24.88
7.61	8.98	7.73	8.46	17.29	15.13	16.72	25.4	22.41	24.9
8.01	9.01	7.75	8.48	17.33	15.15	16.74	25.45	22.44	24.92
8.41	9.04	7.76	8.49	17.37	15.17	16.76	25.5	22.47	24.94
8.81	9.07	7.78	8.51	17.41	15.19	16.78	25.56	22.5	24.96
9.21	9.09	7.79	8.52	17.45	15.21	16.8	25.61	22.52	24.99
9.61	9.12	7.8	8.53	17.49	15.23	16.82	25.66	22.55	25.01
10.01	9.14	7.81	8.55	17.53	15.25	16.83	25.71	22.57	25.03
10.41	9.17	7.83	8.56	17.57	15.27	16.85	25.76	22.6	25.05
10.81	9.19	7.84	8.57	17.61	15.29	16.87	25.8	22.63	25.08
11.21	9.22	7.85	8.58	17.65	15.31	16.89	25.85	22.65	25.1
11.61	9.24	7.86	8.59	17.68	15.33	16.91	25.9	22.67	25.12

The dependence of the thread tension after the guide in the form of a torus depending on the input tension and the radius of curvature of the torus surface in the contact zone

R , mm	Thread tension after the guide in the form of a torus P, cN $\delta = 8^0$								
	Input tension $P_O=20$ cN			Input tension $P_O=25$ cN			Input tension $P_O=30$ cN		
	PAT	WL	CY	PAT	WL	CY	PAT	WL	CY
2.01	35.53	30.62	35.07	45.19	38.62	44.69	55.3	46.8	54.66
2.41	34.46	30.11	34.22	43.46	37.8	43.3	52.69	45.6	52.59
2.81	33.88	29.83	33.74	42.51	37.35	42.51	51.28	44.93	51.42
3.21	33.55	29.67	33.45	41.95	37.08	42.03	50.44	44.53	50.7
3.61	33.36	29.58	33.27	41.61	36.92	41.71	49.92	44.28	50.23
4.01	33.25	29.53	33.15	41.41	36.82	41.51	49.59	44.12	49.91
4.41	33.19	29.51	33.07	41.28	36.77	41.37	49.38	44.03	49.69
4.81	33.17	29.5	33.03	41.21	36.74	41.27	49.25	43.97	49.54
5.21	33.17	29.51	33.00	41.18	36.73	41.21	49.18	43.93	49.44
5.61	33.19	29.52	32.99	41.18	36.73	41.18	49.14	43.92	49.37
6.01	33.23	29.54	32.99	41.19	36.74	41.15	49.13	43.92	49.32
6.41	33.27	29.56	33.00	41.22	36.76	41.14	49.14	43.93	49.29
6.81	33.31	29.59	33.01	41.26	36.78	41.14	49.17	43.95	49.27
7.21	33.36	29.62	33.02	41.31	36.81	41.15	49.21	43.98	49.26
7.61	33.41	29.65	33.04	41.36	36.84	41.16	49.25	44.0	49.27
8.01	33.47	29.68	33.06	41.41	36.87	41.17	49.31	44.03	49.27
8.41	33.53	29.71	33.08	41.47	36.9	41.19	49.37	44.07	49.29
8.81	33.58	29.74	33.1	41.53	36.93	41.21	49.43	44.1	49.3
9.21	33.64	29.77	33.13	41.59	36.97	41.24	49.49	44.14	49.32
9.61	33.7	29.8	33.15	41.66	37.0	41.26	49.56	44.17	49.34
10.01	33.76	29.83	33.17	41.72	37.04	41.28	49.62	44.21	49.37
10.41	33.81	29.86	33.2	41.78	37.07	41.31	49.69	44.25	49.39
10.81	33.87	29.89	33.22	41.85	37.1	41.34	49.76	44.28	49.42
11.21	33.93	29.92	33.25	41.91	37.14	41.36	49.83	44.32	49.45
11.61	33.98	29.95	33.27	41.97	37.17	41.39	49.9	44.36	49.47
12.01	34.04	29.98	33.3	42.04	37.21	41.42	49.97	44.39	49.5

The dependence of the thread tension after the guide in the form of a torus depending on the input tension and the radius of curvature of the torus surface in the contact zone

R, mm	Thread tension after the guide in the form of a torus P, cN $\delta = 8^0$								
	Input tension $P_O=35$ cN			Input tension $P_O=40$ cN			Input tension $P_O=45$ cN		
	PAT	WL	CY	PAT	WL	CY	PAT	WL	CY
2.01	65.91	55.17	65.01	77.1	63.77	75.79	88.94	72.59	87.02
2.41	62.19	53.51	62.12	71.98	61.53	71.88	82.1	69.69	81.89
2.81	60.2	52.58	60.48	69.3	60.3	69.7	78.58	68.1	79.07
3.21	59.03	52.02	59.48	67.72	59.56	68.36	76.54	67.15	77.35
3.61	58.29	51.67	58.82	66.73	59.09	67.48	75.25	66.54	76.23
4.01	57.81	51.44	58.37	66.08	58.77	66.89	74.4	66.13	75.46
4.41	57.5	51.29	58.06	65.65	58.57	66.47	73.83	65.86	74.92
4.81	57.3	51.2	57.84	65.36	58.43	66.16	73.44	65.67	74.52
5.21	57.17	51.14	57.68	65.17	58.34	65.95	73.17	65.55	74.23
5.61	57.09	51.11	57.57	65.04	58.29	65.79	72.99	65.47	74.02
6.01	57.05	51.09	57.49	64.97	58.26	65.67	72.88	65.42	73.86
6.41	57.04	51.09	57.43	64.93	58.24	65.59	72.81	65.39	73.75
6.81	57.05	51.1	57.4	64.92	58.25	65.53	72.77	65.38	73.66
7.21	57.08	51.12	57.38	64.93	58.26	65.49	72.76	65.38	73.6
7.61	57.12	51.15	57.37	64.96	58.28	65.46	72.78	65.39	73.55
8.01	57.17	51.18	57.36	64.99	58.3	65.45	72.8	65.41	73.53
8.41	57.22	51.21	57.37	65.04	58.33	65.44	72.84	65.44	73.51
8.81	57.28	51.24	57.38	65.1	58.36	65.44	72.89	65.47	73.5
9.21	57.34	51.28	57.39	65.16	58.4	65.45	72.95	65.51	73.5
9.61	57.41	51.32	57.41	65.23	58.44	65.47	73.02	65.54	73.51
10.01	57.48	51.35	57.43	65.3	58.48	65.48	73.09	65.58	73.52
10.41	57.55	51.39	57.46	65.37	58.52	65.51	73.16	65.63	73.54
10.81	57.62	51.43	57.48	65.44	58.56	65.53	73.23	65.67	73.56
11.21	57.7	51.47	57.51	65.52	58.6	65.55	73.31	65.71	73.59
11.61	57.77	51.51	57.54	65.6	58.65	65.58	73.39	65.76	73.61
12.01	57.84	51.55	57.56	65.68	58.69	65.61	73.47	65.8	73.64

The dependence of the thread tension after the guide in the form of a torus depending on the input tension and the radius of curvature of the torus surface in the contact zone

R, mm	*Thread tension after the guide in the form of a torus P, cN $\delta = 28^0$*								
	Input tension $P_O=5$ cN			*Input tension $P_O=10$ cN*			*Input tension $P_O=15$ cN*		
	PAT	WL	CY	PAT	WL	CY	PAT	WL	CY
2.01	8.78	7.65	8.34	17.64	15.34	17.17	26.79	23.14	26.32
2.41	8.76	7.65	8.35	17.41	15.23	17.00	26.19	22.86	25.85
2.81	8.77	7.66	8.37	17.31	15.17	16.92	25.88	22.71	25.59
3.21	8.80	7.67	8.40	17.26	15.16	16.88	25.71	22.63	25.44
3.61	8.83	7.69	8.42	17.26	15.16	16.87	25.62	22.59	25.36
4.01	8.87	7.7	8.45	17.27	15.16	16.87	25.59	22.57	25.31
4.41	8.90	7.72	8.47	17.3	15.18	16.88	25.58	22.57	25.28
4.81	8.94	7.74	8.49	17.33	15.2	16.89	25.59	22.58	25.27
5.21	8.98	7.76	8.52	17.37	15.22	16.91	25.62	22.6	25.27
5.61	9.01	7.78	8.54	17.42	15.24	16.93	25.66	22.62	25.28
6.01	9.05	7.8	8.56	17.46	15.27	16.95	25.7	22.65	25.29
6.41	9.08	7.81	8.58	17.51	15.29	16.97	25.75	22.67	25.31
6.81	9.12	7.83	8.60	17.55	15.31	17.00	25.8	22.7	25.33
7.21	9.15	7.85	8.62	17.6	15.34	17.02	25.85	22.73	25.35
7.61	9.18	7.86	8.63	17.64	15.36	17.04	25.91	22.75	25.37
8.01	9.21	7.88	8.65	17.69	15.39	17.06	25.96	22.78	25.4
8.41	9.24	7.89	8.66	17.73	15.41	17.08	26.02	22.81	25.42
8.81	9.27	7.91	8.68	17.78	15.43	17.11	26.07	22.84	25.44
9.21	9.3	7.92	8.69	17.82	15.45	17.13	26.12	22.87	25.47
9.61	9.33	7.93	8.71	17.86	15.47	17.15	26.18	22.9	25.49
10.01	9.35	7.95	8.72	17.91	15.49	17.17	26.23	22.92	25.52
10.41	9.38	7.96	8.73	17.95	15.52	17.19	26.28	22.95	25.54
10.81	9.4	7.97	8.75	17.99	15.54	17.2	26.33	22.98	25.56
11.21	9.43	7.98	8.76	18.03	15.56	17.22	26.38	23.0	25.59
11.61	9.45	7.99	8.77	18.07	15.57	17.24	26.43	23.03	25.61
12.01	9.48	8.00	8.78	18.1	15.59	17.26	26.48	23.05	25.63

The dependence of the thread tension after the guide in the form of a torus depending on the input tension and the radius of curvature of the torus surface in the contact zone

R , mm	Thread tension after the guide in the form of a torus P, cN $\delta = 28^0$								
	Input tension P_O=20 cN			Input tension P_O=25 cN			Input tension P_O=30 cN		
	PAT	WL	CY	PAT	WL	CY	PAT	WL	CY
2.01	36.28	31.1	35.8	46.17	39.24	45.64	56.53	47.56	55.86
2.41	35.16	30.57	34.91	44.34	38.39	44.19	53.78	46.31	53.69
2.81	34.55	30.28	34.4	43.35	37.91	43.35	52.29	45.61	52.46
3.21	34.20	30.11	34.1	42.76	37.63	42.84	51.41	45.19	51.70
3.61	34.00	30.02	33.9	42.41	37.46	42.51	50.87	44.93	51.20
4.01	33.88	29.96	33.78	42.19	37.36	42.3	50.52	44.76	50.87
4.41	33.82	29.94	33.7	42.06	37.3	42.15	50.3	44.66	50.64
4.81	33.8	29.93	33.65	41.99	37.27	42.05	50.17	44.6	50.48
5.21	33.81	29.94	33.63	41.96	37.26	41.99	50.09	44.56	50.37
5.61	33.83	29.95	33.61	41.95	37.26	41.95	50.05	44.55	50.29
6.01	33.86	29.97	33.61	41.97	37.27	41.93	50.04	44.55	50.24
6.41	33.9	30.00	33.62	42.00	37.29	41.92	50.06	44.56	50.21
6.81	33.95	30.03	33.63	42.04	37.32	41.92	50.09	44.58	50.19
7.21	34.01	30.05	33.65	42.09	37.35	41.92	50.13	44.61	50.19
7.61	34.06	30.09	33.67	42.14	37.38	41.93	50.18	44.64	50.19
8.01	34.12	30.12	33.69	42.20	37.41	41.95	50.23	44.67	50.2
8.41	34.18	30.15	33.71	42.26	37.44	41.97	50.29	44.7	50.21
8.81	34.24	30.18	33.73	42.33	37.48	41.99	50.36	44.74	50.23
9.21	34.30	30.21	33.76	42.39	37.51	42.02	50.43	44.78	50.25
9.61	34.36	30.25	33.78	42.46	37.55	42.04	50.5	44.82	50.27
10.01	34.42	30.28	33.81	42.53	37.59	42.07	50.57	44.86	50.3
10.41	34.48	30.31	33.84	42.59	37.62	42.09	50.64	44.89	50.32
10.81	34.54	30.34	33.86	42.66	37.66	42.12	50.71	44.93	50.35
11.21	34.60	30.37	33.89	42.73	37.69	42.15	50.78	44.97	50.38
11.61	34.66	30.40	33.91	42.8	37.73	42.18	50.86	45.01	50.41
12.01	34.72	30.43	33.94	42.86	37.76	42.21	50.93	45.05	50.44

The dependence of the thread tension after the guide in the form of a torus depending on the input tension and the radius of curvature of the torus surface in the contact zone

R , mm	Thread tension after the guide in the form of a torus P, cN $\delta = 28^0$								
	Input tension P_O=35 cN			Input tension P_O=40 cN			Input tension P_O=45 cN		
	PAT	WL	CY	PAT	WL	CY	PAT	WL	CY
2.01	67.41	56.1	66.48	78.89	64.85	77.55	91.07	73.85	89.08
2.41	63.5	54.35	63.43	73.52	62.51	73.42	83.88	70.81	83.68
2.81	61.41	53.38	61.71	70.7	61.22	71.13	80.19	69.15	80.72
3.21	60.17	52.79	60.65	69.04	60.44	69.72	78.03	68.15	78.91
3.61	59.40	52.42	59.96	68.00	59.95	68.8	76.68	67.51	77.73
4.01	58.9	52.18	59.49	67.32	59.62	68.17	75.8	67.09	76.92
4.41	58.57	52.03	59.16	66.87	59.41	67.73	75.2	66.8	76.35
4.81	58.36	51.93	58.93	66.56	59.26	67.42	74.79	66.61	75.93
5.21	58.22	51.87	58.76	66.36	59.17	67.18	74.51	66.48	75.63
5.61	58.14	51.83	58.65	66.23	59.11	67.02	74.32	66.39	75.41
6.01	58.1	51.82	58.56	66.15	59.08	66.89	74.2	66.34	75.24
6.41	58.09	51.82	58.51	66.11	59.07	66.81	74.12	66.31	75.12
6.81	58.1	51.83	58.47	66.1	59.07	66.74	74.09	66.3	75.03
7.21	58.13	51.85	58.45	66.11	59.08	66.7	74.08	66.3	74.96
7.61	58.17	51.88	58.43	66.14	59.1	66.68	74.09	66.31	74.92
8.01	58.22	51.91	58.43	66.18	59.13	66.66	74.12	66.34	74.89
8.41	58.28	51.94	58.44	66.24	59.16	66.66	74.17	66.36	74.87
8.81	58.34	51.98	58.45	66.29	59.2	66.66	74.22	66.4	74.86
9.21	58.41	52.02	58.47	66.36	59.23	66.67	74.28	66.43	74.87
9.61	58.48	52.06	58.48	66.43	59.27	66.68	74.35	66.47	74.87
10.01	58.56	52.1	58.51	66.51	59.32	66.7	74.42	66.51	74.89
10.41	58.63	52.14	58.53	66.58	59.36	66.73	74.5	66.56	74.91
10.81	58.71	52.18	58.56	66.66	59.4	66.75	74.58	66.6	74.93
11.21	58.78	52.22	58.59	66.74	59.45	66.78	74.66	66.65	74.95
11.61	58.86	52.26	58.62	66.82	59.49	66.81	74.75	66.7	74.98
12.01	58.94	52.31	58.65	66.91	59.54	66.84	74.83	66.74	75.01

The dependence of the thread tension after the guide in the form of a torus depending on the input tension and the radius of curvature of the torus surface in the contact zone

R, mm	Thread tension after the guide in the form of a torus P, cN $\delta = 48^0$								
	Input tension $P_O=5$ cN			Input tension $P_O=10$ cN			Input tension $P_O=15$ cN		
	PAT	WL	CY	PAT	WL	CY	PAT	WL	CY
2.01	9.2	7.93	8.7	18.48	15.89	17.95	28.08	23.98	27.56
2.41	9.18	7.92	8.71	18.23	15.76	17.76	27.42	23.67	27.04
2.81	9.19	7.93	8.74	18.11	15.71	17.67	27.07	23.5	26.75
3.21	9.22	7.95	8.76	18.06	15.69	17.63	26.88	23.41	26.58
3.61	9.26	7.97	8.79	18.05	15.69	17.62	26.78	23.37	26.48
4.01	9.3	7.99	8.82	18.07	15.7	17.62	26.74	23.35	26.43
4.41	9.34	8.01	8.85	18.1	15.71	17.63	26.74	23.35	26.4
4.81	9.38	8.03	8.88	18.14	15.74	17.64	26.75	23.36	26.39
5.21	9.43	8.05	8.9	18.19	15.76	17.66	26.79	23.38	26.39
5.61	9.47	8.07	8.93	18.24	15.79	17.69	26.83	23.41	26.4
6.01	9.51	8.09	8.95	18.29	15.81	17.71	26.88	23.43	26.41
6.41	9.55	8.11	8.97	18.34	15.84	17.74	26.93	23.46	26.43
6.81	9.58	8.13	8.99	18.39	15.87	17.76	26.99	23.49	26.46
7.21	9.62	8.15	9.01	18.45	15.89	17.79	27.05	23.52	26.48
7.61	9.66	8.16	9.03	18.5	15.92	17.81	27.11	23.56	26.51
8.01	9.69	8.18	9.05	18.55	15.95	17.84	27.17	23.59	26.53
8.41	9.73	8.2	9.07	18.6	15.97	17.86	27.23	23.62	26.56
8.81	9.76	8.21	9.09	18.65	16.0	17.89	27.3	23.65	26.59
9.21	9.79	8.23	9.1	18.7	16.02	17.91	27.36	23.68	26.61
9.61	9.82	8.24	9.12	18.75	16.05	17.93	27.42	23.71	26.64
10.01	9.85	8.26	9.13	18.79	16.07	17.95	27.48	23.75	26.67
10.41	9.88	8.27	9.15	18.84	16.09	17.98	27.54	23.78	26.69
10.81	9.91	8.28	9.16	18.89	16.12	18	27.59	23.81	26.72
11.21	9.94	8.3	9.18	18.93	16.14	18.02	27.65	23.83	26.75
11.61	9.97	8.31	9.19	18.98	16.16	18.04	27.71	23.86	26.77
12.01	9.99	8.32	9.2	19.02	16.18	18.06	27.77	23.89	26.8

The dependence of the thread tension after the guide in the form of a torus depending on the input tension and the radius of curvature of the torus surface in the contact zone

R , mm	Thread tension after the guide in the form of a torus P, cN $\delta = 48^0$								
	Input tension $P_O=20$ cN			Input tension $P_O=25$ cN			Input tension $P_O=30$ cN		
	PAT	WL	CY	PAT	WL	CY	PAT	WL	CY
2.01	38.06	32.25	37.54	48.49	40.71	47.92	59.44	49.38	58.72
2.41	36.81	31.66	36.54	46.45	39.76	46.29	56.37	47.98	56.29
2.81	36.13	31.33	35.97	45.34	39.23	45.36	54.71	47.2	54.91
3.21	35.74	31.15	35.63	44.69	38.92	44.79	53.73	46.74	54.06
3.61	35.52	31.04	35.41	44.29	38.73	44.42	53.12	46.45	53.5
4.01	35.39	30.99	35.28	44.05	38.62	44.18	52.74	46.27	53.13
4.41	35.32	30.96	35.19	43.9	38.56	44.01	52.49	46.15	52.88
4.81	35.3	30.95	35.14	43.82	38.52	43.9	52.34	46.09	52.7
5.21	35.31	30.96	35.11	43.79	38.51	43.83	52.26	46.05	52.57
5.61	35.33	30.97	35.09	43.79	38.51	43.79	52.22	46.04	52.49
6.01	35.37	31.0	35.09	43.81	38.53	43.76	52.21	46.04	52.44
6.41	35.42	31.03	35.1	43.84	38.55	43.75	52.22	46.05	52.4
6.81	35.48	31.06	35.11	43.89	38.58	43.75	52.26	46.07	52.38
7.21	35.54	31.09	35.13	43.95	38.61	43.76	52.3	46.1	52.38
7.61	35.6	31.12	35.15	44.01	38.65	43.77	52.36	46.14	52.38
8.01	35.67	31.16	35.18	44.08	38.68	43.79	52.43	46.17	52.39
8.41	35.73	31.2	35.2	44.15	38.72	43.81	52.5	46.21	52.4
8.81	35.8	31.23	35.23	44.22	38.76	43.84	52.57	46.25	52.42
9.21	35.87	31.27	35.26	44.29	38.8	43.87	52.65	46.29	52.45
9.61	35.94	31.3	35.29	44.37	38.84	43.9	52.73	46.34	52.47
10.01	36.01	31.34	35.32	44.45	38.88	43.93	52.81	46.38	52.5
10.41	36.08	31.38	35.35	44.52	38.92	43.96	52.89	46.42	52.53
10.81	36.15	31.41	35.38	44.6	38.96	43.99	52.97	46.47	52.56
11.21	36.22	31.45	35.41	44.67	39.0	44.02	53.05	46.51	52.6
11.61	36.28	31.48	35.44	44.75	39.04	44.05	53.14	46.56	52.63
12.01	36.35	31.52	35.47	44.83	39.08	44.08	53.22	46.6	52.66

The dependence of the thread tension after the guide in the form of a torus depending on the input tension and the radius of curvature of the torus surface in the contact zone

R, mm	*Thread tension after the guide in the form of a torus P, cN* $\delta = 48^0$								
	Input tension $P_O=35$ cN			*Input tension $P_O=40$ cN*			*Input tension $P_O=45$ cN*		
	PAT	WL	CY	PAT	WL	CY	PAT	WL	CY
2.01	70.97	58.27	69.98	83.17	67.42	81.72	96.13	76.83	94
2.41	66.6	56.33	66.56	77.16	64.82	77.1	88.11	73.46	87.95
2.81	64.26	55.25	64.63	74.02	63.39	74.54	83.99	71.62	84.63
3.21	62.89	54.6	63.45	72.17	62.53	72.96	81.59	70.51	82.61
3.61	62.02	54.2	62.67	71.01	61.98	71.93	80.08	69.8	81.28
4.01	61.47	53.93	62.15	70.25	61.62	71.23	79.1	69.33	80.38
4.41	61.1	53.76	61.78	69.75	61.38	70.74	78.43	69.01	79.74
4.81	60.87	53.65	61.52	69.41	61.22	70.38	77.98	68.8	79.28
5.21	60.72	53.58	61.34	69.19	61.12	70.13	77.66	68.66	78.94
5.61	60.63	53.55	61.21	69.04	61.06	69.94	77.46	68.56	78.69
6.01	60.59	53.53	61.11	68.96	61.02	69.8	77.32	68.5	78.51
6.41	60.58	53.54	61.05	68.92	61.01	69.71	77.24	68.47	78.37
6.81	60.59	53.55	61.01	68.91	61.01	69.64	77.2	68.46	78.27
7.21	60.63	53.57	60.98	68.92	61.02	69.59	77.2	68.47	78.2
7.61	60.67	53.6	60.97	68.96	61.05	69.56	77.21	68.48	78.15
8.01	60.73	53.63	60.97	69	61.08	69.55	77.25	68.51	78.12
8.41	60.8	53.67	60.98	69.06	61.11	69.54	77.3	68.54	78.1
8.81	60.87	53.71	60.99	69.13	61.15	69.55	77.36	68.58	78.09
9.21	60.95	53.76	61.01	69.21	61.2	69.56	77.43	68.62	78.1
9.61	61.03	53.8	61.03	69.29	61.24	69.57	77.51	68.66	78.11
10.01	61.11	53.85	61.06	69.37	61.29	69.6	77.59	68.71	78.12
10.41	61.2	53.89	61.09	69.46	61.34	69.62	77.68	68.76	78.14
10.81	61.28	53.94	61.12	69.55	61.39	69.65	77.77	68.81	78.17
11.21	61.37	53.99	61.15	69.64	61.44	69.68	77.87	68.86	78.2
11.61	61.46	54.04	61.18	69.73	61.49	69.71	77.96	68.91	78.23
12.01	61.55	54.08	61.22	69.83	61.54	69.75	78.06	68.97	78.26

The dependence of the thread tension after the guide in the form of a torus depending on the input tension and the radius of curvature of the torus surface in the contact zone

R, mm	Thread tension after the guide in the form of a torus P, cN $\delta = 68^0$								
	Input tension $P_O=5$ cN			Input tension $P_O=10$ cN			Input tension $P_O=15$ cN		
	PAT	WL	CY	PAT	WL	CY	PAT	WL	CY
2.01	9.99	8.44	9.39	20.08	16.92	19.43	30.54	25.55	29.91
2.41	9.97	8.44	9.4	19.77	16.77	19.21	29.74	25.18	29.28
2.81	9.99	8.45	9.43	19.63	16.71	19.1	29.32	24.98	28.93
3.21	10.03	8.47	9.46	19.57	16.68	19.05	29.09	24.87	28.73
3.61	10.07	8.49	9.5	19.57	16.68	19.03	28.98	24.82	28.62
4.01	10.12	8.51	9.54	19.59	16.7	19.03	28.93	24.8	28.55
4.41	10.18	8.54	9.57	19.63	16.72	19.05	28.93	24.81	28.52
4.81	10.23	8.57	9.6	19.68	16.74	19.07	28.95	24.82	28.5
5.21	10.28	8.59	9.63	19.74	16.77	19.09	28.99	24.84	28.51
5.61	10.33	8.62	9.66	19.8	16.8	19.12	29.05	24.87	28.52
6.01	10.38	8.64	9.69	19.86	16.84	19.15	29.11	24.91	28.54
6.41	10.43	8.66	9.72	19.93	16.87	19.18	29.18	24.94	28.56
6.81	10.48	8.69	9.75	19.99	16.9	19.21	29.25	24.98	28.59
7.21	10.52	8.71	9.77	20.06	16.93	19.25	29.32	25.02	28.62
7.61	10.57	8.73	9.8	20.12	16.97	19.28	29.4	25.06	28.65
8.01	10.61	8.75	9.82	20.19	17	19.31	29.47	25.1	28.69
8.41	10.65	8.77	9.84	20.25	17.03	19.34	29.55	25.13	28.72
8.81	10.7	8.79	9.86	20.31	17.06	19.37	29.62	25.17	28.75
9.21	10.74	8.81	9.88	20.37	17.09	19.4	29.7	25.21	28.79
9.61	10.77	8.83	9.9	20.43	17.12	19.43	29.78	25.25	28.82
10.01	10.81	8.84	9.92	20.49	17.15	19.45	29.85	25.29	28.85
10.41	10.85	8.86	9.94	20.55	17.18	19.48	29.92	25.32	28.89
10.81	10.89	8.88	9.96	20.6	17.2	19.51	30.0	25.36	28.92
11.21	10.92	8.89	9.97	20.66	17.23	19.53	30.07	25.39	28.95
11.61	10.95	8.91	9.99	20.71	17.26	19.56	30.14	25.43	28.98
12.01	10.99	8.93	10.0	20.77	17.28	19.58	30.21	25.46	29.01

The dependence of the thread tension after the guide in the form of a torus depending on the input tension and the radius of curvature of the torus surface in the contact zone

R, mm	Thread tension after the guide in the form of a torus P, cN $\delta = 68^0$								
	Input tension $P_O=20$ cN			Input tension $P_O=25$ cN			Input tension $P_O=30$ cN		
	PAT	WL	CY	PAT	WL	CY	PAT	WL	CY
2.01	41.45	34.39	40.85	52.9	43.45	52.25	64.97	52.76	64.17
2.41	39.94	33.69	39.64	50.44	42.33	50.28	61.27	51.11	61.23
2.81	39.13	33.3	38.95	49.11	41.7	49.15	59.28	50.18	59.56
3.21	38.66	33.08	38.53	48.32	41.33	48.47	58.1	49.63	58.53
3.61	38.39	32.96	38.27	47.85	41.11	48.02	57.38	49.29	57.87
4.01	38.24	32.89	38.11	47.56	40.98	47.73	56.92	49.08	57.42
4.41	38.17	32.86	38.01	47.39	40.9	47.54	56.63	48.94	57.11
4.81	38.14	32.85	37.94	47.3	40.86	47.41	56.45	48.86	56.9
5.21	38.15	32.86	37.91	47.26	40.85	47.32	56.35	48.82	56.75
5.61	38.18	32.88	37.9	47.26	40.86	47.27	56.31	48.81	56.65
6.01	38.23	32.91	37.89	47.29	40.87	47.24	56.3	48.81	56.59
6.41	38.29	32.94	37.9	47.33	40.9	47.23	56.32	48.83	56.54
6.81	38.36	32.98	37.92	47.39	40.94	47.23	56.37	48.86	56.52
7.21	38.44	33.02	37.94	47.46	40.97	47.24	56.43	48.89	56.52
7.61	38.52	33.06	37.97	47.54	41.02	47.26	56.5	48.93	56.52
8.01	38.6	33.11	38.0	47.63	41.06	47.28	56.58	48.98	56.54
8.41	38.69	33.15	38.03	47.71	41.11	47.31	56.66	49.02	56.56
8.81	38.77	33.2	38.07	47.8	41.16	47.34	56.76	49.07	56.58
9.21	38.86	33.24	38.1	47.9	41.2	47.37	56.85	49.12	56.61
9.61	38.94	33.28	38.14	47.99	41.25	47.41	56.95	49.18	56.64
10.01	39.03	33.33	38.18	48.08	41.3	47.45	57.05	49.23	56.68
10.41	39.11	33.37	38.21	48.18	41.35	47.48	57.15	49.28	56.72
10.81	39.2	33.41	38.25	48.27	41.4	47.52	57.25	49.34	56.76
11.21	39.28	33.46	38.29	48.37	41.45	47.56	57.35	49.39	56.8
11.61	39.37	33.5	38.32	48.46	41.5	47.6	57.46	49.44	56.84
12.01	39.45	33.54	38.36	48.55	41.54	47.64	57.56	49.49	56.88

The dependence of the thread tension after the guide in the form of a torus depending on the input tension and the radius of curvature of the torus surface in the contact zone

R, mm	*Thread tension after the guide in the form of a torus P, cN* $\delta = 68^0$								
	Input tension $P_O=35$ cN			*Input tension $P_O=40$ cN*			*Input tension $P_O=45$ cN*		
	PAT	WL	CY	PAT	WL	CY	PAT	WL	CY
2.01	77.73	62.34	76.63	91.29	72.21	89.68	105.76	82.41	103.37
2.41	72.47	60.04	72.49	84.07	69.13	84.1	96.12	78.4	96.05
2.81	69.67	58.76	70.17	80.29	67.43	81	91.18	76.22	92.05
3.21	68.02	57.99	68.74	78.08	66.41	79.1	88.31	74.9	89.61
3.61	66.99	57.51	67.81	76.69	65.76	77.86	86.51	74.07	88.02
4.01	66.32	57.2	67.18	75.79	65.34	77.02	85.33	73.51	86.93
4.41	65.89	56.99	66.74	75.19	65.06	76.42	84.53	73.14	86.17
4.81	65.61	56.87	66.43	74.79	64.87	76.0	83.99	72.89	85.61
5.21	65.43	56.79	66.21	74.52	64.75	75.69	83.62	72.72	85.21
5.61	65.33	56.75	66.05	74.35	64.68	75.47	83.38	72.61	84.91
6.01	65.29	56.73	65.94	74.26	64.64	75.3	83.22	72.54	84.69
6.41	65.28	56.73	65.86	74.21	64.63	75.19	83.13	72.51	84.52
6.81	65.3	56.75	65.81	74.2	64.63	75.11	83.09	72.5	84.4
7.21	65.34	56.78	65.79	74.22	64.65	75.05	83.08	72.5	84.32
7.61	65.4	56.82	65.77	74.27	64.68	75.02	83.11	72.52	84.26
8.01	65.47	56.86	65.77	74.33	64.72	75.0	83.16	72.55	84.23
8.41	65.56	56.9	65.78	74.41	64.76	75.0	83.22	72.59	84.21
8.81	65.65	56.95	65.8	74.49	64.81	75.01	83.3	72.64	84.2
9.21	65.74	57.01	65.82	74.58	64.86	75.02	83.39	72.69	84.2
9.61	65.84	57.06	65.85	74.68	64.91	75.04	83.48	72.74	84.22
10.01	65.95	57.12	65.89	74.79	64.97	75.07	83.59	72.8	84.24
10.41	66.05	57.17	65.92	74.9	65.03	75.1	83.7	72.86	84.26
10.81	66.16	57.23	65.96	75.01	65.09	75.14	83.81	72.92	84.3
11.21	66.27	57.29	66.0	75.12	65.15	75.18	83.92	72.99	84.33
11.61	66.38	57.34	66.04	75.24	65.21	75.22	84.04	73.05	84.37
12.01	66.49	57.4	66.08	75.35	65.27	75.26	84.16	73.12	84.41

The dependence of the thread tension after the guide in the form of a torus depending on the input tension and the radius of curvature of the torus surface in the contact zone

R , mm	Thread tension after the guide in the form of a torus P, cN δ =88⁰								
	Input tension P_O=5 cN			Input tension P_O=10 cN			Input tension P_O=15 cN		
	PAT	WL	CY	PAT	WL	CY	PAT	WL	CY
2.01	11.48	9.38	10.66	23.06	18.79	22.19	35.12	28.41	34.3
2.41	11.45	9.37	10.68	22.65	18.6	21.9	34.06	27.92	33.46
2.81	11.48	9.39	10.72	22.47	18.52	21.75	33.5	27.67	33
3.21	11.53	9.42	10.77	22.4	18.49	21.69	33.21	27.53	32.73
3.61	11.6	9.45	10.81	22.39	18.49	21.66	33.06	27.47	32.58
4.01	11.67	9.48	10.86	22.43	18.51	21.67	33.01	27.45	32.49
4.41	11.74	9.51	10.91	22.48	18.54	21.69	33.0	27.45	32.45
4.81	11.82	9.55	10.96	22.55	18.58	21.72	33.04	27.47	32.44
5.21	11.89	9.58	11.0	22.63	18.62	21.75	33.1	27.5	32.44
5.61	11.96	9.62	11.04	22.72	18.66	21.79	33.18	27.54	32.46
6.01	12.03	9.65	11.08	22.81	18.7	21.84	33.26	27.59	32.49
6.41	12.1	9.68	11.12	22.9	18.75	21.88	33.36	27.64	32.52
6.81	12.16	9.71	11.15	22.99	18.79	21.92	33.46	27.69	32.56
7.21	12.23	9.74	11.19	23.08	18.83	21.96	33.56	27.74	32.6
7.61	12.29	9.77	11.22	23.17	18.88	22.01	33.67	27.79	32.65
8.01	12.35	9.8	11.25	23.26	18.92	22.05	33.77	27.84	32.69
8.41	12.41	9.82	11.28	23.35	18.96	22.09	33.88	27.89	32.74
8.81	12.47	9.85	11.31	23.43	19.0	22.13	33.98	27.95	32.79
9.21	12.53	9.88	11.34	23.52	19.04	22.17	34.09	28.0	32.83
9.61	12.58	9.9	11.37	23.6	19.08	22.21	34.19	28.05	32.88
10.01	12.63	9.92	11.39	23.68	19.12	22.25	34.3	28.1	32.92
10.41	12.69	9.95	11.42	23.76	19.16	22.29	34.4	28.15	32.97
10.81	12.74	9.97	11.44	23.84	19.19	22.32	34.5	28.19	33.02
11.21	12.79	9.99	11.46	23.92	19.23	22.36	34.6	28.24	33.06
11.61	12.83	10.01	11.49	23.99	19.27	22.39	34.69	28.29	33.1
12.01	12.88	10.03	11.51	24.07	19.3	22.43	34.79	28.33	33.15

The dependence of the thread tension after the guide in the form of a torus depending on the input tension and the radius of curvature of the torus surface in the contact zone

R , mm	*Thread tension after the guide in the form of a torus P, cN* $\delta = 88^0$								
	Input tension $P_O=20$ cN			*Input tension* $P_O=25$ cN			*Input tension* $P_O=30$ cN		
	PAT	WL	CY	PAT	WL	CY	PAT	WL	CY
2.01	47.77	38.28	47.01	61.13	48.45	60.35	75.27	58.92	74.36
2.41	45.77	37.37	45.4	57.87	46.99	57.71	70.39	56.78	70.43
2.81	44.7	36.88	44.48	56.1	46.18	56.22	67.76	55.59	68.21
3.21	44.08	36.59	43.93	55.07	45.7	55.3	66.21	54.88	66.85
3.61	43.73	36.43	43.59	54.45	45.42	54.72	65.26	54.44	65.97
4.01	43.54	36.35	43.37	54.08	45.25	54.33	64.66	54.16	65.38
4.41	43.44	36.31	43.24	53.86	45.15	54.08	64.29	53.99	64.97
4.81	43.42	36.3	43.16	53.75	45.11	53.91	64.06	53.9	64.69
5.21	43.44	36.32	43.11	53.7	45.09	53.8	63.94	53.84	64.5
5.61	43.48	36.35	43.1	53.71	45.1	53.73	63.88	53.83	64.37
6.01	43.56	36.39	43.1	53.75	45.13	53.69	63.88	53.84	64.29
6.41	43.64	36.43	43.11	53.82	45.17	53.68	63.92	53.86	64.23
6.81	43.74	36.48	43.14	53.9	45.21	53.68	63.98	53.9	64.21
7.21	43.84	36.54	43.17	54	45.27	53.7	64.07	53.95	64.2
7.61	43.96	36.59	43.21	54.11	45.32	53.73	64.17	54.0	64.21
8.01	44.07	36.65	43.25	54.23	45.38	53.76	64.28	54.06	64.23
8.41	44.19	36.71	43.3	54.35	45.45	53.8	64.4	54.12	64.26
8.81	44.3	36.77	43.35	54.47	45.51	53.84	64.53	54.19	64.3
9.21	44.42	36.83	43.39	54.6	45.57	53.89	64.66	54.26	64.34
9.61	44.54	36.89	43.44	54.73	45.64	53.94	64.8	54.33	64.39
10.01	44.66	36.95	43.49	54.86	45.71	53.99	64.94	54.4	64.44
10.41	44.78	37.0	43.54	54.99	45.77	54.04	65.08	54.47	64.49
10.81	44.9	37.06	43.59	55.12	45.84	54.1	65.22	54.54	64.54
11.21	45.01	37.12	43.65	55.25	45.9	54.15	65.36	54.61	64.6
11.61	45.13	37.17	43.7	55.38	45.97	54.21	65.5	54.69	64.66
12.01	45.24	37.23	43.75	55.51	46.03	54.26	65.64	54.76	64.72

The dependence of the thread tension after the guide in the form of a torus depending on the input tension and the radius of curvature of the torus surface in the contact zone

R , mm	Thread tension after the guide in the form of a torus P, cN $\delta = 88^0$								
	Input tension $P_O=35$ cN			Input tension $P_O=40$ cN			Input tension $P_O=45$ cN		
	PAT	WL	CY	PAT	WL	CY	PAT	WL	CY
2.01	90.33	69.75	89.09	106.43	80.95	104.6	123.72	92.55	120.96
2.41	83.38	66.77	83.57	96.9	76.96	97.15	111	87.38	111.2
2.81	79.69	65.11	80.48	91.93	74.77	93.03	104.5	84.56	105.88
3.21	77.52	64.12	78.59	89.02	73.45	90.51	100.73	82.87	102.64
3.61	76.17	63.5	77.35	87.21	72.62	88.87	98.37	81.79	100.53
4.01	75.3	63.1	76.51	86.02	72.07	87.75	96.83	81.08	99.1
4.41	74.74	62.85	75.93	85.24	71.71	86.97	95.8	80.6	98.08
4.81	74.38	62.68	75.52	84.72	71.48	86.41	95.1	80.28	97.35
5.21	74.16	62.59	75.23	84.38	71.33	86.01	94.63	80.07	96.82
5.61	74.03	62.54	75.03	84.17	71.23	85.71	94.31	79.93	96.43
6.01	73.98	62.52	74.89	84.05	71.19	85.5	94.12	79.85	96.14
6.41	73.98	62.53	74.79	84	71.17	85.35	94.01	79.81	95.93
6.81	74.01	62.55	74.73	84	71.18	85.25	93.96	79.79	95.77
7.21	74.07	62.59	74.69	84.04	71.21	85.18	93.96	79.81	95.66
7.61	74.16	62.64	74.68	84.1	71.25	85.14	94.0	79.84	95.59
8.01	74.26	62.7	74.68	84.19	71.3	85.12	94.07	79.88	95.55
8.41	74.38	62.76	74.7	84.3	71.36	85.12	94.17	79.93	95.52
8.81	74.51	62.83	74.73	84.42	71.43	85.13	94.28	80	95.52
9.21	74.64	62.9	74.76	84.55	71.5	85.15	94.4	80.07	95.53
9.61	74.78	62.97	74.8	84.69	71.57	85.19	94.54	80.14	95.55
10.01	74.92	63.04	74.85	84.83	71.65	85.22	94.68	80.22	95.58
10.41	75.07	63.12	74.9	84.98	71.73	85.27	94.83	80.3	95.62
10.81	75.22	63.2	74.95	85.14	71.81	85.32	94.99	80.38	95.66
11.21	75.37	63.27	75	85.29	71.89	85.37	95.15	80.46	95.71
11.61	75.52	63.35	75.06	85.45	71.97	85.43	95.31	80.55	95.77

Щербань Волдимир Юрійович,
Галавська Людмила Євгеніївна,
Колиско Оксана Зенонівна,
Щербань Юрій Юрійович,
Єліна Тетяна Вікторівна,
Колиско Мар'яна Ігорівна

МАТЕМАТИЧНІ МОДЕЛІ КОМП'ЮТЕРНОГО ЗАБЕЗПЕЧЕННЯ ДЛЯ ВИЗНАЧЕННЯ ТЕХНОЛОГІЧНИХ ЗУСИЛЬ ПРИ ВИРОБНИЦТВІ ТЕХНІЧНИХ ТКАНИН ТА ТРИКОТАЖУ ДЛЯ ВІЙСЬКОВИХ ПОТРЕБ

(англійською мовою)